The

GEOLOGICAL BULLETIN

of the

PUNJAB UNIVERSITY

Number Nine *December* 1972

CONTENTS

THE STUDY OF GEOCHEMISTRY OF THE ALTERATION PRODUCTS OF THE SUSALGALI GRANITE GNEISS, NEAR AHL, DISTRICT HAZARA, N.W.F.P., PAKISTAN

BY

FAZAL-UR-REHMAN

Geology Department, Punjab University, Lahore.

Abstract : *On the Battal-Mansehra road and close to the Ahl rest house north of Abbotabad, Hazara district, there is a huge deposit of soft, friable, white-looking material. This has been repeatedly investigated, in the past, by many workers taking it as a deposit of kaolin clay ; the reports have been both in favour as well as against this assumption. However, these reports were almost never based on detailed technical investigation which had been the cause of widely variable conclusions.*

The present paper has been written on the basis of chemical, microscopic, differential thermal and infra-red spectrophotometric analyses and also on the basis of geochemical relationships which exist between the soft, friable deposit and the immediately associated Susalgali granite gneiss. Moreover it has been discovered that the deposit has got the same mineralogy and almost the same chemical composition as that of the surrounding granite gneiss and the deposit can not be other than but an alteration product of the surrounding rock.

INTRODUCTION

Near and around P.W.D. Rest House, Ahl (Lat. 34° 33′ 20″N Long. 73° 9′ 39″E) widely spread white powdery material has been attracting attention of geologists long since. The Geological Survey of Pakistan has called it a deposit of Kaolin clay. While carrying out geochemical work on the Mansehra-Amb State area (Rehman, 1966) the writer got interested to carry out a detailed investigation.

The deposit is flanked on all sides by the Susalgali granite gneiss, whereas the Susalgali granite gneiss is a major and an older member of the Granite Complex which exists in the Mansehra area, District Hazara (Shams, 1966, 1969). The deposit is covered by a layer of alluvium which is of variable thickness, varying from 1′ to 15′. The material of the deposit consists of 30 to 40 per cent coherent rock fragments which vary in size from coarse sand to pebble, and 60 to 70 per cent gray matrix of a soft, friable, fine material most of which feels gritty. Only 10 per cent of the material feels slick and non-gritty.

The material along the fresh cuts, 6 to 12 inches deep, is easily disintegrable by crumbling between the fingers, whereas the material, still deeper, is comparatively more integrated. It may be due to fact that most of the fine, soluble material (and also if any traces of calcite and magnestite were present) might have gone into solution in the rain water, and thus weakening the cohesion of the residual material, on the surface of the cuts.

SAMPLING

The sampling was started from the fresh portion of surrounding Susalgali granite gneiss and after continuing through the deposit, it was stopped when the other end of Susalgali granite gneiss was met with again. The rock samples were collected

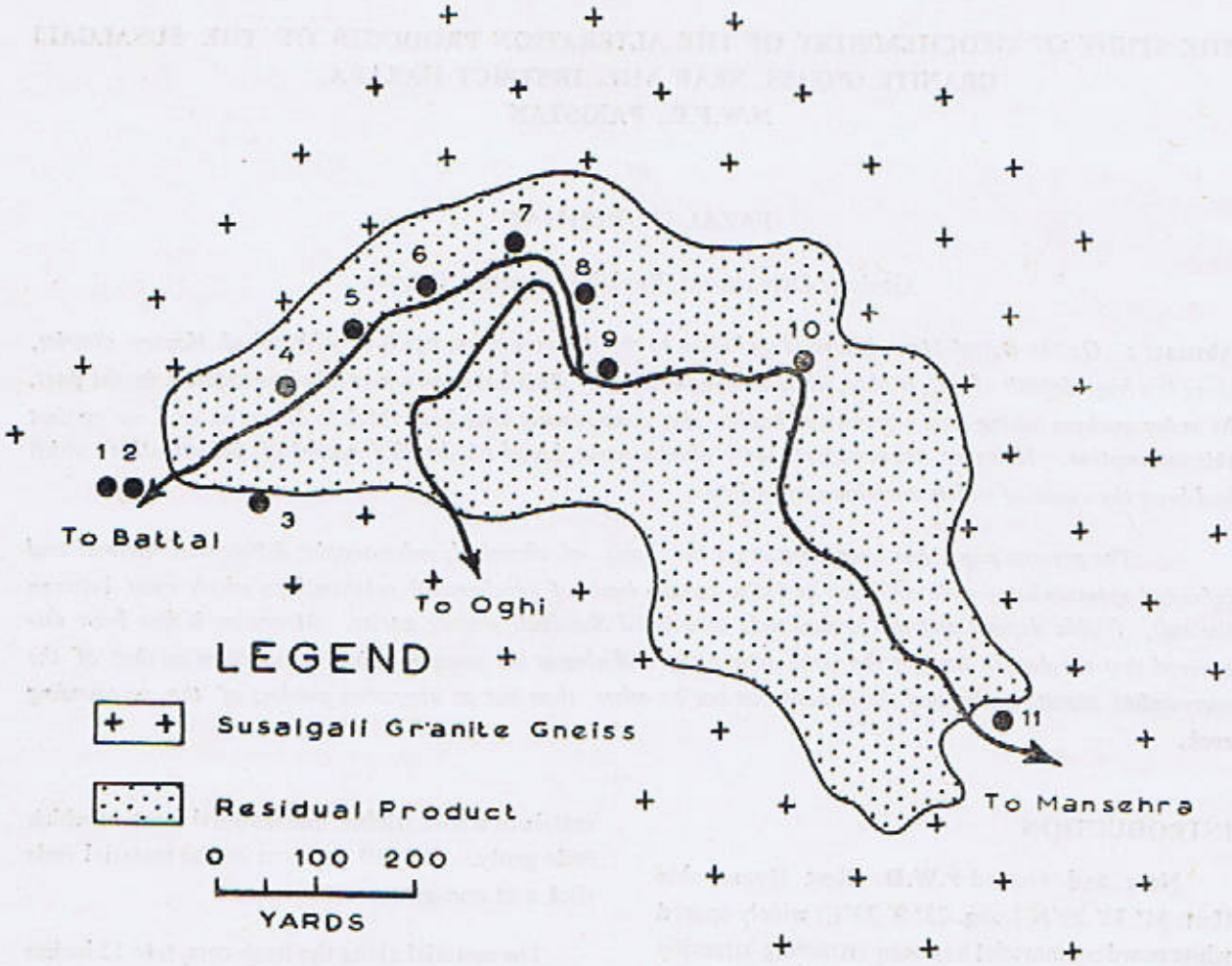

Fig. 1. Map showing locations of the selected samples (Mumtaz-ud-Din, 1950.)

along the fresh road cuts, after removing the surface material upto the depth of 6"-12" till more integrated rock material was observed.

Eleven different rock samples, physically distinct in colour, coherence, and particle size, were collected from different sites of the deposit and the surrounding Susalgali granite gneiss during a traverse made along the Battal-Mansehra road. The locations of these sample have been marked on Fig. 1.

CHEMISTRY OF THE SAMPLES

(*a*) Chemical Analyses.

The scheme employed for chemical analyses can be summerised as follows :

(*i*) *Estimation of* SiO_2, TiO_2, Al_2O_3, Fe_2O_3 (*total*), *MnO contents.*

These contents of the selected rock samples have been estimated spectrophotometrically (Shapiro & Brannock, 1956).

(*b*) *Estimation of Na_2 O and K_2 O contents.*

These contents of the above samples have been estimated by the use of a flamephotometer. (Shapiro & Brannock 1956).

(*c*) *Estimation of Ca O and Mg O contents.*

These contents of the above samples have been determined volumetrically by the use of versene reagent (EDTA) in the presence of Murexide and Erichrome Black-T respectively. (Welcher, 1961, Flaschka, 1959).

(*d*) *Estimation of Fe O content.*

The FeO content of the above samples have been estimated volumetrically by the use of standard solution of K Mn O_4, after decomposing the rock powder by HF and H_2 SO_4. (Riley, 1958)

(*e*) *Estimation of P_2 O_5 content.*

The P_2 O_5 content of these rock samples have been estimated colorimetrically after decomposing the rock powder by HF and HNO_3 and producing colour with the help of vanadomolybdate. (Snell, 1949).

The results of the chemical investigations have been given in Table 1.

TABLE 1

Chemical Analyses

Sr. No.			1	2	3	4	5	6
Rock No.*			7880	7881	7882	7883	7884	7885
Wt. Percentage of	SiO_2	..	61.15	61.05	61.28	60.10	59.02	60.42
	TiO_2	..	0.18	0.24	0.11	0.21	0.18	0.15
	Al_2O_3	..	20.57	21.34	24.40	23.24	25.22	24.49
	Fe_2O_3	..	3.30	2.68	2.01	4.31	3.85	3.37
	Fe O	..	1.37	1.23	1.30	0.72	0.75	1.06
	Mn O	..	0.12	0.18	0.06	0.12	0.12	0.18
	Mg O	..	3.80	3.80	2.40	1.80	1.75	1.40
	Ca O	..	1.96	1.96	1.78	2.10	0.70	0.84
	Na_2O	..	2.97	2.68	2.48	2.97	3.19	3.19
	K_2O	..	3.88	4.23	3.29	3.30	4.09	3.35
	P_2O_5	..	0.20	0.20	Tr	Tr.	Tr.	0.10
	H_2O	..	0.78	0.85	0.89	1.08	1.08	1.34
Total :		..	100.28	100.44	100.00	99.95	99.95	99.89

*Numbers correspond to catalogue register.

TABLE I (*continued*)

Sr. No.			7	8	9	10	11
Rock No.			7886	7887	7888	7889	7890
Wt. percentage of	SiO_2	..	55.65	53.53	50.05	54.13	63.93
	TiO_2	..	0.20	0.20	0.15	0.08	0.08
	Al_2O_3	..	27.71	29.85	30.94	30.59	20.47
	Fe_2O_3	..	2.97	4.15	5.25	3.75	3.48
	Fe O	..	1.16	0.38	0.48	0.21	0.28
	Mn O	..	0.19	0.20	0.18	0.12	0.06
	Mg O	..	1.37	0.70	1.03	0.68	2.98
	Ca O	..	0.78	1.26	1.74	0.62	0.68
	Na_2O	..	3.41	4.03	3.31	2.48	2.89
	K_2O	..	4.23	3.39	4.93	6.29	4.21
	P_2O_5	..	0.20	0.20	Tr.	Tr.	Tr.
	H_2O	..	2.05	2.08	1.95	1.25	.095
Total :		..	99.92	99.97	100.01	100.20	100.01

Method of Calculation of Rock Composition.

(*i*) The writer has calculated the rock compositions in terms of their normative mineral molecules. The results have been given in the Table 2. Moreover he has calculated the ratio of residual alumina and residual silica.*

The above chemical investigations clearly reflect upon the fact that the chemical composition of the samples which may be suitable for the production of *clay minerals* is possessed only by the 7, 8, 9 & 10 samples, otherwise the rest of the samples do not possess sufficient proportion of alumina, after satisfying the feldspar constituents, to promote the formation of clay minerals. The results have been graphically represented on the Fig. 2.

(*ii*) In addition, the weight percentages of Al_2O_3, MgO, CaO K_2O, and Na_2O were calculated in terms of gram moles in order to determine the residual character $(Al_2O_3+K_2O/MgO+CaO+Na_2O)$ in each case, (Table 3).

The values as calculated above, clearly show that the residual character or the alteration effect increases progressively as we go inside the deposit. These values have been graphically plotted in Figs. 3 & 4, and it has been found that maximum alteration effect is observed for sample No. 10.

*(The theoretical ratio of Al_2O_3/SiO_2 in case of a clay member of kaolin group having formula $Al_2Si_2O_5(OH)_4$, $2H_2O.Al_2Si_2O_5(OH)_4$ } is = 0.83 (Shand, 1952).

TABLE 2

C.I.P.W. Normative Mineral molecules

Sr. No.			1	2	3	4	5	6
Rock No.			7880	7881	7882	7883	7884	7885
	Q	..	19.20	19.19	26.51	22.93	20.45	25.24
	or	..	22.74	25.19	19.46	19.46	24.46	19.74
	ab		25.20	22.70	21.12	25.20	26.99	26.99
	an	..	9.76	9.76	8.73	10.56	3.61	4.09
	C	..	7.92	8.74	13.49	10.84	14.15	14.10
	hy	..	9.50	9.62	6.65	4.50	4.38	3.50
	mt	..	4.41	4.04	3.04	2.39	2.48	3.43
	hm	..	1.28	—	—	2.69	2.18	1.06
	il	..	—	—	—	—	—	—
	ap	..	—	—	—	—	—	—
Ratio C/Q		..	0.41	0.46	0.51	0.47	0.69	0.56

Sr. No.			7	8	9	10	11
Rock No.			7886	7887	7888	7889	7890
	Q	..	15.68	13.29	6.84	12.12	25.00
	or	..	25.19	20.02	29.08	37.25	25.08
	ab	..	28.93	34.32	27.88	21.12	24.37
	an	..	4.00	6.14	8.53	3.17	3.45
	C	..	16.03	17.23	17.05	18.48	9.86
	hy	..	3.43	1.75	2.58	1.70	7.45
	mt	..	3.67	1.18	1.65	0.72	0.95
	hm	..	0.42	3.39	4.19	3.23	2.78
	il	..	—	—	—	—	—
	ap	..	—	—	—	—	—
Ratio C/Q		..	1.02	1.29	2.49	1.41	0.39

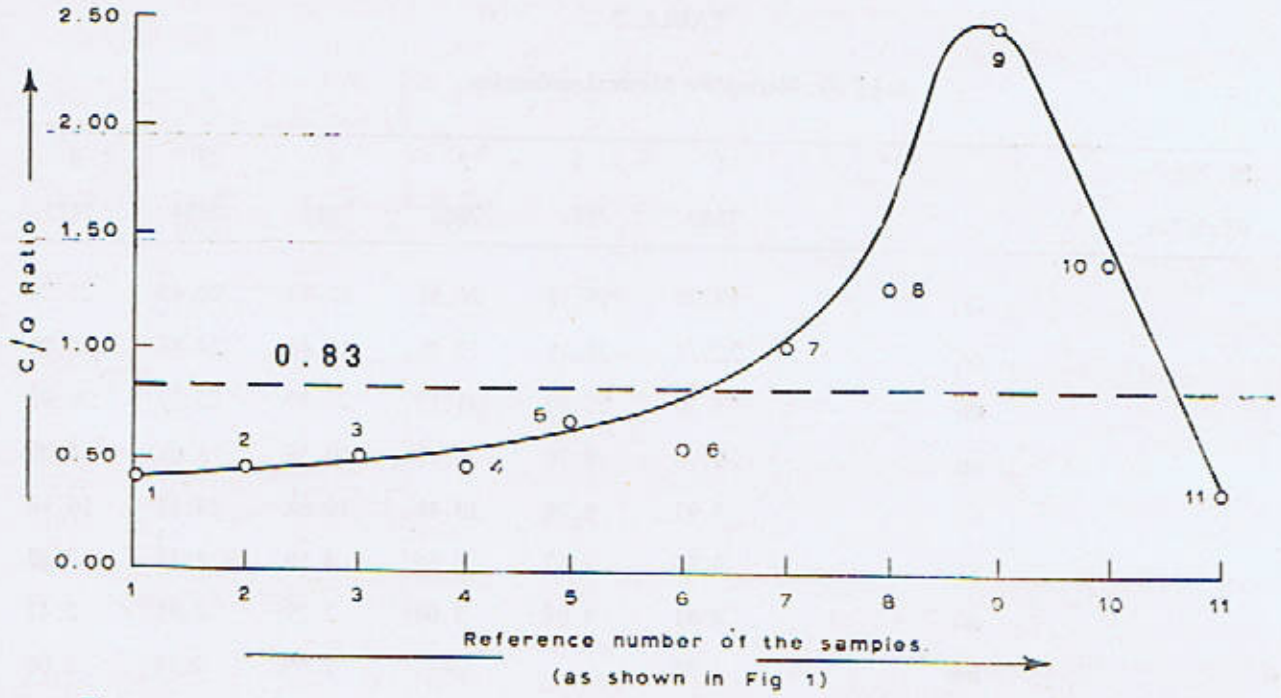

Fig. 2. Curve showing relationship between ratio of normative mineral molecules of Corundum & Quartz (C/Q) and the distribution of different altered granite gneiss samples. Dotted line shows theoratical ratio of C/Q for clay members of Kaolin group. It also shows that the sample Nos. 7, 8, 9 & 10 were capable of producing clay minerals.

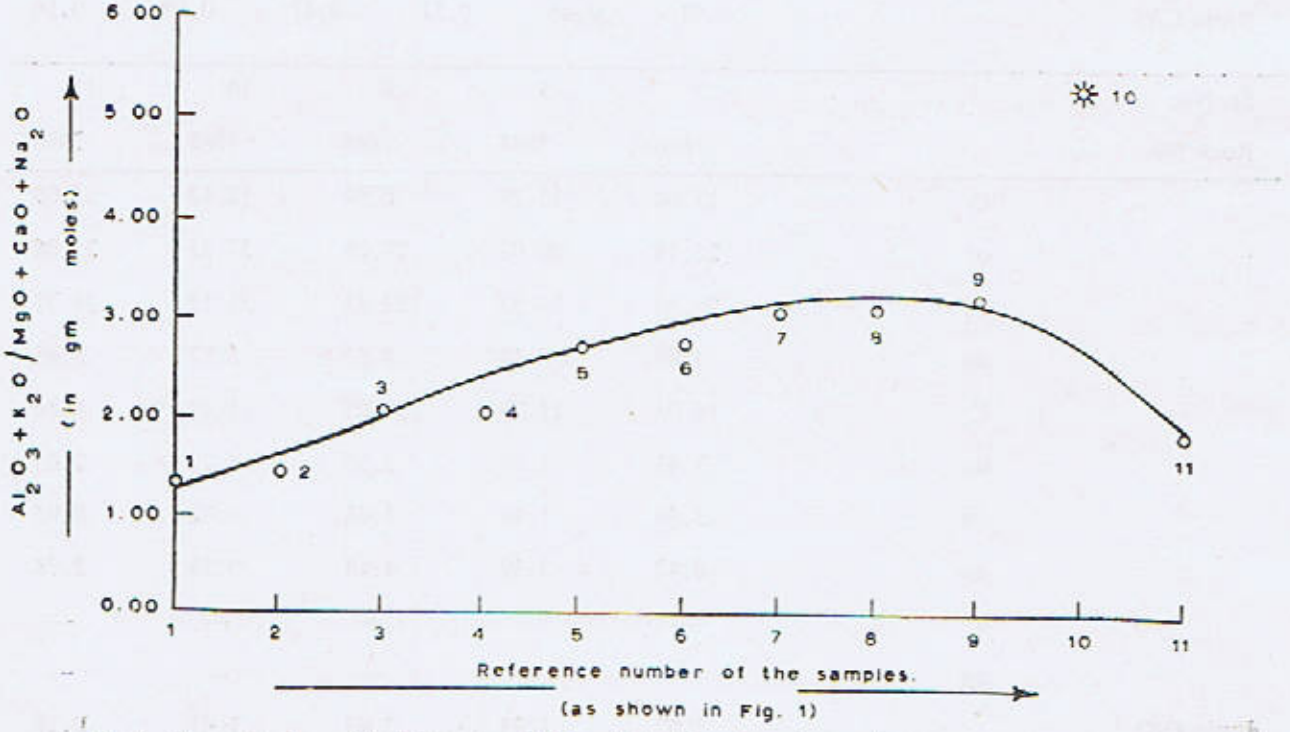

Fig. 3. Curve showing residual character of different altered granite gneiss samples.
*Sample No. 10 has got the maximum value for $Al_2O_3+K_2O/MgO+CaO+Na_2O$ fraction.

TABLE 3

Residual Character

Sr.* No.	Composition in terms of gm. moles Al_2O_3	K_2O	MgO	CaO	Na_2O	Value of residual fraction $Al_2O_3+K_2O/MgO+CaO+Na_2O$	
1.	0.20167	0.0413	0.0950	0.0350	0.0479	0.2430 0.1779	= 1.3659
2.	0.2092	0.0450	0.0950	0.0350	0.0432	0.2542 0.1732	= 1.4677
3.	0.2392	0.0350	0.0600	0.0318	0.0400	0.2742 0.1318	= 2.0804
4.	0.2278	0.0351	0.0450	0.0375	0.0479	0.2629 0.1304	= 2.0161
5.	0.2473	0.0435	0.0437	0.0125	0.0515	0.2908 0.1077	= 2.7001
6.	0.2401	0.0356	0.0350	0.0150	0.0515	0.2757 0.1015	= 2.7163
7.	0.2717	0.0450	0.0342	0.0149	0.0550	0.3167 0.1031	= 3.0718
8.	0.2926	0.0361	0.0175	0.0225	0.0650	0.3287 0.1050	= 3.1305
9.	0.3033	0.0524	0.0256	0.0311	0.0534	0.3557 0.1102	= 3.2278
10.	0.2999	0.0669	0.0170	0.0111	0.0400	0.3668 0.0681	= 5.3862
11.	0.2007	0.0448	0.0745	0.0211	0.0466	0.2455 0.1332	= 1.8431

*The numbers correspond to those of Table No. 1.

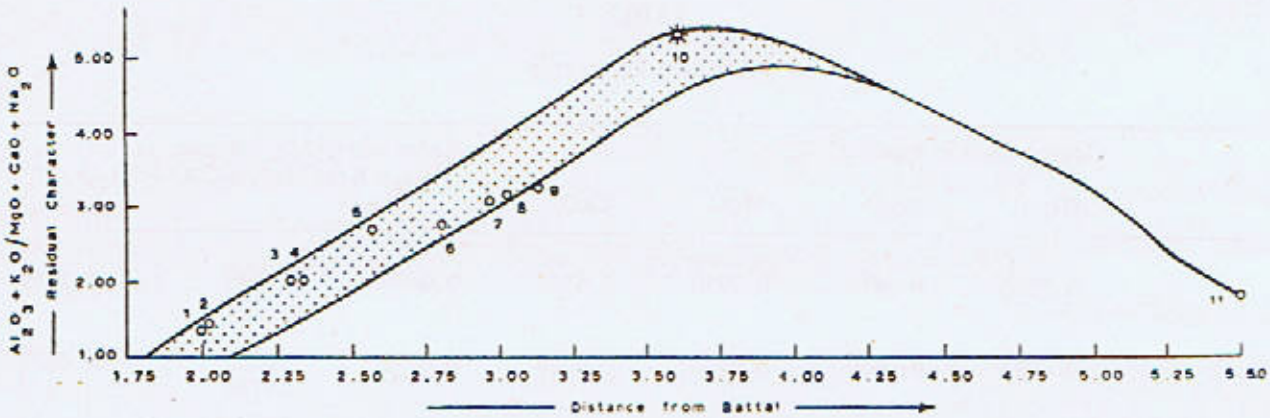

Fig. 4 Diagram showing the residual character of altered zone of the Susalgali granite gneiss near Ahl. The dotted area shows range of residual character.

MICROSCOPIC ANALYSES

The optical examination has shown that the fresh granite gneiss samples essentially consist of alkali feldspars 53 per cent, quartz 20 per cent, plagioclase 15 per cent, and accessories like tourmaline, garnet, and iron ore 4 per cent. Whereas the samples of gray looking, friable material consist of the same mineralogy with the of addition sericite. Their proportions, however, have been found different in different samples. The sericite content is generally present between 3 to 10 per cent of the rock material.

DIFFERENTIAL THERMAL ANALYSES

As by the microscopic examination one cannot be very sure about the absence or presence of clay minerals, therefore the samples were subjected to the differential thermal analysis.

Most of the samples, of comparatively more slicky nature, were investigated by the use of the differential thermal technique. One thermogram (thermal curve) was obtained in each case (Fig. 5) which clearly showed that none of the samples could give any prominent endothermic, exothermic peak characteristic of any of the known clay minerals, however, the rock samples 8, 9 & 10 showed very tiny endothermic peaks in the temperature range between 500 C° to 540 C° (Perkins, 1957). It is, therefore, proved that the clay minerals, if at all they are present, are found in trace amounts. So, most of the friable slick material is something other than clay minerals.

Moreover, it has been observed from the thermograms for rock samples Nos. 7, 8, 9 & 10 that there is a small endothermic peak in the temperature range of 570 C° to 580 C° which indicates the conversion of α-quartz to β-quartz (Grimshaw, et al., 1948).

INFRARED SPECTROPHOTOMETRIC ANALYSES

In order to understand the difference in mineralogy, if there was any, the samples of the surrounding Susalgali granite gneiss and those of the deposit were subjected to infrared spectrophotometric investigations. It has been observed from the various curves (scans) Fig. 6, that the samples of the granite gneiss and those of the gray friable material do not have any difference in mineralogy. From the size of different peaks it is, however, very clear that the relative proportions of different minerals in different samples are different. Moreover it is evident from different peaks that the samples of the friable gray material essentially consist of α-quartz, microcline, micas (biotite,

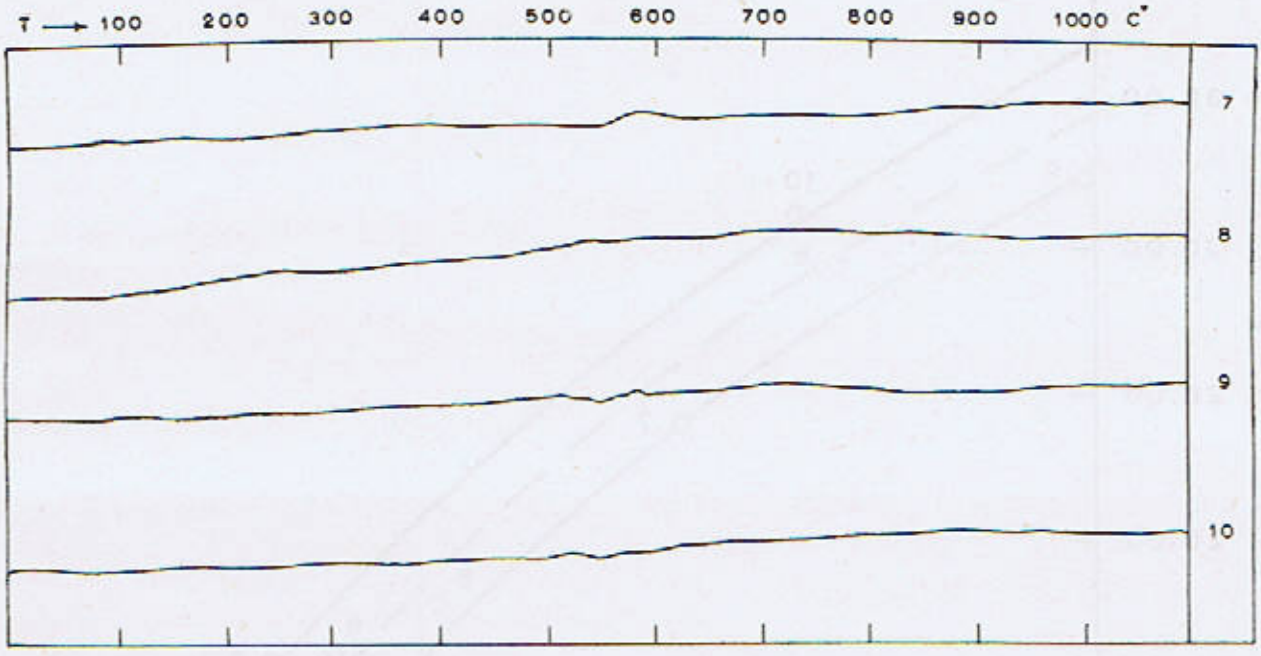

Fig. 5. Differential Thermal curves for different samples of the altered Susalgali Granite Gneiss.

muscovite and sericite), and plagioclase. Garnet is also present in traces.

DISCUSSION:

From the above, I.R.A. and optical investigations, it is clear that there is no difference in the mineralogy of the samples of the friable material and those of the surrounding Susalgali granite gneiss (Fig. 6). Therefore this white looking friable mass is nothing other than the alteration product of the Susalgali granite gneiss.

The physical appearance and the high alumina content of the samples Nos. 7, 8 & 10 are undoubtedly misleading the research workers who may consider it a clay deposit. Normally it can be expected from the rocks with this much high aluminia, to produce sufficient amount of clay minerals. It is clear from Fig. 2, which shows that 7, 8, 9 & 10 were capable of producing clay minerals as their C/Q ratio is above the critical value. Whereas actually it has been proved by D.T.A. investigations that the presence of clay minerals in these samples is not more than traces, as indicated by the very tiny peaks observed in the temperature range between 500 C° and 540 C° (Fig. 5).

X-ray studies (Farooqi and Qureshi, 1966) have also shown that the clay minerals may exist in a small proportion (if any) in the highly friable, slick and gray looking samples only.

The nature of residual character of this part of the Susalgali granite gneiss, which has undergone alteration due to certain reasons, is quite obvious from Figs. 3 & 4 which show that this character goes on increasing as we move from granite gneiss to the altered zone, and the maximum effect is around the location of sample No. 10.

Moreover it is observed (Fig. 7) that Al_2O_3 and SiO_2 behave antipathitic to one another, which means, when Al_2O_3 is increasing SiO_2 is decreasing and *vice versa*.

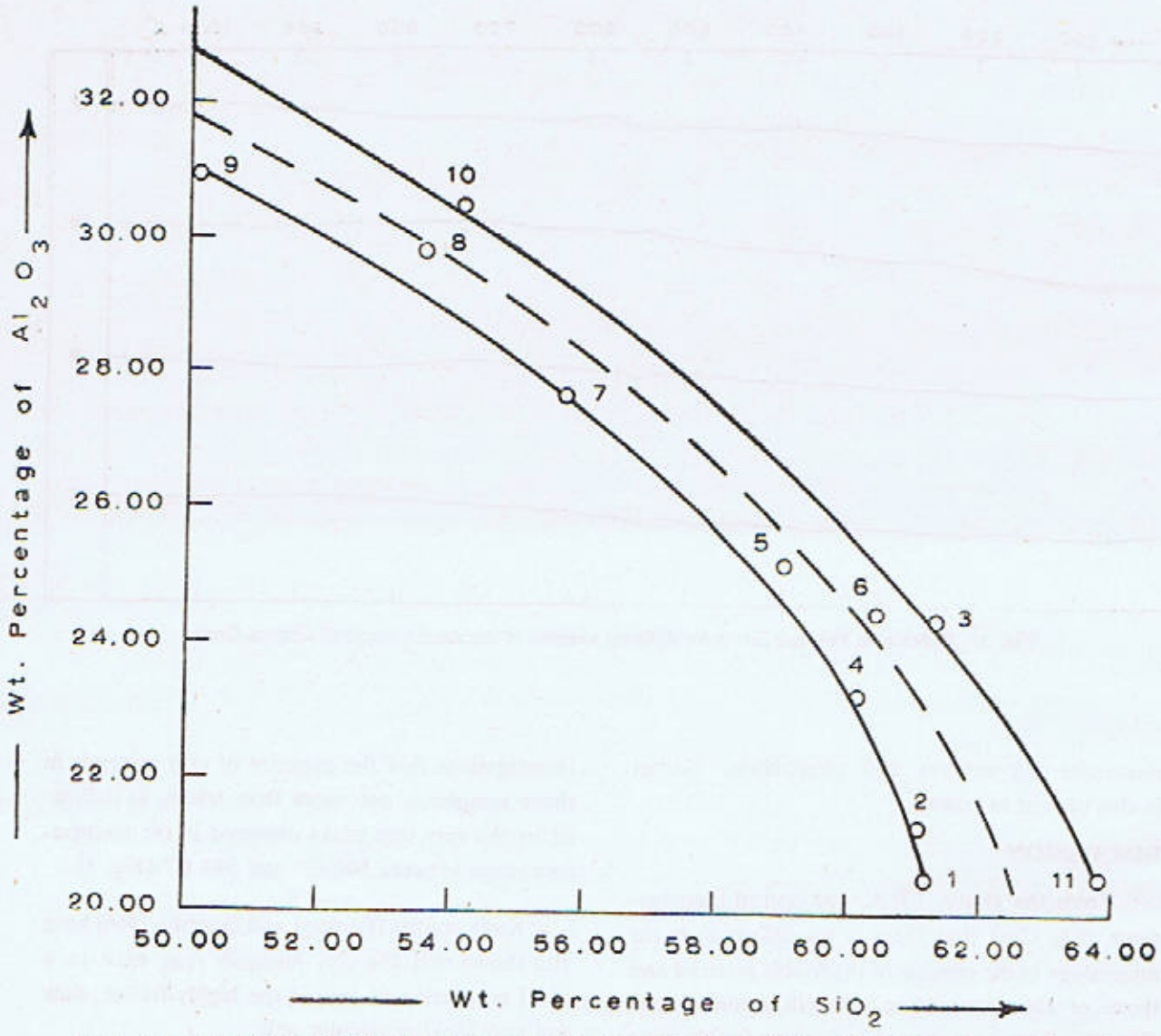

Fig. 7 Varation of Al_2O_3 with respect to SiO_2 in the altered granite zone. Area, within the continuous lines, shows the spread of plots, whereas the broken line shows the deduced variation trend.

CAUSE OF ALTERATION

After knowing that there is no difference in the mineralogy of the surrounding granite gneiss and that of the altered granite product, it is necessary to trace the cause of this alteration.

Normally the alteration of the granite is brought about by either hydrothermal solutions or chemical weathering and in both the cases the alkali feldspars are very apt to undergo alteration but quartz, muscovite, etc. are comparatively more stable. Usually the decomposition products are either (*i*) very fine grained variety of hydromica, called sericite (white mica), or (*ii*) when all the potassium (or Na or Ca) has been consumed, then the residual alumina (after satisfying the composition of feldspars) fulfills the requirements for the production of hydrous silicates of alumina (clay

minerals like kaolinite dickite,, halloysite etc.). Therefore in the present situation either hydrothermal solutions or chemical weathering has been the cause of this alteration of granite gneiss into a soft, friable and white looking slicky mass. It may be possible that. in the past, there might have been a big lake formed by rain on the surrounding high outcrops which could have caused partial alteration of feldspars into sericite (as at present met with) by the continuous chemical action of this accumulated rain water.

However, there is one more possibility for the alteration of this part of the Susalgali granite gneiss. According to Folk (1947) this might have been due to the alkaline solutions associated with metalliferrous ore deposits. This possibility needs confirmation either by drilling through this altered zone or by some indirect method like seismic and gravity survey

CONCLUSIONS

From the above investigations and discussion it may be concluded that this friable white looking slicky mass is nothing other than an alteration product of the surrounding Susalgali granite gneiss, and it is nearly without clay minerals (except for the very small proportions present around the locality of sample No. 10). In future, investigations can be carried out in order to evaluate the speculation regarding this alteration product due to alkaline solutions associated with metalliferrous ore deposit.

ACKNOWLEDGEMENTS

The author in indebted to Prof. F.A. Shams, Head of Geology Department, Punjab University for his invaluable guidance, criticism and encouragement. I am also grateful to Dr. S.F.A. Siddiqui, for his cooperation during field excursion, and laboratory investigations.

REFERENCES

Farooqi, F.A., and Qureshi, H., 1966 Mineralogy of Ahl Kaolinite. *Pak. Jour. Sci. Res.*, **18**, 68-74.

Flaschka, H., 1959 EDTA TITRATIONS. 60-63, 67-69, 100. Methuen and Co. Ltd., London.

Folk, R.L., 1947 The alteration of the feldspar and its products as studied in the laboratory. *Amer. Jour. Sci.*, **245**, 388.

Folk, R.L., 1955 Note on the significance of turbid feldspars. *Amer. Min.*, **40**, 356.

Grimshaw, R.W., Westerman, A., and Roberts, A.L., 1948 A symposium on silica inversions : I. Thermal effects accompanying the inversion of silica. *Trans. Brit. Ceram. Soc.* 47, 269-76.

Mumtazuddin, M., 1950. Unpublished report, Geol. Surv. Pakistan.

Perkins, A.T., and Mitchell, H.L., 1957 Differential thermal analysis of organic compounds. *Trans Kans. Acad. Sci.* **60**, 437. 440.

Rehman, F.U., 1966 The geochemistry of the granites and the associated rocks of the Mansehra Area, district Hazara. Unpublished Ph.D. thesis, Punjab University.

Riley, J.P., 1958 The rapid analysis of Silicate Minerals. *Analytica Chimica Acta*, **19**, 413-428.

Shand, S.J., 1952 ROCKS FOR CHEMISTS, 110. Thomas Murby & Co. London.

Shams, F.A., and Rehman, F.U., 1966 The petrochemistry of the granitic complex of the Mansehra-Amb State. *Journ. Sci. Res., Punjab Univ., Lahore.* **1** (2). 47-55.

Shams, F.A., 1969 Geology of the Mansehra-Amb State area, northwest Pakistan, *Geol. Bull. Punjab Univ.*, **8**, 1-29.

Shapiro, L., and Brannock, W.W., 1956 Rapid analysis of silicate rocks. *U.S. Geol. Surv. Bull.*, 1036-C.

Snell, F.D., and Snell, C.T., 1949 COLORIMETRIC METHODS OF ANALYSIS, D. Van Nostrand Co., Inc., London.

Welcher, F.J., 1961 ANALYTICAL USES OF EDTA. D. Van Nostrand Co. Inc., London, 103-106, 141.

Received December, 1969

APPENDIX I

Index to the analyses given in Table I

Sr. No.	*Cat. No.*	*Rock*	*Map No.*	*Grid Reference*
1.	7880	Gneissic granite	43 F/2	200599
2.	7881	,,	,,	200599
3.	7882	,,	,,	200599
4.	7883	Altered granite	,,	200599
5.	7884	,,	,,	200599
6.	7885	,,	,,	200599
7.	7886	,,	,,	200599
8.	7887	,,	,,	199599
9.	7888	,,	,,	199599
10.	7887	,,	,,	199599
11.	7890	Granite gneiss	,,	195599

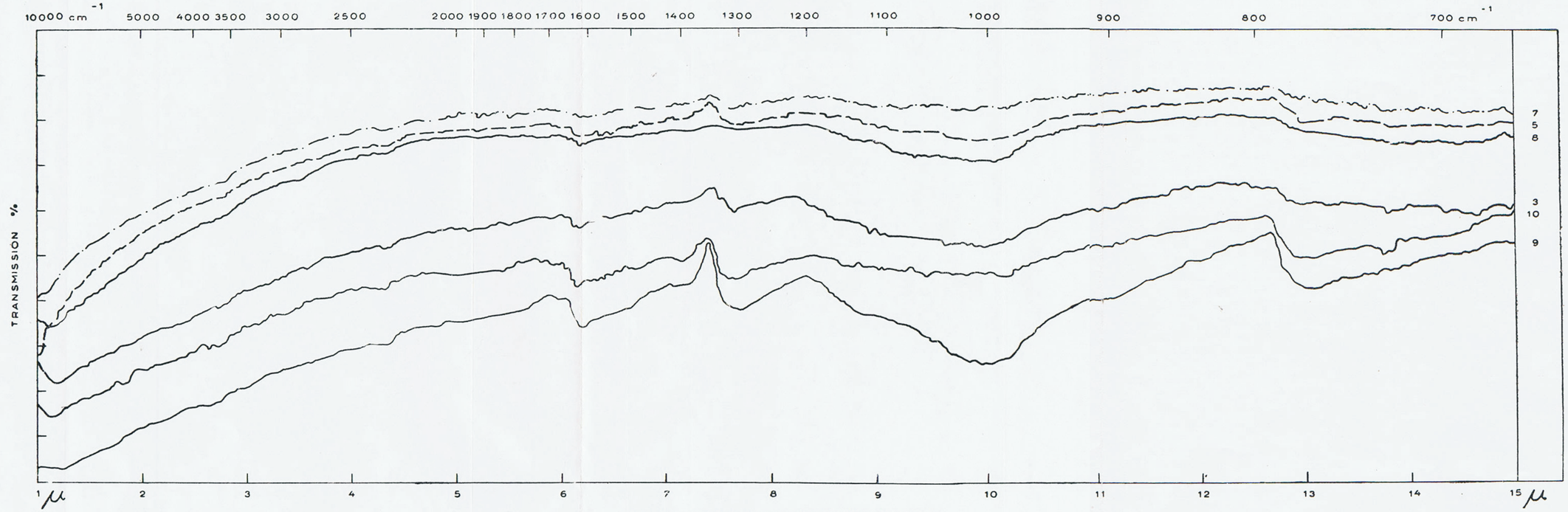

Fig. 6. Infra-red spectra for different samples of altered Susalgali granite gneiss.

RESPONSE OF MAGNETOGRAPHS TO EARTHQUAKES AT THE QUETTA OBSERVATORY, BALUCHISTAN, PAKISTAN

BY

AZIZ-UR-RAHMAN

Geology Department, Punjab University, Lahore

Abstract : *The effects of earthquakes on the Ruska normal-run magnetographs at the Quetta Observatory were studied. The magnitudes of these earthquakes varied from 4 to 7, their depth of foci from 8 to 225 km and their epicentral distances from 22 to 775 km. The earthquakes registered a blurring effect on the magnetograms, which seemed to be mechanical in nature. Due to lack of sensitivity of the instruments, the hypothetical effects due to piezomagnetic and electrical conductivity of the rocks below the observatory could not be detected.*

INTRODUCTION

The Geophysical Observatory at Quetta (Lat. 30° 11.2′N and Long. 66° 57.0′E ; Geomagnetic coordinates: $\phi = 21.6°, \Lambda = 139.7°$ and $\psi = -8.6°$) is situated at a distance of 9.6 km west of the city of Quetta. There is considerable folding and faulting in the area, and the station itself rests on a major fault plane, at an elevation of 1713 meter above mean sea level.

The magnetic variographs—normal-run (20mm/hr) Ruska-type have been housed in a vault in the massive Jurassic limestone, about 60 meter above the foot-hill of northern slopes of the Chiltan mountain range. The mean sensitivities of the variometers, during the period under study, were H, 2.95γ/mm ; Z, 3.55γ/mm and D, 5.0γ/mm or 0.5′/mm.

SEISMOLOGICAL RESPONSE OF MAGNETOGRAPHS

Chapman and Bartels (1940), beside others, have observed the earthquake effects on the magnetograms. The onset times on the magnetograms agreed with the times of arrival of the seismic disturbances. The infra-sensitive seismographic behaviour of magnetographs is such, that the east-west component of the ground movement is recorded by D-, the north-south component by the H- and the vertical ground motion by the Z-variographs.

During the period from 1955 to 1967, fifteen earthquakes, of appreciable intensities, were studied for their effects on the magnetographs located at Quetta. In Table 1, the seismological data are given for nine of these earthquakes, whose epicentres with respect to Quetta are shown in Fig. 1. This selection is based on the fact, that quiet magnetic conditions prevailed at the time of recording these earthquakes, so that the response of the magnetographs was studied on a smooth record of various magnetic elements. The amplitudes of the disturbances, as indicated on the magnetograms, were of the order of 1 to 2 mm. However, due to the blurring of the traces of the magnetograms and poor time resolution, quantitative measurements could not be carried out. The characteristics of a typical earthquake record was a sharp cut-out at the onset

TABLE 1

Earthquakes Recorded on the Magnetographs of Quetta Observatory

S.No.	Date	Arrival Time G.M.T.			Epicentre	△(km)	Region
1.	11-2-55	00	59	95	30.5N, 67.0E	25	Quetta
2.	18-2-55	22	48	33	30.5N, 67.0E	25	Quetta
3.	28-1-64	14	09	17.1	36.5N, 70.9E	775	Hindukush
4.	14-3-65	15	53	06.6	36.3N, 70.7E	730	Hindukush
5.	7-2-66	04	26	13.9	29.8N, 69.7E	250	Barkhan
6.	7-2-66	23	06	34.5	30.2N, 69.8E	250	Loralai
7.	6-6-66	07	46	16.2	36.3N, 71.2E	750	Hindukush
8.	1-8-66	21	02	59.6	30.0N, 68.7E	160	Duki
9.	11-5-67	08	33	14.4	22.4km S-W of Quetta	22.4	Chiltan Hills

TABLE 1 (*Cont.*)

S.No.	Depth of Focus (km)	Average Magnitude	*Intensity (M.M.S.)*		*Recording of Main Shock*			Remarks
			Epi-C	Quetta	D	Z	H	
1.	8—10	5	VI-VII	V	good	nil	good	Recording of H stopped
2.	8	6	VIII	VI-VII	good	good	good	Shift in Z. Recording of D stopped.
3.	207	6.3	VII	I	good	nil	good	H overlaped by base-line.
4.	219	7.5	VIII	III	good	good	good	
5.	33	6.5	VIII-IX	I	good	fair	good	Several after-shocks recorded on D, H.
6.	10	6	VIII-IX	I	good	fair	good	
7.	225	6.5	VII	I	good	nil	good	
8.	33	6.5	IX	V	good	good	good	Shift in H. Recording of D stopped
9.	~15	~4.5	VI	V	good	nil	fair	Shift in D

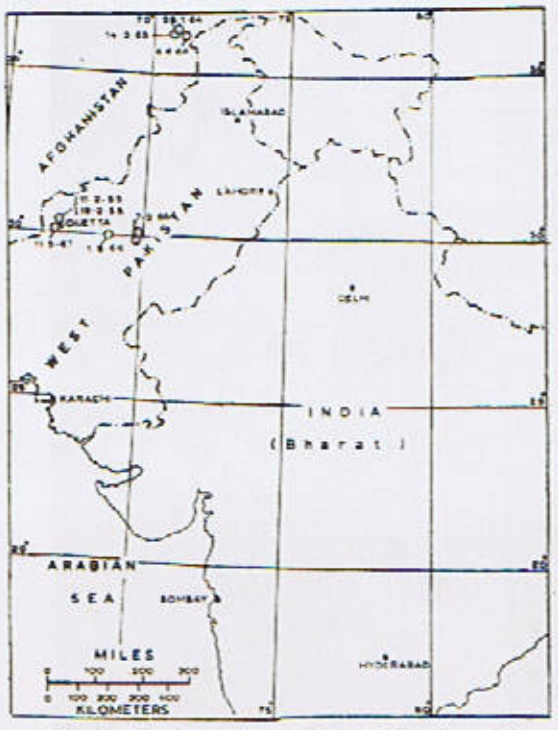

Fig. 1. Location of epicentres of the nine earthquakes and observatories.

time, accompanied by disappearing or blurring of the trace. The blurring was due to the damped oscillations of the magnet system of the magnetograph. The reappearing of the trace, after the blurring, indicated a decrease in the amplitude of the ground motion. However, the duration of the blurring seemed to be a factor related to the sensitivity of the instrument. In certain cases, the Z-trace, unlike H-and D-trace, showed a sharp cut-out on both sides of the blurred gap. Since the Z-variograph was a pivoted instrument, its mechanical oscillations due to ground motion were not expected to be appreciable, as compared to those of H- and D-variographs. Some typical records of H-, D- and Z-traces are shown in Fig. 2.

The relevant portion of the nine magnetograms are reproduced in Figures 3 and 4. The salient features of some of these are discussed below :

Fig. 3 (*a*) Arrival time:11 Feb. 1955 at 00 59 59 GMT.
Description : The recording of H stopped due to the relative displacement of the light source and the mirror, as a result of the shock. This showed, that the motion recorded was translatory, as it was also expected. A lateral shifting of the suspended magnet system has caused the disappearance of the trace. This was contrary to the views ecperessed by Eleman (1966). The light intensity of trace D decreased after the shock, which was again due to shifting of the light source. The earthquake was not recorded on the Z-trace.

Fig. 3 (*b*). Arrival time : 18 Feb. 1955 at 22 48 33 GMT.
Description : The Z-trace was displaced to a lower value by about 10γ. This displacement resulted in a change of sensitivity, brought about by a shift in the magnetic system with

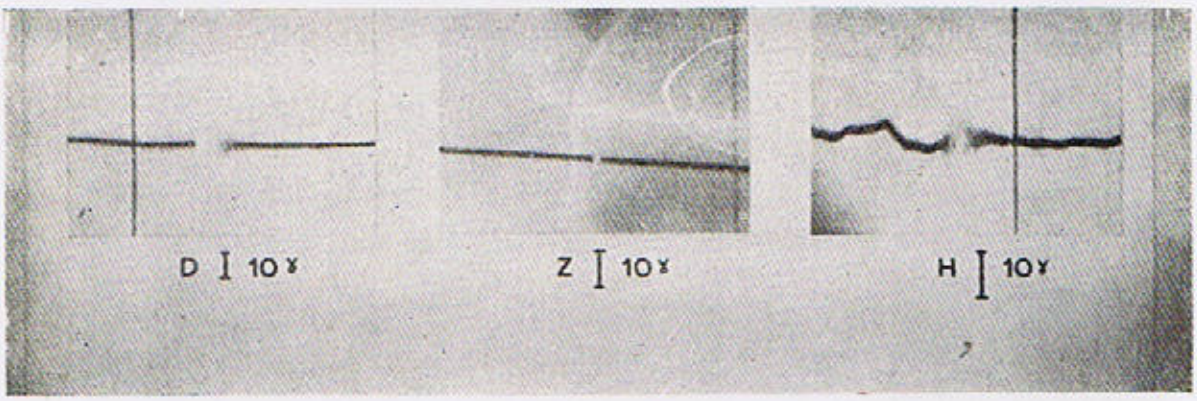

Fig. 2. Some typical, H—, D— and Z— traces of magnetographs during an earthquake at Quetta.

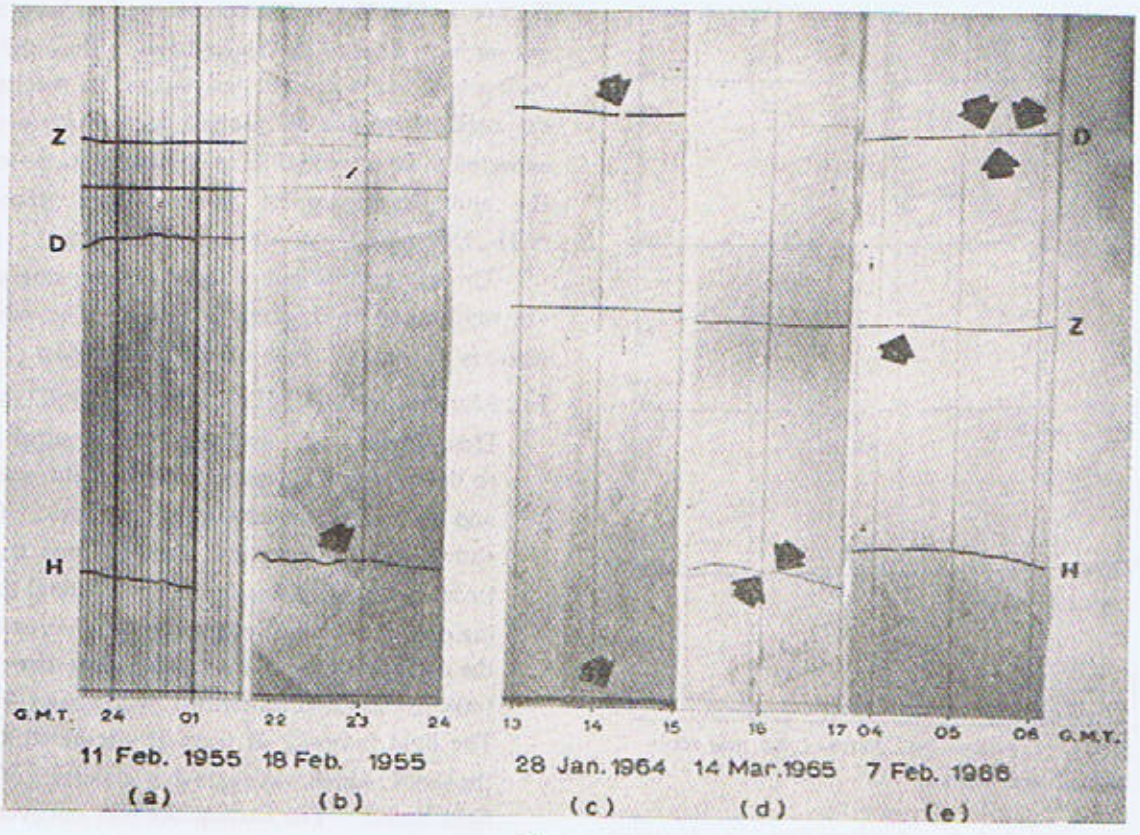

Fig. 3.

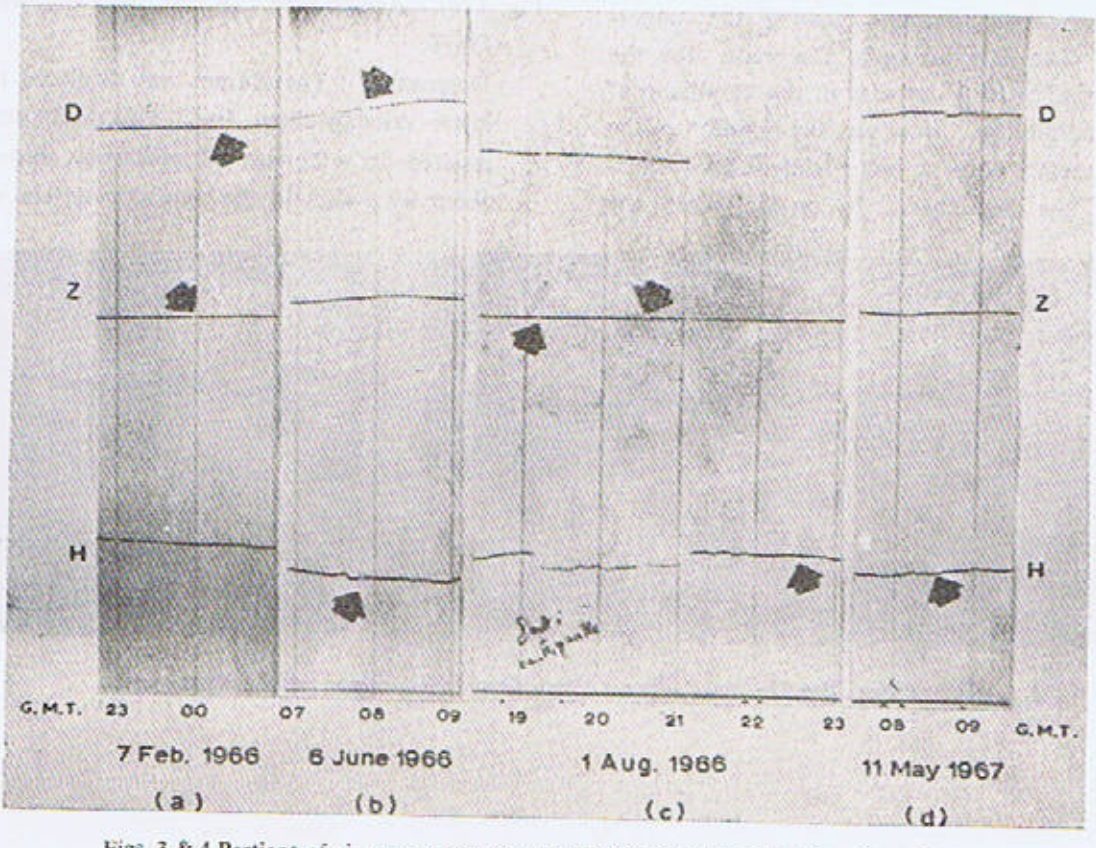

Figs. 3 & 4 Portions of nine magnetograms recorded during a typical earthquake at Quetta.

respect to the auxialary magnet of the Z-variograph. Thus the instrument became so insensitive, that it did not record the after-shocks, which were clearly recorded by the H-variograph. The recording of D-trace had stopped, probably due to shifting of the light source.

Fig. 4 (*b*). Arrival time : 6 June 1966 at 07 46 16.2 GMT.

Description : The main shock was more clearly recorded on D- and H- rather than on Z-trace. The recording on H-trace showed an amplitude of about 2 mm.

This earthquake was also recorded on a La Cour magnetograph, having nearly the same sensitivity as that of the Ruska magnetograph under study, at Hyderabad (India) Magnetic Observatory (Srivastava 1967). The arrival time of this earthquake, at Hyderabad was reported as 07 49 00 GMT. It was interesting to note, that at Hyderabad the quality of record of earthquake on Z-trace was far better that at Quetta, although the sensitivities of the Z-variometers at Quetta and Hyderabad were nearly the same, i.e., 3.55/mm and 3.6γ/mm respectively. Both the magnetograms recorded at Quetta and Hyderabad are reproduced for comparison in Fig. 5.

Fig. 4 (*c*) Arrival time : Aug. 1966 at 21 02 59.6 GMT.

Description : Before the main shock there were two clearly recorded fore-shocks. The fore-shock at 19 10 00 GMT, which was recorded on D-, Z-and H-traces, had shifted the H-trace

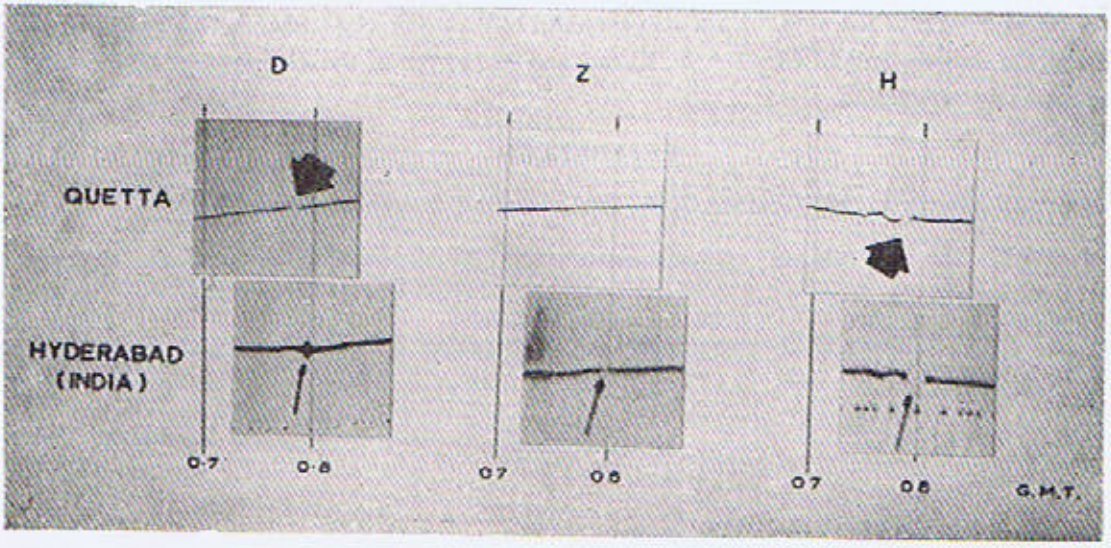

Fig 5. Magnetograms recorded at Quetta and Hyderabad (India).

towards a lower value. This shifting was probably reversed on the arrival of the main shock. The shift in H-trace, which persisted for about two hours, to a value about 12γ higher than the normal, could be explained on the basis of some mechanical disturbance.

CONCLUSIONS

From the above observations it could be concluded that :

1. The magnetic variometers at the Quetta observatory generally record a well marked horizontal component of the earthquake wave. Although the suspended magnet system in the case of D- and H-variougraphs, and the pivoted system of the Z-variograph, have more or less the same type of response, the recording on Z-variograph remained indiscernible in some of the cases.

2. It has not been possible to delineate the piezomagnetic or the electrical conductivity components with a Ruska type of instrument, because of its low sensitivity and its moving magnet systems.

3. As reported by Eleman (1966), that the amplitudes of the records of earthquakes are proportional to the value of Z at the observatory, no verification of this statement could be found by comparing the magnetograms recorded at Quetta and at Hyderabad, due to a Hindukush earthquake of 6 June 1966. The difference in the value of Z at both of these observatories could be judged from the fact, that their Geomagnetic Latitudes differ by 14°. The absence of this evidence could of course be attributed to different geological and surficial conditions at the two observatories.

4. The directional response of the magnetographs has not been found to be systematic. Three of the earthquakes studied, had the locations of their epicentres due east of the observatory (Fig.1). However, the magnetograms showed no difference in the quality of the records of D-and H-variographs.

5. The earthquake intensity (M.M.S.) at Quetta seemed to have a marked effect on the response of the Z-variograph, particularly when the intensity was of the order of I (M.M.S.).

ACKNOWLEDGEMENTS

I am grateful to Mr. K. U. Siddiqui, Director of Geophysical Observatory, Quetta, who permitted me to have an access to the data. I am also thankful to Professor F. A. Shams, Geology Department, University of the Punjab, and to M/s S.A.A. Kazmi and M. Idrees of the Geophysical Observatory for useful comments and discussion.

REFERENCES

Chapman, S., and Bartels, J. 1940 GEOMAGNETISM. Oxford, Clarendon Press, 330.

Eleman, F., 1966 The response of magnetic instruments to earthquake waves. *Jour. Geomag. & Geoelect.* **18** (1), 43.

Srivastava, B.J., 1967 Effects of thunderstorms and earthquakes on the Hyderabad magnetographs. *Ibid.*, **19** (4), 289.

Received December, 1969

A PORTABLE LONG-PERIOD VERTICAL SEISMOMETER

BY

GULZAR AHMAD*

Department of Earth Sciences, University of Leeds, U.K.

Abstract : *A long period vertical seismograph of Galitzin and LaCoste-Romberg type has been described, which can be used in the field for the recording of surface waves of Rayleigh type, generated in quarry blasts.*

INTRODUCTION

In order to record the long-period surface waves of Rayleigh type, generated in quarry blasts, a vertical seismometer is needed, which would register them with sufficient amplification. Until recently, seismometers with eigen frequencies in the range 5-10 c.p.s. have been used for this purpose, since the main interest has been to record the different high frequency phases only.

The following are the characteristics required in a seimometer for observing the surface waves :

(1) It must be reasonably shockproof during transportation in the field in automobiles, etc.

(2) It must be light enough for easy handling in the field.

(3) It should possess a flat amplitude characteristic in the period range 0.5-10 seconds. Also, the amplification should not be so high that the microseismics, lying in this range, may cause distortion of the records. Although the microseismics is dependent upon the area under study, however, their amplitudes are generally of the order of the order of μ.m. (Hardtwig, 1962); therefore the magnification should not exceed 10,000.

(4) The eigen-period as well as the equilibrium position should be more or less constant for at least 1 to 2 hours, so that these may be adjusted in this duration. Since this was not as strict a specification as required for the observatory seismometers, so the simple steel springs might be used to keep the costs low.

In the Institute of Applied Geophysics of the Munich University, such a seismometer, which is described below, was constructed.

PRINCIPLE OF THE INSTRUMENT

General : The Electro-dynamic seismographs consist of three essential parts : seismometer, galvanometer and the recording apparatus. The galvanometer was first used by Galitzin for seismic work and since then the technique has been used more widely. In all the Galitzin seismographs, a coil fixed to the seismometer moves in a permanent magnetic field and the current induced thereby is recorded through the galvanometer.

The astatic system of Galitzin and the La Coste—Romberg modification

In Figure 1 the important parts of the seismometers are shown schematically, m the mass is shown as a solid sphere at the end of an arm of length r. The spring of length l is fixed to a rigid support at B and the moveable part of the seismometer at A. The arms d and r are fixed rigidly to each other and can rotate about a horizontal axis through O. c makes an angle x with the vertical. Helbig (1962) has derived the following expres-

*Dr. Gulzar Ahmad was student of Geology Department, Punjab University, Lahore, 1958—1960.

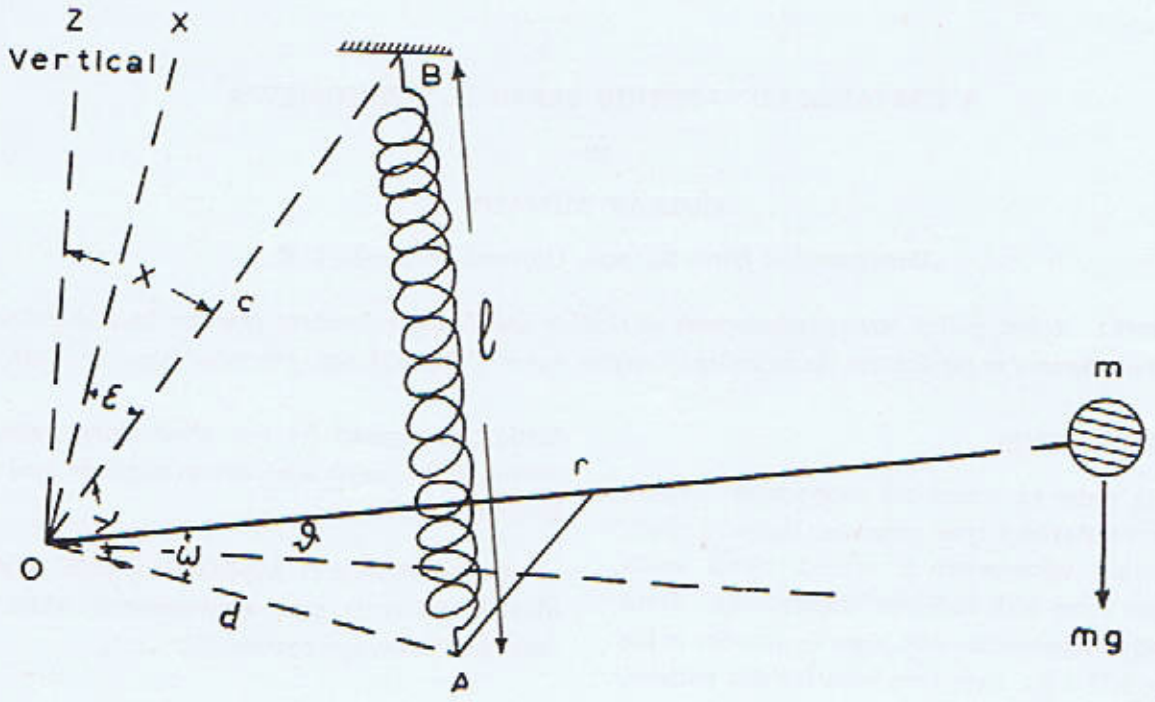

Fig. 1. Schematic diagram of seismometer to show its important parts.

sions for the sensitivity E, defined as the ratio of the change of angle ($d\theta$) to the change of relative gravity acceleration (dg/g), the sensitivity e, defined as the ratio of the linear deflexion of the arm ($p = r\theta$) to the change in absolute gravity acceleration that is dp/dg, eigen frequency ω_o, torque D as :

$$D = m\,g\,r\cos\theta_o - k(l-l_o)\,c\,d\cos\epsilon/l \qquad (1)$$

$$1/E = dg/g.d\theta = \tan\epsilon - \tan\theta_o + c\,d\,l_o\cos\epsilon/(l-l_o)l^2$$

$$= -\tan\xi\,\frac{1+\tan^2\theta_o}{1+\tan\theta_o\tan\xi} + \frac{c\,d\cos\epsilon\,l_o}{(l-l_o)\,l^2} \qquad (2)$$

Since $\omega_o^2 = -\dfrac{dD}{d\theta}/K = -\cos\theta/e = -g\cos\theta/r.E$

therefore $e = \dfrac{\partial D}{\partial g}\Big/\dfrac{(dD).}{d\theta}\dfrac{\partial p}{\partial\theta} = -\dfrac{\partial p.}{\partial\theta}\dfrac{\partial D}{\partial g}\Big/$

$(K.\omega_o^2)$

K = the moment of inertia about the axis through O,

l_o = the initial length of the spring,

k = the spring constant,

and $\epsilon = \theta - \omega + x = \theta - \xi$,

In this seismometer the so called "zero-length-spring", which has been introduced by La Coste in 1934, was used. Since with such a spring $l_o = 0$, the above expressions become :

$$\frac{1}{E} = -\tan\xi\,\frac{1+\tan^2\theta_o}{1+\tan\theta_o\tan\xi} \qquad (2a)$$

$$\omega_o^2 = -g\cos\theta_o(\tan\epsilon - \tan\theta_o)/r \qquad (3a)$$

The expression (2a) showed how the sensitivity of the instrument could be increased : the right-hand-side of this expression must tend to zero.

In order to investigate the influence of the variations in the adjustable part of the system, i.e. c, x, and θ upon the natural period, ω_o^2 is differentiated :

$$K\,\omega_o^2 = -\frac{dD}{d\theta} = m\,g\,r\sin\theta_o - k\,c\,d\sin\epsilon$$

$$-K\,d\omega_o^2 = -m\,g\,r\cos\theta_o\,d\theta_o + k\,c\,d\cos\epsilon\,d\epsilon + k\,d\sin\epsilon\,dc$$

and with $d\epsilon = d\theta_o + dx$,

we get further

$$-K\,d\omega_0^2 = -(m\,g\,r\cos\theta_0 - k\,c\,d\cos\epsilon)\,d\theta_0 + k\,c\,d\cos\epsilon\,dx + k\,d\sin\epsilon\,dc$$
$$= k\,c\,d\cos\epsilon\,dx + k\,d\sin\epsilon\,dc$$

since

$D = O = m\,g\,r\cos\theta_0 - k\,c\,d\cos\epsilon$ in equilibrium. ($l_0 = 0$ here)

$$-K\,d\omega_0^2 = m\,g\,r\cos\theta_0\,dx + k\,d\sin\epsilon\,dc$$

we have further

$$d\omega_0^2 = -8\pi^2\,dT/T^3 \quad \text{and} \quad K = m\,r^2$$

Therefore

$$dT = \frac{g\,T^3\cos\theta_0}{8\,\pi^2\,r}\,dx + \frac{g\,T^3\cos\theta_0}{8\,\pi^2\,rc}\tan\epsilon\,dc \quad (4)$$

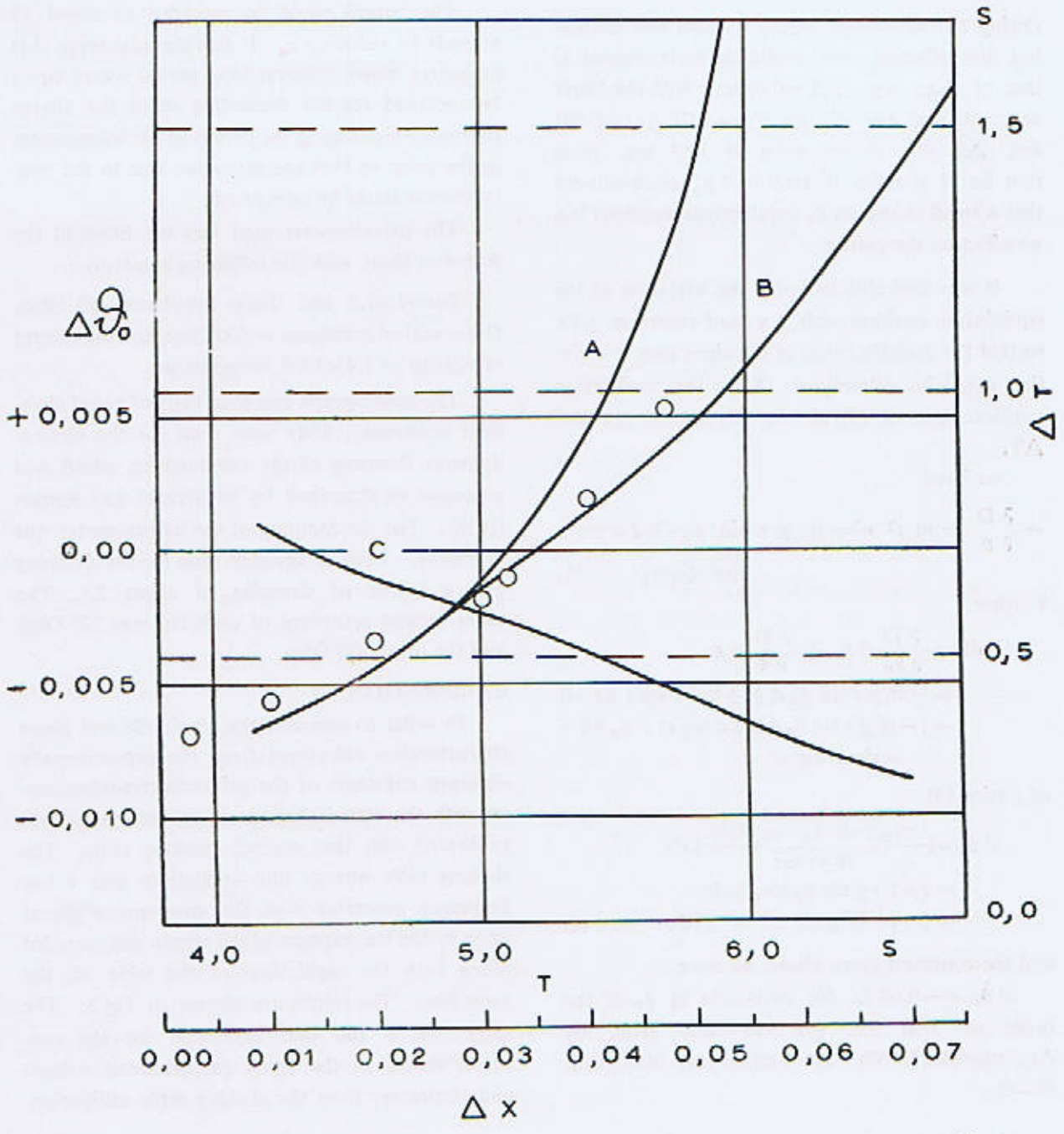

Fig. 2. Curves showing relationship between Δ° and Δx. The coordinate axes belong to the curves after following:—

to A : ΔT and ΔX,

to B : T and ΔT,

to C : ΔT and $\Delta\theta_0$.

(for explanation see text)

Eq. (4) shows the influence of x and c on the change in T. Both of the coefficient depend upon the third power of T. It can be shown that $\triangle T = -0.686$ S For $\triangle x = 0.01$ with the constants of our seismometer, i.e. r≅22.5 cm, T=5, so $\theta_o = 3.4°$. Fig. 2 shows the relation between $\triangle \theta_o$ and $\triangle x$. $\triangle x$ was changed in steps of 0.01.

Owing to the change in$\triangle x$, c would also change, but this influence was negligible as compared to that of $\triangle x$. e.g. $\triangle T = 0.059 \triangle c$ with the above constants and $\epsilon = 5°$; for $\triangle x = 0.01, \triangle c = 0.001$ cm, $\triangle T$ was of the order of 10^{-5} sec. Note that Eq. 4 contains no term in d θ_o which showed that a small change in θ_o (equilibrium position) has no effect on the period.

It was desirable to know the variation of the equilibrium position with $\triangle x$ (and therefore $\triangle T$), so that the possible range of the eigen period variation could be determined. Since the equilibrium position occurs in (4) above, connecting $\triangle x$ and $\triangle T$,

we have

$$-\frac{\partial D}{\partial \theta} = m\ r^2\ \omega^2 = m\ g\ r\ \sin\ \theta_o - k\ d\ c\ \sin\ \epsilon \quad \text{(see above)} \qquad (5)$$

Further

$$dD = \frac{\partial D}{\partial \theta_o} d\theta_o + \frac{\partial D}{\partial \epsilon} d\epsilon$$
$$= -m\ g\ r \sin\theta_o\ d\theta_o + k\ d\ c \sin\epsilon\ d\epsilon = 0$$
$$= (-m\ g\ r \sin\theta_o + k\ d\ c \sin\epsilon)\ d\theta_o + k\ c\ d \sin\epsilon\ dx = 0$$

or , using (5)

$$d\theta_o = \left(\frac{m\ g\ r \sin\theta_o - m\ r^2\omega^2}{m\ r^2\ \omega_o^2}\right) dx$$
$$= (-1 + g \sin\theta_o / r.\omega_o^2)\ dx$$
$$= (-1 + T^2\ g \sin\theta_o / 4\pi^2\ r)\ dx \qquad (6)$$

and the constants given above, we have :

d $\theta_o = -0.64\ dx$, for variations in θ_o of the order of 3°.4. Eq. (6) was also given by Archangelski (1960). He derived (4) also with dc=0.

From (4) and (6) it is obvious that the eigen period could be controlled through x alone. For the calculations of $T - \triangle T$ curve in Fig. 2 (as for $T - \triangle \theta_o$) both of the formulae have been taken into account, since they are coupled with each other. In $T - \triangle T$, $\triangle T$ is the change in T, when $\triangle x$ was varied by 0.01 for a given T.

The period could be extended to about 12 seconds by reducing x. It has the advantage that in quarry blasts different long period waves could be recorded (period depending upon the charge strength) by changing the period of the seismometer in the field, so that the distortion due to the microseismics could be minimised.

The galvanometer used was the EG-6 of the Ruhstrat Firm, with the following constants :

Period=1.5 sec. Inner resistance=60 Ohm, Outer critical resistance = 530 Ohm, and the current sensitivity = 1.4×10^{-8} Amp/mm/m.

The seismograph has four coils of equal electrical resistance. They were used for the electrodynamic damping of the seismometer, which was measured as described by Savarenski and Kirnos (1958). The air damping of the galvanometer was negligible. Each of the coils used for the damping gave a degree of damping of about 2.6. The outer critical resistance of each coil was 320 Ohm and the inner 200 Ohm.

CALIBRATION

In order to compare the amplitude and phase characteristics calculated from the experimentally obtained constants of the galvanometer-seismometer with the actual characteristics, the system was calibrated with the vertical shaking table. The shaking table was set into oscillations with a low frequency generator with the seismometer placed upon it, and the response of the system was recorded along with the oscillations of the table on the same film. The results are shown in Fig 3. The solid line is the one calculated for the constants shown in the figure (experimental values) and circles are from the shaking table calibration.

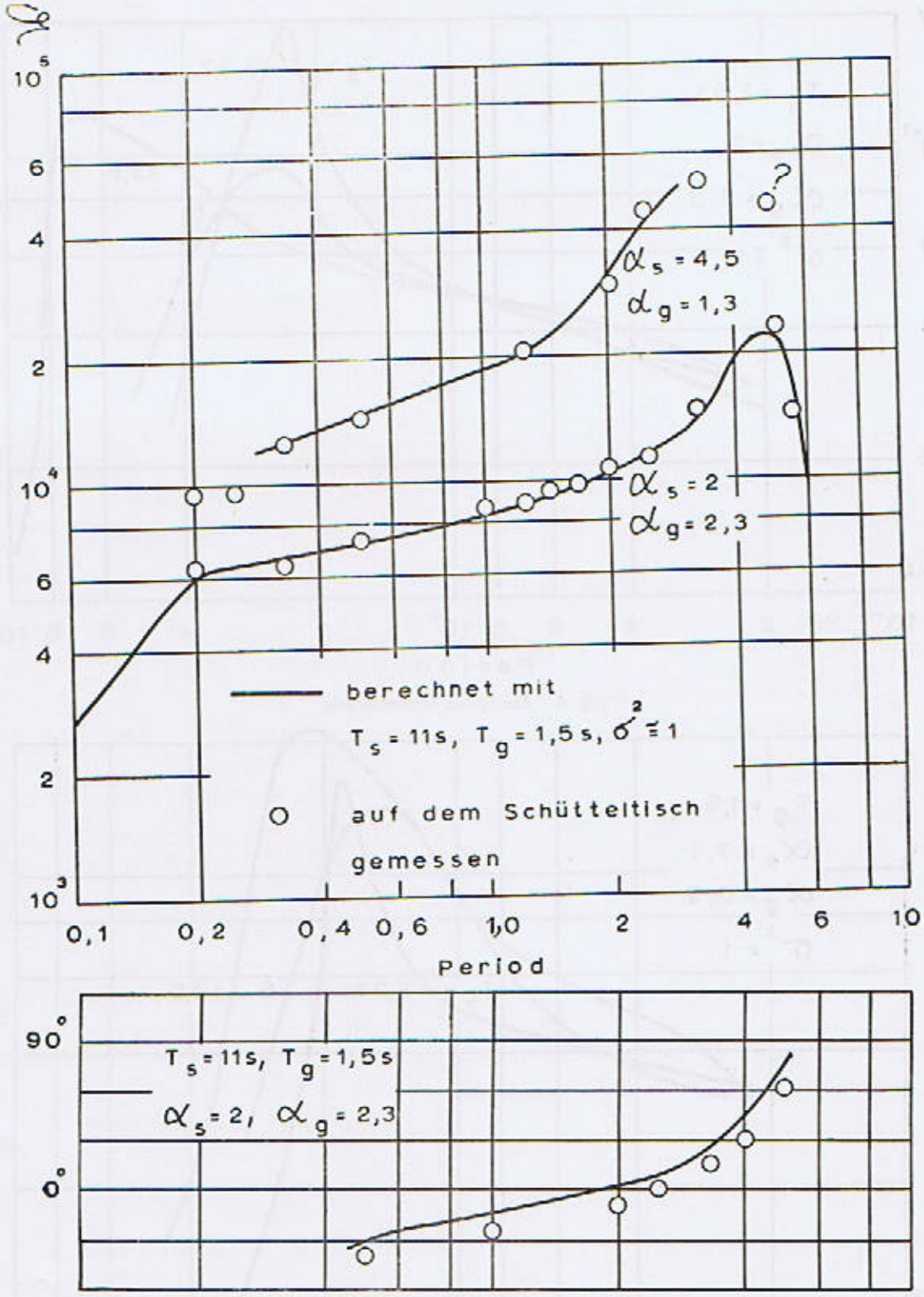

Fig. 3. Amplitude and phase characteristics calibration on the vertical shake table (berechnet mit=calculated from, auf dem Schutteltisch gemessen=measured on the shake table)

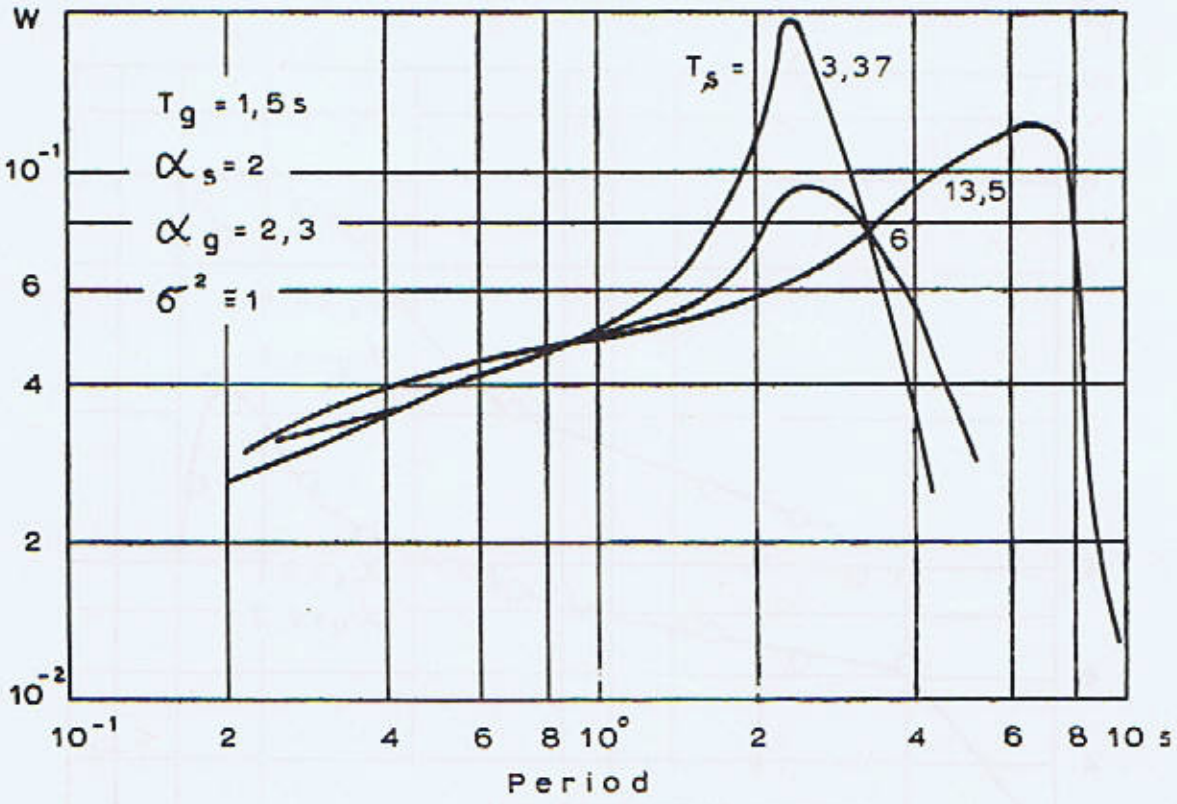

Fig. 4. Amplitude Characteristic

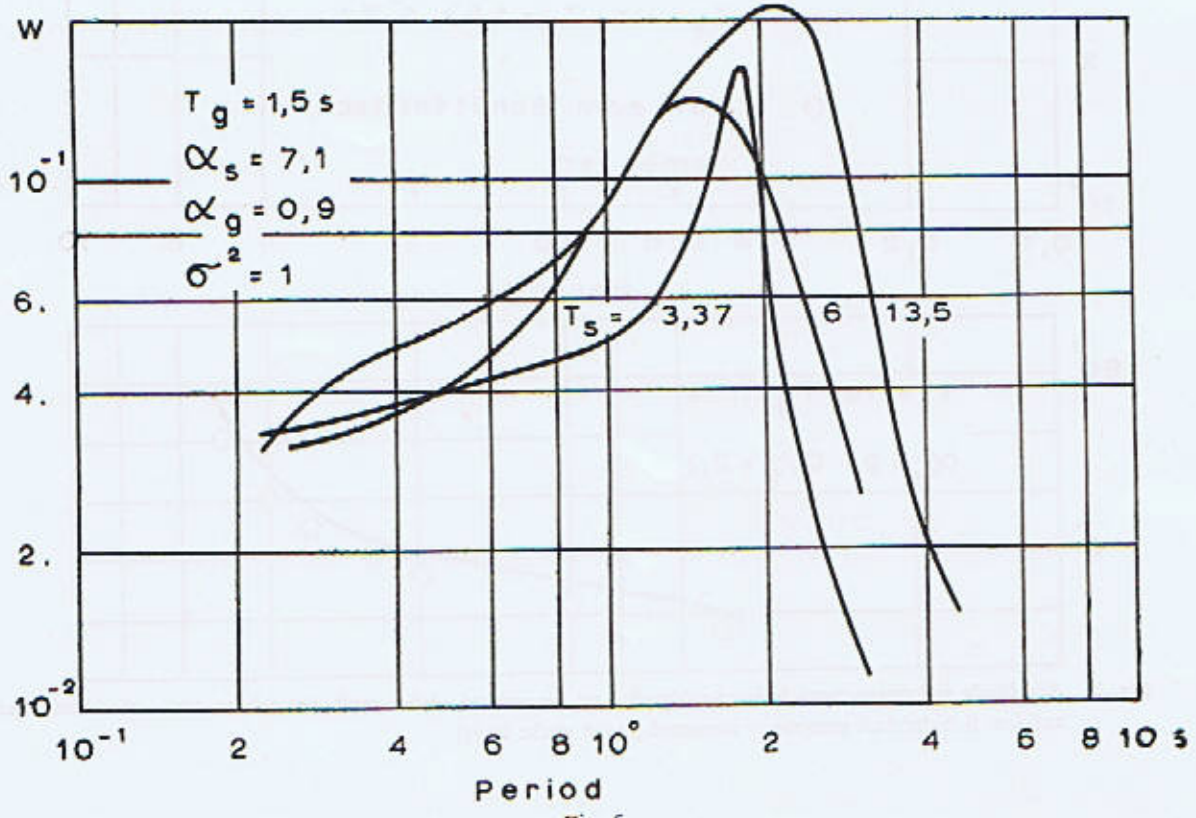

Fig. 5

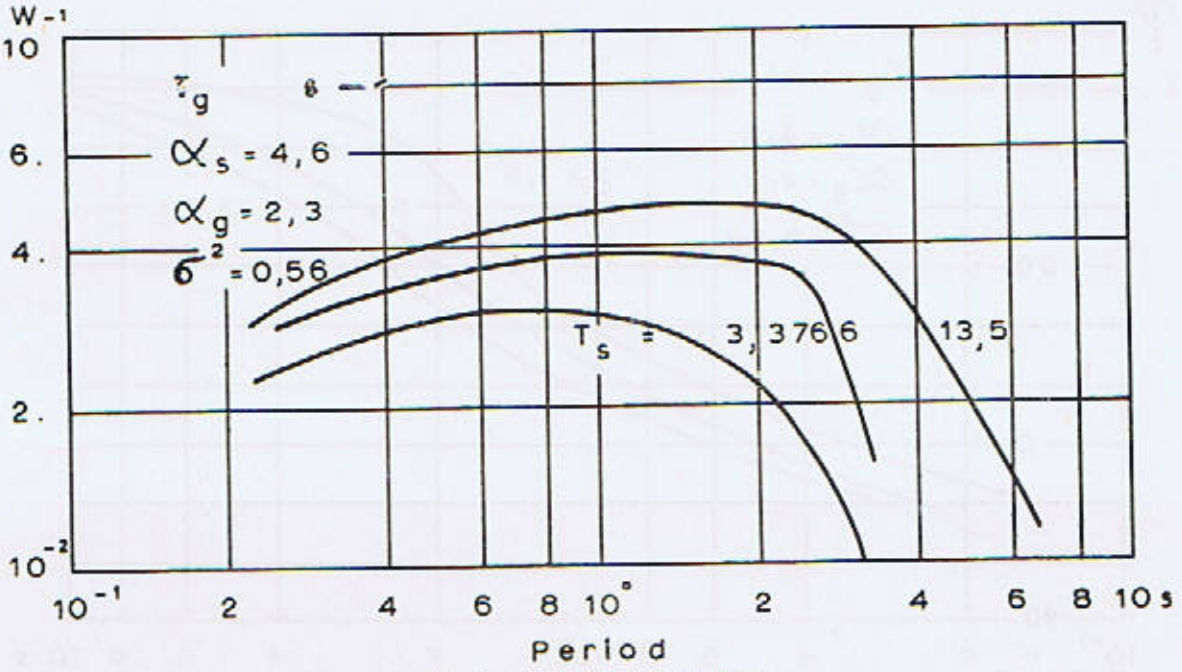

Fig. 6. Amplitude characteristic.

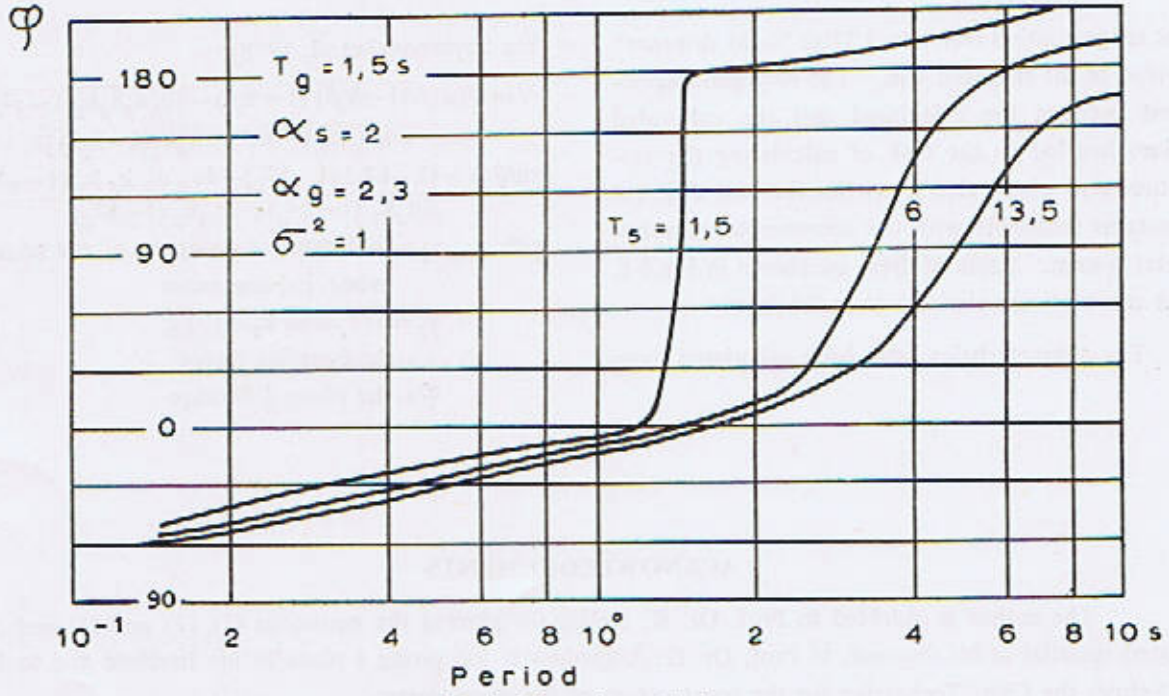

Fig. 7. Phase characteristic

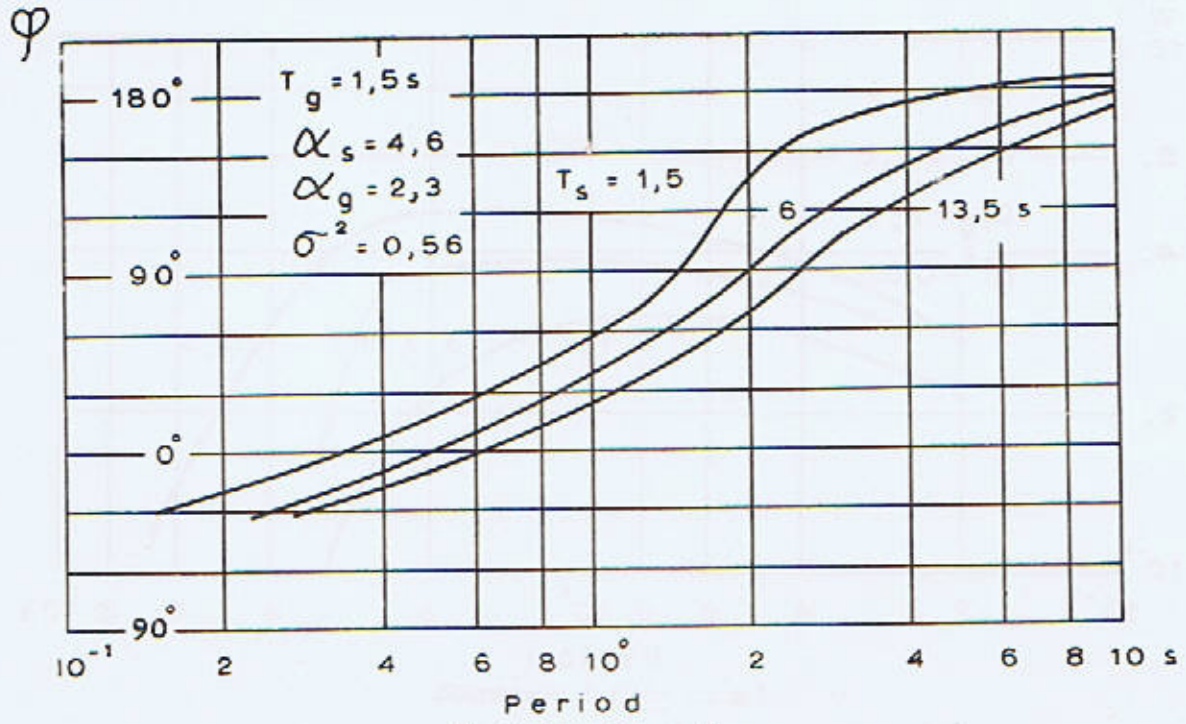

Fig. 8. Phase characteristic

The magnification refers to 2.37 m "light distance" instead of the standard 1 m. The very good agreement between the calculated and the calibrated values has led to the task of calculating the amplitude and phase characteristics for the different constants realisable with the seismometer-galvanometer system. Some of them are shown in Fig.4-8. The constants are also shown in the figures.

The characteristics have been calculated from (See Savarenski et al. 1958):

$$V = 1/(\omega\sqrt{(1-k_g^2)(1-k_s^2)-4\alpha_g\alpha_s k_g k_s(1-\sigma^2)})^2 + 4(\alpha_g k_s(1-k_g^2)+\alpha_s k_g(1-k_s^2))^2$$

$$\tan\varphi = -\frac{(1-k^2{}_s)(1-k^2{}_g)-4\alpha_s\alpha_g k_s k_g(1-\sigma^2)}{2\alpha_s k_g(1-k^2{}_s)+2\alpha_g k_s(1-k^2{}_g)}$$

with α_s, α_g = th degree of damping of the seismometer, galvanometer

$k_s = T/T_s$ and $k_g = T/T_g$,

σ = the coupling factor

φ = the phase difference

ACKNOWLEDGEMENTS

The author is indebted to Prof. Dr. K. Helbig for placing the equations (1), (2) and (3) and the related material at his disposal, to Prof. Dr. G. Angenheister for giving a place in his Institute and to Mr. L. Lehner the Chief Technician for the construction of the seismometer.

REFERENCES

Archangelski, V.T., 1960 Questions concerning the theory of the long period vertical Seismometer. *Bull. Izw. Acad. Sce. USSR*, 955-960.

Hardtwig, E. 1962 THEORIEN ZUR MIKROSEISMISCHEN BODENUNRUHE, *Akad. Verlag Leipzig.*

Helbig, K. 1962 Personal communication.

Savarenski, E.F., and Kirnos, D.P. 1958 ELEMENTE DER SEISMOLOGIE UND SEISMOMETRIE. *Akad. Verlag. Berlin*

Received January, 1970.

MINERALOGY OF SERPENTINITE FROM TLERI MUHAMMAD JAN AREA, NORTH OF HINDUBAGH, ZHOB DISTRICT, BALUCHISTAN, PAKISTAN

BY

MUHAMMAD ASHRAF, M. WAHEED QURESHI and F.A. FARUQI

Glass & Ceramics Division, P.C.S.I.R. Laboratories, Lahore

Abstract : *Serpentine samples were collected from serpentinite of Tleri Muhammad Jan Area. The serpentine mineralogy was studied by chemical, optical, static dehydration, differential thermal (D.T.A.) and X-ray diffraction analyses. The data obtained are discussed and the mineralogy of the serpentine group explained. The serpentinite has been found to consist of chrysotile, antigorite, lizardite and accessories as chromite, carbonates, talc and magnetite.*

INTRODUCTION

The purpose of this investigation was to determine the mineralogy of serpentine minerals occuring in the host rocks. The samples are so fine-grained that it is practically impossible to separate fibres of chrysotile from an antigorite matrix. The rocks are however massive. brittle or sheared. Chemical analysis, D.A.T. X-ray diffraction and static dehydration methods are applied to three representative samples of the above in order to compare and correlate the minerals of the serpentine group present in different samples of Tleri Muhammad Jan serpentinites (Ashraf, 1966).

OCCURRENCE

The samples are taken from a long and narrow ultrabasic body whose outcrops strike in an east west direction, along the northern flank of the Zhob valley. The serpentinized body is traversed by three streams namely the Malguzar, the Shakh and the Ragha in the vicinity of Tleri Muhammad Jan village. The ultrabasic rocks i.e., dunite, harzburgite and peridotite are thoroughly serpentinized. The contact of ultrabasic body with country rocks is quite sharp. There is no metamorphism of great significance except shearing and granulation along the fault planes where breccia of siderite-talc-serpentine composition and granulation on talc are observed. The chromite occurs as dense black lenses of sachhoroidal grains. Harzburgite and pyroxenite occur as dykes with chilled margins in both the cases. Even xenolith of dunite-serpentine was observed in harzburgite serpentine in the Shakh stream. The dykes of harzburgite are not wider than fifty feet and are enough in length to cover all the three streams accross. Pyroxenite dyke is only exposed in the Malguzar stream where it shows very coarse grains of pyroxene. The width of the serpentinite outcrop in this area ranges

from 400 to 850 yards. Although the rocks are mainly composed of serpentine minerals, the presence of relict grains of pyroxene and olivine gives some clue to the identity of the original ultrabasic rocks. These indicate that dunite, harzburgite and peridotite were the original rock types. These are intruded by dolerite dykes. Serpentine derived from dunite can be easily recognized in the field by the absence of bronze colour orthopyroxene crystals in it.

The present study has been carried out only on samples of serpentine derived from dunite.

PETROGRAPHY

In hand-specimens the rock is generally light to dark green in colour with a fine-grained texture. The rock is either very sheared or massive. The sheared material (S-1)* is sometimes powdery and contains minor amounts of dolomite, magnesite, talc and chromite. The non-sheared (S-2, S-3)* serpentinite also has traces of magnesite, dolomite and talc. The mineralogy of the rock is difficult to ascertain in hand specimens as antigorite and chrysotile are not easily distinguishable. In some cases chrysotile can be detected when it occurs in coarse veinlets.

Under the microscope the rock consists of almost colourless, bluish-grey, pale-green to greenish serpentine minerals with minor amount of accessories.

Chrysotile

Fibrous chrysotile occurs in veinlets as cross-fibres. Chrysotile in most cases is colourless ; it sometimes shows anomalous bluish interference colours, which may be due to increase of iron in the structure. Moreover the arrangement of chrysotile veinlets in most rocks is more or less of a mesh structure forming parallelograms and rectangles. In this type of mesh structure a network of longitudinally divided corss-fibre veins enclose an area of isotropic or nearly isotropic materials. The corss-fibre chrysotile grows in typical sinuous cross-cutting veinlets. Under high magnification the meshes are composed of bipartite rims or collars of cross-fibre alpha serpentine and isotropic cores of gamma serpentine. The gamma serpentine is often in matted growth leading to isotropism of the aggregates. In the sheared samples like S-1, a distinctly new foliation is observed, where dominant collars cut across the subordinate and the gamma serpentine fibres of the core are arranged normal to the shearing. This sort of shearing has made a part of the serpentine body as serpentine schist. Moreover S-1 is evidently almost notihng but chrysotile serpentine, as shown by other experimental procedures, because strong shearing does not favour the formation of antigorite.

Antigorite

Antigorite is colourless to pale green in thin sections. It occurs as very fine-grained plates which are mostly anhederal in form. It shows a ramifying sort of network arrangement with other serpentine minerals. In some thin sections however, transition from mesh serpentine has been observed on occasion while in others it is observed that with the mesh structure some coareser grains have also developed. According to Francis (1956) antigorite has replaced mesh serpentine at Glen Urquhart (Scotland), where shearaing stress generally accompanied antigorite formation. This does not apply in the case of highly sheared sample S-1, as has been confirmed by other tests ; this sample is much richer in chrysotile and has only subordinate antigorite as compared to S-2 and S-3. The latter are brittle and massive samples, and show somewhat higher antigorite contents. The role of chemical environments as suggested by Hess *et al.* (1952) appears very likely ; that olivine yields chrysotile, and enstatile yields antigorite.

*(S-1), (S-2) and (S-3) are field numbers of specimens.

Serpophite

It occurs in some sections as isotropic or nearly isotropic material formed in the core of chrysotile veinlet mesh. It is usually colourless and shows very weak interference colours. This could be an amorphous mineraloid of serpentine, olivine or enstatite (Deer *et al.* 1962). It is also observed that sometimes the core of a mesh structure is full of ore dust ; probably chromiferous (Francis 1956).

Bastite

It occurs as medium to coarse grained with subhedral and euhedral forms. Due to the preservation of original cleavages, straight extinction is clearly shown by the pseudomorphs. It exhibits grey interference colours of the first order. Multiple twinning is very common in most pseudomorphs. According to Francis (1962) Pseudomorphism is along (010) parting of the orthopyroxene which according to Winchell (1951) is now (001) cleavage of bastite, which is clearly evident due to the very low interference colours of bastite.

Accessories

Minor amounts of the other recognizable minerals are : chromite, dolomite, magnetite and traces of magnesite, and talc. Chromite usually occurs as reddish brown, fine to medium grained anhederal crystals, which sometimes show rings of magnetite around a few grains. Some grains of chromite show nodules of serpentine in them. Magnetite occurs either as individual grains or as dust. Dolomite usually occurs in very fine to medium veinlets and also as scattered grains.

CHEMICAL COMPOSITION

The chemical analysis was made on the three types of samples. SiO_2 and Al_2O_3 were determined in accordance with standard silicate analysis method. CaO and MgO were determined by E.D.T.A. method. Fe_2O_3 was determined colorimetrically using EEL colorimeter by ammonical thioglycollic acid method. FeO, MnO and Cr_2O_3 were determined by Siel's, sodium bismuthate and sodium peroxide methods respectively. CO_2 was determined with the help of calcimeter. H_2O was found out after substracting the amount of $-H_2O$ at 110°C and CO_2 from loss on ignition.

The percentage chemical composition of the different samples is listed in Table 1. Microscopic identification revealed that the three samples are natural mixtures of chrysotile, antigorite, chromite, dolomite, magnetite etc. Where mostly magnetite and chromite are present in extremely fine grained as well as dusty cloud and are hardly separable. The coarser grains of magnetite, chromite and dolomite were separated anyhow by manual method, under the microscope. Consequently the respective samples could not be thoroughly purified. Anyhow a purity of about 99% was achieved.

Due to the identical chemical composition of serpentines, it is understood that all serpentine group minerals are of polymorphic forms, though some small chemical differences are associated with each variety. On the basis of this difference all the polymorphs can be differentiated. It has been suggested by Deer *et. al.* (1962) that antigorite contains higher trivalent (Al) ion content than chrysotile but not always. Lizardite is also expected to have high Al content. Therefore, from the analyses it could be judged that S-3, S-2 and S-1 have some amount of Al in decreasing order and therefore, contain some antigorite and possible lizardite as well.

DIFFERENTIAL THERMAL ANALYSIS

For the determination of differential thermal properties samples were heated from room temperature to 1000°C at a rate of 200°C per hour.

The D.T.A. curves are plotted in Figs. 1, 2 & 3. In Fig. 1 and 3 the small exothermic and endothermic peaks in the curves upto 600°C are due to the minor accessories present in the raw samples. After about 600°C the peaks are very prominent.

TABLE—I

Chemical Analyses

No.		S-1	S-2	S-3	*Serpentine* Glen Urquhart	Chrysotile Quebac	Antigorite New Zealand
SiO_2	..	35.20	38.81	37.18	37.53	41.97	43.45
Al_2O_3	..	1.04	1.90	3.25	0.72	0.10	0.81
TiO_2	..	n.d	n.d	n.d	0.09	—	0.02
Fe_2O_3	..	2.95	2.13	1.78	5.12	0.38	0.88
FeO	..	1.88	0.33	0.54	1.78	1.57	0.69
Cr_2O_3	..	0.83	0.20	0.59	0.33	—	n.d
CaO	..	0.21	0.13	0.19	1.32	—	0.04
MgO	..	39.57	40.59	41.18	37.99	42.50	41.90
MnO	..	0.04	0.03	trees	0.17	—	—
H_2O	..	16.87	14.80	14.31	11.75	13.56	12.29
H_2O^-	..	0.51	0.11	0.44	0.68	—	0.00
CO_2	..	0.03	0.02	0.03	2.04	—	—
	..	99.13	99.05	99.49	99.52	100.08	100.12

Number of ions on the basis of 18 (O, OH)

Si	..	3.578	3.50	3.584	—	3.886	4.044
Al	..	0.140	0.216	0.368	—	0.001	—
Fe^{+3}	..	0.230	0.152	0.127	—	0.014	—
		3.948	3.868	4.079		3.901	4.044
Mg	..	5.976	5.874	5.957	—	5.864	5.810
Fe^{+2}	..	0.017	0.026	0.043	—	0.122	0.054
Mn	..	0.002	0.002	—	—	—	—
CaO	..	0.026	0.014	0.107	—	—	0.004
Al	..	—	—	—	—	—	0.088
Fe^{+3}	..	—	—	—	—	—	0.060
Cr	..	0.015	0.015	0.046	—	—	—
(OH)	..	8.000	8.000	8.000	—	8.188	7.628
		6.036	5.931	6.153		5.986	6.016

The mineral analysis has been recalculated following Faust's method (1956).

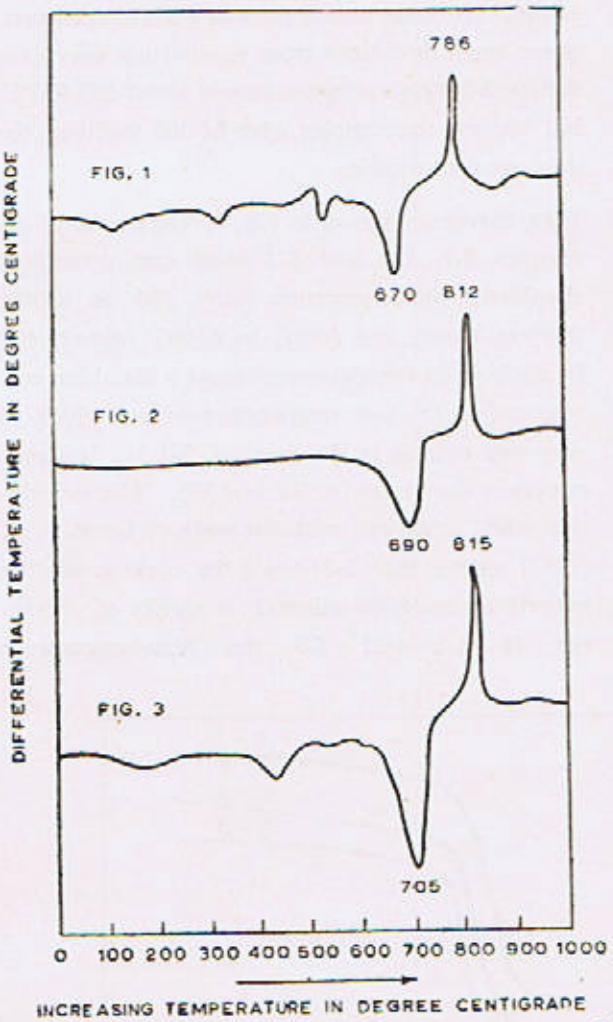

Figs. 1,2,3. Differential thermal analysis curves of Serpentine S-1, S-2 & S-3.

The curves begin their descent with minimum at 670°, 680°, and 705°C respectively. These endothermic peaks are produced on the expulsion of chemically bonded water in serpentine. These peaks are narrower and deeper in samples S-1 and S-3 than S-2. At the end of endothermic reaction the curves return to the baseline at about 680°, 720° and 725°C respectively, and continue along until 770°, 780° and 815°C respectively where an exothermic reaction begins and reaches a maximum at temperatures 786°, 812° and 815°C respectively. Subsequently the curves first drop steeply and then remain above the baseline upto 1000°C.

A detailed analysis of the three curves has been carried out according to the procedure followed by Faust *et al.* (1962). In the temperature range 85°, to 200°C Figs. 1 and 3 show shallow troughs at about 120° and 150°C which indicates a loss of uncombined water (H_2O). According to Gheith (1952) the endotherms between 200°-600°C are mostly due to the presence of chromite and the exotherms are due to oxidation of magnetite to maghemite, while Pabst (1952) and others called it incandescence in serpentine at this temperature. Caillere (1934) believes that this phenomenon is related to the major exothermic peak.

The major endothermic curves in the temperature range 600° to 750°C., are related to the decomposition and loss of water from the serpentine structure, culminating with the destruction of the crystal structures at 685°, 725°C.

The particle size may be responsible for the size and temperature of the peak. The effect of the particle size on the D.T.A. of chrysotile and antigorite was determined by Martinez (1961) who states that with the decrease in the particle size peak temperature for the endotherm decreases from 710° in coarse fibres to 670°C in fine chrysotile. The particle size does not affect appreciably the exothermic peak temperature but the sharpness and the height increases with the grinding time. Platy mineral (antigorite) also behaves in a very similar manner to chrysotile.

Faust *et al.* (1962) has classified serpentine minerals into groups of clinochrysotile (A), clinochrysotile globetype (B), clinochrysotile plus orthochrysotile (C), chrysotile plus lizardite (D), lizardite plus clinochrysotile (E), and antigorite. Comparing with their groups serpentine S-1 comes within their A, or (D) groups. Sample S-2 could be out of any A,B,C, or D group. Sample, S-3 has minerals of A, B, and C group. Moreover, from the pure antigorite curves it is observed that the endothermic trough has temperature between 790° to 802°C.

Samples S-2 and S-3 have higher temperature of endotherms than S-1, They, therefore, contain more of chrysotile and lizardite than antigorite mineral. Comparing S-1 with F-15 of group D in Table-13, it is found that both the samples have mineralogy very close to each other ; for example, S-1 has endotherm at 670°C, while F-51 at 671°C and exotherm 786°C vice 784°C which indicates chrysotile plus lizardite (C>L). S-2 as compared to F-164, endotherm for S-2, 690° and for F-164, 687°C, exotherms for S-2, 812°C and for F-164, 816°C. Thus S-2 is clinochrysotile plus some orthochrysotile. S-3 with reference to F-61 has endotherm at 705°C, exotherms at 815° and at 814°C respectively.

STATIC DEHYDRATION METHOD

For the static dehydration analyses a heating of 10 hours at each temperature was used to permit samples to attain equilibrium at each temperature. Some small deviations from equilibrium may have occurred between temperatures of about 500-600°C, but because the samples were heated together, the data are comparable.

TGA curves are shown in Fig. 4. The curves of the samples S-1, S-2 and S-3 show one prominent shoulder in the temperature range 580 to 630°C, 590° to 640°C and 600°C to 650°C respectively. In addition all the specimens shows a shoulder, corresponding to low temperature-water, which is very well defined in the case of S-1 but less prominent in the curves for S-2 and S-3. This correlation when compared with the work of Faust *et al.* (1962) shows that S-1 could be rock consisting entirely of deweylite mineral : a variety of chrysotile. In S-2 and S-3 the high-temperature shoulder occurs at a higher temperature than in S-1, which according to Faust should contain a little higher content of antigorite than S-1. Comparatively S-2 has more antigorite and S-3 has still more. This is also in agreement with D.T.A. curves.

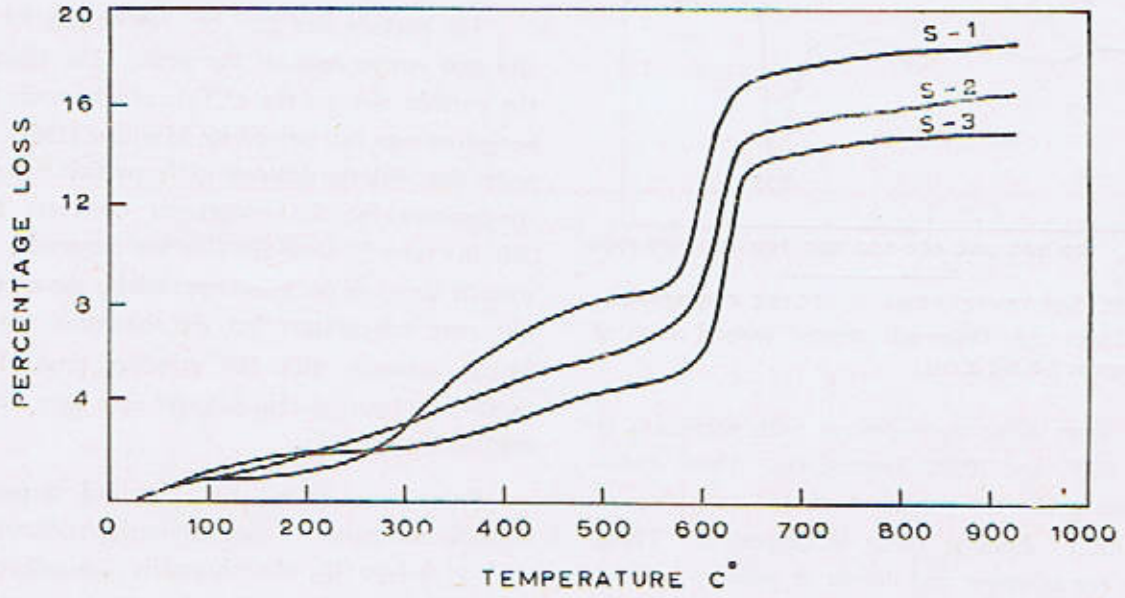

Fig. 4. Static dehydration curves.

X-RAY STUDIES

Powder photographs of serpentine were made on a 19 cm. camera using Ni filtered Cu-Kα radiation. The measurement of the spacings are given in Table - II.

TABLE—II

X-ray Diffraction Data for Serpentine Minerals

S—1 'dA' mixture	S—2 'dA' mixture	S—3 'dA' mixture	ASTM Clino-chrysotile	ASTM Ortho-chrysotile	ASTM Lizardite	ASTM Antigorite
7.36/VS 4.58/M	7.36/VS 4.58/M	7.36/VS 4.57/M	7.36/VS 4.58/M	7.36/VS —	7.36/VS —	— —
4.25/M	—	—	—	—	—	4.26/MW
3.66/M	3.66/MS	3.66/MS	3.66/VS	3.66/S	—	—
2.65/W	—	—	—	—	2.65/MS	—
2.50/W	2.50/MS	2.50/M	—	—	—	2.495/S
2.45/MW	—	2.46/W	—	—	—	2.46/MW
1.535/M	1.535/M	1.535/M	—	—	—	1.535/MW
—	—	1.750/F	—	—	—	1.755/M
—	—	1.28/F	—	—	1.279/MW	—
—	—	1.31/M	—	1.31/M	—	—
—	—	0.943/F	—	—	0.944/W	—

The 'd' values obtained for all the three samples are listed in Table II for the differentiation of minerals present in the serpentinite rocks. The X-ray patterns shows that the rocks are composed of orthochrysotile, clinochrystile, lizardite, antigorite and the accessories, chromite, talc, magnetite, dolomite and magnesite. The relevent 'd' values were compared with ASTM powder diffraction file (1963) for their indentification.

From the X-ray studies of three types of serpentine it is evident that both types of chrysotile, ortho and clinochrysotile are present in the admixture and the strongest of lines are those for clinochrysotile.

Other 'd' values are for lizardite and antigorite. Antigorite has very prominent medium intensity values (Table-II).

CONCLUSION

1. Under the microscope, three different physical forms of serpentine samples appeared to be consisting of chrysotile, antigorite, serpophite and bastite, with accessories of chromite, magnetite, dolomite, talc and magnesite.

2. Chemical compositions of the three types of samples confirm high amount of chrysotile.

3. D.T.A. & T.G.A. studies show that it is

possible to distinguish polymorphic forms of serpentine.

4. X-ray studies confirm the presence of the following minerals in the order cited. Clino-chrysotile with orthochrysotile, antigorite, lizar-dite, and accessories such as chromite, dolomite, magnetite, talc and magnesite.

REFERENCES

Ashraf, M., and Qureshi, M.W., 1966 M.Sc. Field Report. Geol. Dept., Punjab Univ., Lahore.

Caillere, S. 1934 Sur L' incandescence des certaines serpentines apres leurs dehydration. *C.R. Acad. Sci. Paris*. 198, 1354.

Deer, W.A. Howie, R.A. and Zussman, J. 1962 ROCK FORMING MINERALS, **3**, Longmans, Green and Co. Ltd., London, 170-187.

Faust, G.T., and Fahey, J.J., 1962 Static dehydration method for the determination of Serpentine Group Minerals. *U.S. Geol. Surv., Prof. Paper*, 384-A, 48.

Faust, G.T., and Fahey, J.J., 1962 D.T.A. of Serpentine Group Minerals : *U.S. Geol. Surv., Prof. Paper*, 384-A, 51.

Francis, G.H. 1956 The serpentine mass in Glen Urqauhart, Inverness-shire, Scotland, *Amer. Jour. Sci.*, **254**, 201.

Gheight M.A. 1952 D.T.A. of certain iron oxides and oxides hydrates, *Ibid.*, **250**, 677.

Hess, H.H., Smith. R.J. and Dengo, G., 1952 Antigorite from the vicinity of Caracas, Venezuela, *Amer. Mineral.* **37**, 68.

Martinez, E., 1961 The effect of particle size on the thermal properties of serpentine minerals. *Ibid.*, **46**, 901.

Pabst, A., 1952 The Metamict state, *Ibid.*, **37**, 137.

Powder Diffraction File. 1963, A.S.T.M. Philadulphia, U.S.A.

Whittaker, E.J.W. and Zussman, J. 1956. The characterization of serpentine minerals by X-ray diffraction. *Min. Mag.*, **31**, 107.

Winchell, A.N. and Winchell, H. 1951. ELEMENTS OF OPTICAL MINERALOGY, Pt. II, John Wiley and Sons, New York, 551.

Received March, 1970

THE DETERMINATION OF GOLD BY RADIOCHEMICAL AND NON-DESTRUCTIVE NEUTRON ACTIVATION ANALYSES IN SOME SULPHIDE ORE SAMPLES FROM PAKISTAN

BY

FAZAL-UR-REHMAN*

Geologisk Mineralogisk Museum, University of Oslo, Sars Gate-1, Oslo-5, Norway.

Abstract : *Four sulphide ore samples were selected from different localities in Pakistan, and were analysed by both radiochemical as well as by non-destructive neutron activation techniques. Only the results on gold are being presented in this paper. The nuclear reactor JEEP-II located at Kjeller (Norway), has been used as a source of neutrons. The samples were irradiated at a flux* 1.5×10^{13} *n/cm²/sec for one hour in case of radiochemical neutron activation experiment, and for half an hour in case of non-destructive neutron activation experiment. Following irradiation and "cooling" for two days, the respective samples were used directly for non-destructive analysis, whereas others were put to gold radiochemistry.* ^{198}Au*, half life* 2.697 *days, has been assayed in both the experiments. A lithium-drifted germanium detector, Ge (Li), has been used, along with a* 16 *bit computer (NORD-*1*) with* 4*K memory, to measure the gold activity.*

INTRODUCTION

Neutron activation analysis (NAA) has been used in the determination of gold in rocks, ores and other geological material for the last many years. The application of NaI(Tl) detectors in neutron activation analysis for the determination of gold in ore samples, at submicrogram level, has been reported by Chow and Beamish (1967) and Crocket *et al.* (1968). Lithium-drifted germanium detectors, Ge (Li), have been used by Lamb *et al.* (1966) and de Lange *et al.* (1968, 1969) for nondestructive estimation of gold in ores, and by Rehman *et al.* (1972) for radiochemical estimation of gold in ores, metallic concentrates and their associated tailings with submicrogram quantities of this element.

EXPERIMENTAL

Ge(Li) detector and electronics

The co-axial germanium detector used in this study was a product of ORTEC Inc. (Model No. 8001-20P). Its size is 32.6 × 34.4mm dia × mm length, the drift depth is 10.6 mm, the diffusion depth is 0.7 mm, and the total active volume is 23.6 cm^3. The detector is operated in vacuum at a cryogenic temperature of 77°K with a bias voltage of 1900 volts. The output signals from the detector are fed into a preamplifier (ORTEC 118A), a selectable active filter amplifier (ORTEC 44OA) and a baseline restorer (ORTEC 438). The resultant pulses are analyzed by an analog-to-digital converter (HEWLETT PACKARD-

*Permanent address
Geology Department, Punjab University, Lahore, Pakistan.

5416A) interfaced to a NORD-1, 16 bit computer with 4K memory (supplied by A/S NORSK DATAELEKTRONIKK). Pulser timing with a research pulser (ORTEC 448) was used to correct the dead time for the total system (Anders, 1969). The resolution for 1332 KeV gamma ray peak of ^{60}Co was 3.5 KeV (FWHM).

Irradiation and radiochemical treatment

Nearly 100-200 mg of thoroughly homogenised samples were accurately weighed, wrapped in aluminium foil and irradiated in the JEEP-II reactor located at Kjeller (Norway) for one hour at a flux of 1.5×10^{13} n/cm^2/sec, along with three gold monitors in duplicate (prepared by pipetting 100μl of each standard solution, having gold content of 3.06 μg/ml, 15.30 μg/ml and 30.60 μg/ml, respectively, on one inch square aluminium foil, evaporating to dryness and finally wrapping like the samples). The samples were then cooled for two days and then subjected to a radiochemical treatment (Brown and Goldberg, 1949). It involved mainly three steps ;

1. Decomposition of the sample,
2. Extraction of gold to avoid bulk activity of the sample,
3. Precipitation of gold.

The whole radiochemical procedure (Rehman *et al.*, 1972) is represented in Fig. 1.

For the non-destructive purposes, 50-100 mg of the samples were weighed, sealed in small polyethylene envelopes and irradiated for 30 minutes along with the gold monitors (prepared as above, using polyethylene sheet instead of aluminium foil and finally sealing them in small polyethylene envelopes like the samples).

Counting procedure and yield determination

After finishing with the radiochemistry, the gold metal, thus obtained from each case, was subjected to radioactivity measurement. For the purpose of non-destructive analysis, the samples were counted directly, after "cooling" for two days. The radioactivity measurements were based on 411.8 KeV gamma ray of ^{198}Au, half life 2.697 days (de Silva Filhe *et. al.* 1965). The counting times were between 20 min. to 120 min. depending on the gold content of the samples. The gold peaks were measured by computing total absorption peak areas (Sterlinski, 1970).

In case of radiochemical results the chemical yield was found between 70-90%.

RESULTS AND DISCUSSION

The experimental results obtained by radiochemical neutron activation analysis have been presented in Table 1, whereas those obtained by non-destructive neutron activation analysis are shown in Table 2. In some cases the deviation from the mean value has been found much higher than that what could be expected from the analytical error but it can be certainly explained on the basis of inhomogeneity of gold distribution in these samples. To check the accuracy, a Nordic reference sample, namely ASK-sulphide ore, was also analysed during this work and the results obtained were found in good consistency with the gold value already established, 60 ppb, (Johansen & Steinnes, 1970). Furthermore the precision was checked by making a separate run of twelve replicates of one ore sample from Killingdal mine (Norway), which was included in these experiments as a "House Standard", and gave a mean value of 213 ppb with a standard deviation of 2.2 as shown by the results given below, 210.8, 212.2, 215.4, 216.9, 214.4. 215.2, 210.8, 212.2, 213.7, 210.6, 210.7, 214.8.

$\bar{x}$	=	213.1
s^2	=	4.84
s	=	2.20
C	=	0.64%

$\bar{x}$, s^2, s, and C represent the normal standard values (Shaw, 1969).

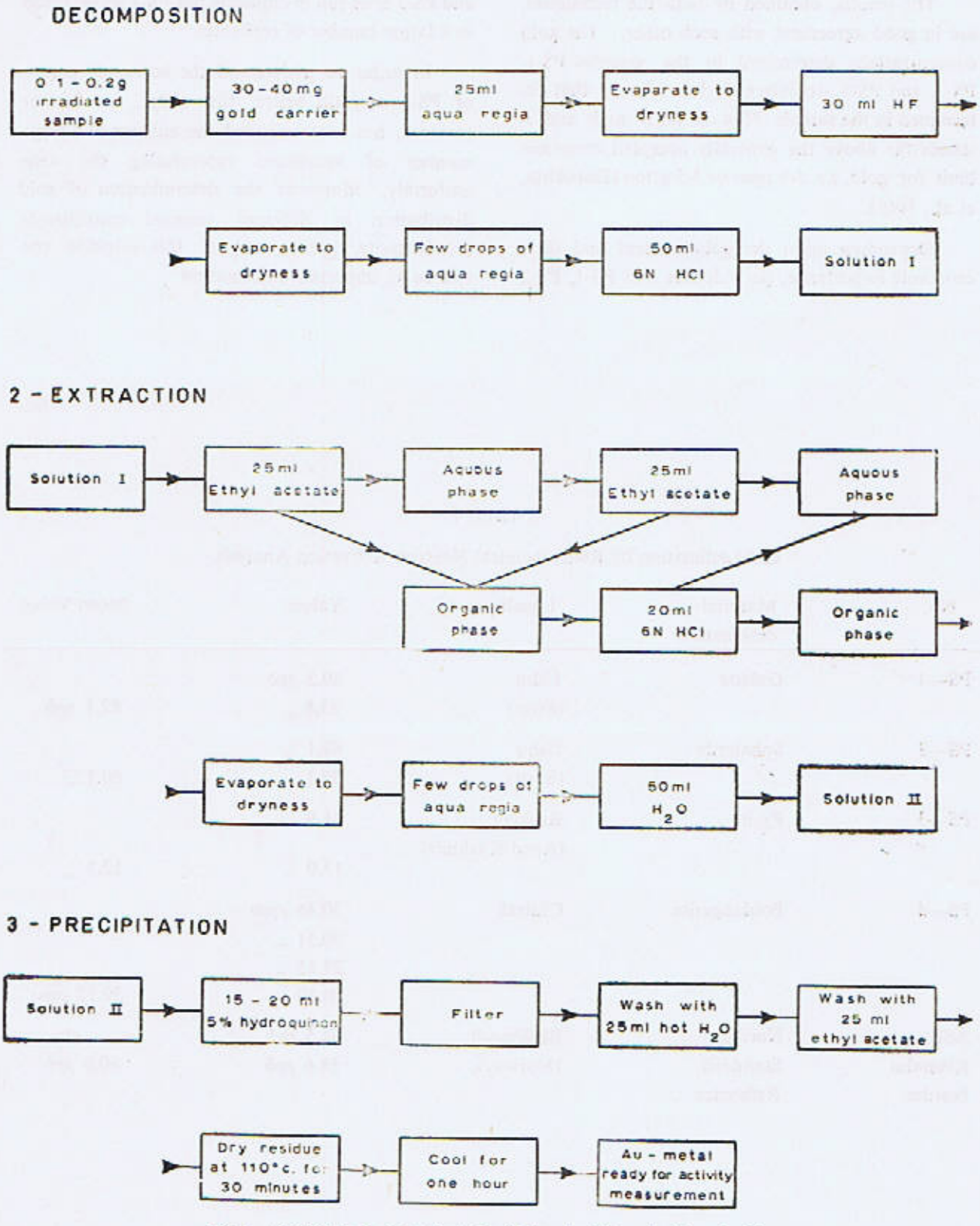

Fig. 1. Schematic representation of radiochemical determination of gold.

The results, obtained by both the techniques, are in good agreement with each other. The gold concentrations determined in the samples PS-1, PS-2, and PS-3 are extremely low whereas that determined in the sample PS-4 is fairly high and it stands far above the generally accepted economic limit for gold, *i.e.* 3-5 ppm or 3-5 g/ton (Dorokhin, et al., 1969).

Depending upon the gold content and their economic importance, the sulphide ores PS-1, PS-2 and PS-3 were run in duplicate but PS-4 was assayed in a larger number of replicates.

In order to understand the economic nature of PS-4 ore still better, the writer, for further research, has recommended the analysis of a large number of specimens representing the area uniformly. Moreover the determination of gold distribution in different mineral constituents (boulangerite, pyrite etc.) of this sulphide ore will be an important information.

TABLE I

Gold estimation by Radiochemical Neutron Activation Analysis.

No.	Material designation	Locality	Values	Mean Value
PS—1	Galena	Ushu (Swat)	80.3 *ppb* 83.8 ,,	82.1 *ppb*
PS—2	Sphalerite	Ushu (Swat)	62.1 ,, 58.1 ,,	60.1 ,,
PS—3	Pyrite	Reshian (Azad Kashmir)	11.9 ,, 13.0 ,,	12.5 ,,
PS—4	Boulangerite	Chitral	30.46 *ppm* 30.51 ,, 29.15 ,, 30.50 ,,	30.15 *ppm*
ASK—Kismalm Norden	Nordic Standard Reference	Bleikvassli (Norway)	62.5 *ppb* 58.6 *ppb*	60.6 *ppb*

TABLE 2

Gold estimation by Non-destructive Neutron Activation Analysis.

No.	Material designation	Locality	Values	Mean value	Other information
PS—1	Galena	Ushu (Swat)	99.9 *ppb*		
			96.3 ,,	97.1 *ppb*	
PS—2	Sphalerite	Ushu (Sawat)	59.9 ,,		
			60.7 ,,	60.3 ,,	
PS—3	Pyrite	Reshian (Azad Kashmir)	16.5 ,,		
			13.5 ,,	14.0 ,,	
PS—4	Boulangerite	Chitral	32.59 *ppm*		
			30.95 ,,		
			39.10 ,,		
			34.95 ,,		
			30.26 ,,		
			38.36 ,,		
			34.86 ,,		
			29.48 ,,		
			33.30 ,,		
			28.82 ,,		
			33.20 ,,	33.26 *ppm*	s^2—11.43 s—3.38 C—1.02 (Shaw, 1969)
A S K—Kismalm Norden	Nordic Standard Reference	Bleikvassli (Norway)	60.8 *ppb*		
			58.9 ,,	59.9 *ppb*	

ACKNOWLEDGEMENTS

The specimens analyzed in this study were obtained from Dr. S.F.A. Siddiqui, Geology Department, Punjab University, Lahore, Pakistan and the author is obliged to him. Grateful acknowledgements are made also to Prof. K.S. Heier and A.O. Brunfelt, Mineralogisk-Geologisk Museum for their permission to use the facilities available at the University of Oslo, during this work. Aslo sincere thanks are due to Norwegian Agency for International Development for the award of a Postdoctorate Research Fellowship.

REFERENCES

Anders, O.U., 1969 Experiences with the Ge (Li) detector for high-resolution gamma ray spectrometry and a practical approach to the pulse pileup problem. *Nucl. Instr. and Meth.*, **12**, 205.

Brown, H.S., and Goldberg, E.D., 1949 The radiometric determination of gold and rhenium in iron meteorites. *U.S. Atomic Energy Commission Report, AECU-495.*

Chow, A. and Beamish, F.E., 1967 An experimental evaluation of Neutron Activation, Wet Assay and Fire Assay methods of determining gold in ores. *Talenta*, **14**, 219-231.

Crocket, J.H., Keays, R.R. and Hsieh, S., 1968 Determination of some precious metals by Neutron Activation analysis. *J. Radioanal. Chem.*, **1**, 487-507.

de Lange, P.W., de Wet, W.J., Turkstra, J. and Venter, J.H., 1968 Nondestructive Neutron Activation analysis of small samples of Witwatersrand Ore for gold. *Anal. Chem.* **40**, (2), 451-454.

de Lange, P.W., Venter, J.H. and de Wet, W.J., 1969 Nondestructive Neutron Activation analysis of gold and uranium in residue samples of different ore bodies. J. *Radioanal. Chem.* **2**, 219-228.

de Silva Filho, J.G., Abrao, A., and Lima, F.W., 1965 *Inst. Energa Atomica, Publ.* I.E.A. 98, Sao Paulo, Brazil.

Dorokhin, I.V., Bgfacheva, E.N., Druzhinin, A.V., Sobolevsky, V.I., and Gobunor, E.N., 1969 ECONOMIC MINERAL DEPOSITS. Higher School Publishing House, Moscow, 120

Johansen, O., and Steinnes, E., 1970 Private communication, Institute for Atomic Energy, Kjeller, Norway.

Lamb, J.F., Prussin, S.G., Harris, J.A. and Hollander, J.M., 1966 Application of lithium drifted germanium gamma ray detectors to Neutron Activation analysis. Nondestructive analysis of a sulphide ore. *Anal. Chem.*, **8**, (7), 813-818.

Rehman, F.U., Brunfelt, A.O., and Heier, K.S., 1972 Gold, silver and mercury from Norwegian sulphide mines. *Norges Geol. Unders.* (In Press)

Shaw, D.M., 1969 HANDBOOK OF GEOCHEMISTRY. I, 324-325, Springer Verlag, Berlin.

Sterlinski, S., 1970 Features of the modified Covell Method for computation of total absorption peak areas in complex Gamma-ray Spectra. *Anal. Chem.* **42**, (2), 151-155.

Received January, 1970

PRELIMINARY STUDIES ON THE ECONOMIC GEOLOGY OF BAUXITE/LATERITE DEPOSITS, KATTHA AREA, SALT RANGE, PUNJAB, PAKISTAN

BY

MUHAMMAD ASHRAF, M. WAHID QURESHI and F. A. FARUQI

Glass & Ceramics Division, P.C.S.I.R. Laboratories, Lahore

Abstract : *A new bauxite/laterite zone was discovered which crops out intermittently over a distance of more than ten miles in the Salt Range, north of Kattha. The zone ranges from less than a foot to over 23 feet in thickness. Samples analysed average 50% Al_2O_3 and the area is believed to hold promise for containing important amount of bauxite suitable as an ore for the manufacture of aluminium, chemicals and refractories. The bauxite is thought to have formed by deep weathering on an old erosion surface over the Permian rocks, now overlain unconformably by rocks of the Paleocene age.*

INTRODUCTION

Bauxite and laterite rocks crop out in an irregular east-west trending zone a few miles north of Kattha Masral which is sixteen miles north of Khushab, Sargodha District Index map Fig. 1. In general the bauxite beds dip northwards between 15° to 20° and crop out at an altitude of about 2,000 feet to 2,500 feet above sea level. The ore zone can be approached by unmetalled motorable roads from Kattha Masral and Chamil as well as from Sultan Mehdi Ziarat.

The area under discussion is about 90 square miles in size. In the past, some work was done on the regional geology of the Salt Range, including the project area, by Wynne (1878), Fox (1924) and Gee (1944). The area, composed of aluminous rocks, has been mapped for the first time by Ashraf during 1968-69, using enlargements (1.5 times) of topographic sheets Nos. 43 D/6 & D/10 of the Survey of Pakistan. The main object of the present investigation has been to study and evaluate the economic potential of the area.

Geomorphologically the terrain represents a dissected cuesta. The relief is moderate. The altitude varies from about 740 feet in south-west to 3,388 feet in the north-west. The scarp slope is quite steep while the dip slope is gentle and merges into the Potwar Plateau to the north. Vegetation is present at higher elevations where trees and shrubs are abundant. Climate is semi-arid to arid.

GEOLOGY

(*i*) **General** : The sequence of sedimentary rock in the Kattha area ranges from Cambrian to Eocene in age. The rocks of Permocarboniferous age are bordered by two major unconformities above and below it ; the higher unconformity is marked by bauxite and laterite.

The best exposures of different rock units are seen on both sides of Patiala Wahan (stream) where Cambrian formations consist of bright red marl and rock salt, dull red to purple sandstone and dark grey micaceous shales. The Carboniferous rocks are composed of an unsorted boulder bed, olive

green sandstones and shales, dark red purple sandstone, light coloured sandstone and grit, and dark purple and lavender coloured clay. The rocks of Permain age conformably overly the Carboniferous strata. Lithologically Permian rocks are sandy to pure crystalline limestone with abundant brachiopods. The laterite/bauxite material occurs irregularly above the uneven and unconformable plane of the Permian rocks with variations in the grade of ore in the vertical succession as well as from one locality to another. The rocks of the Paleocene age, represented by calcareous sandstone, conformably overly the bauxite/laterite horizon, which is sometimes glauconitic. Further upwards, this sandstone passes into a yellow-brownish foramniferal limestone, olive shales and friable white sandstone with hardly a few ferromagnesian minerals. The overlying nummulitic limestone portion of Eocene age is one of the most developed horizon. The limestone is nodular in character which spreads for a considerable distance and conceals the bauxite/laterite outcrops at many places.

STRATIGRAPHIC COLUMN

Eocene-Paleocene

Patala Formation (Patala Shales)	Light grey foramniferal shales with coal seams at places and sandstone
Lockhart Limestone (Khairabad Limestone)	Yellow brown seminodular foramniferal limestone
Hangu Formation (Dhak Pass beds)	Impure limestone and shales

....Unconformity marked by laterite/bauxite....

Permian

Chidru Formation (U. Productus)	Yellow gey limestones and calcareous sandstones with basal dull green shales. Presence of brachiopods.
Wargal Formation (M. Productus)	Thickly bedded, grey limestone with brachiopods.
Amb Formation (L. Productus)	Brown and gery calcareous sandstones and impure limestones with brachiopods.

Carboniferous

..... Unconformity .....

Cambrian

(*ii*) **Laterite** : The laterite of the Kattha area occurs irregularly above the uneven plane of Permian with some variation in the intensity of lateritization. The characteristic features of the laterite therefore are variable with degree of lateritization. The lower most portion is frequently brecciated Fig. 2 a, c but gradually converges to pisolitic and somewhat massive habit, and finally becomes perfectly pisolitic and sometimes containing oolites as well. The basal brecciated portion consists of lateritic material and unweathered rock fragments of argillaceaus sandstone, limestone, and shales. The laterite throughout the area varies in colour from cherry red to red, pinkish red, brownish green to brownish red. The thickness of the outcrops is variable from some inches to over 23 feet, but 10 feet to 15 feet thick outcrops are common west of Kattha-Pail road, and east of Narianwala. The laterite is altogather absent in the north-eastern escarpment of Kalra Wahan and instead a dark brownish-red ferruginous sandstone is present.

(*iii*) **Bauxite** : It is present mostly above the laterite material. The overall length of the outcrop is about ten miles while the thickness is variable from a few feet to over 23 feet (thickness from place to places is shown in Fig. 1 and in Table 1.) The characteristic features of the bauxite are much more variable than laterite. It occurs as a loose rock which on hammering becomes somewhat powdery. Its colour is not constant and varies from white to cream and buff coloured and is sometime mottled. At places bauxite is white but joints are incrusted with red iron compounds, probably goethite and hematite. The top 1-2 feet of bauxite at many places is white in colour and well leached making the rock lighter in density and poorer in alumina than bulk of the rock ; the latter being generally buff to cream coloured and high in alumina (chemical analyses, Table 1).

44/45

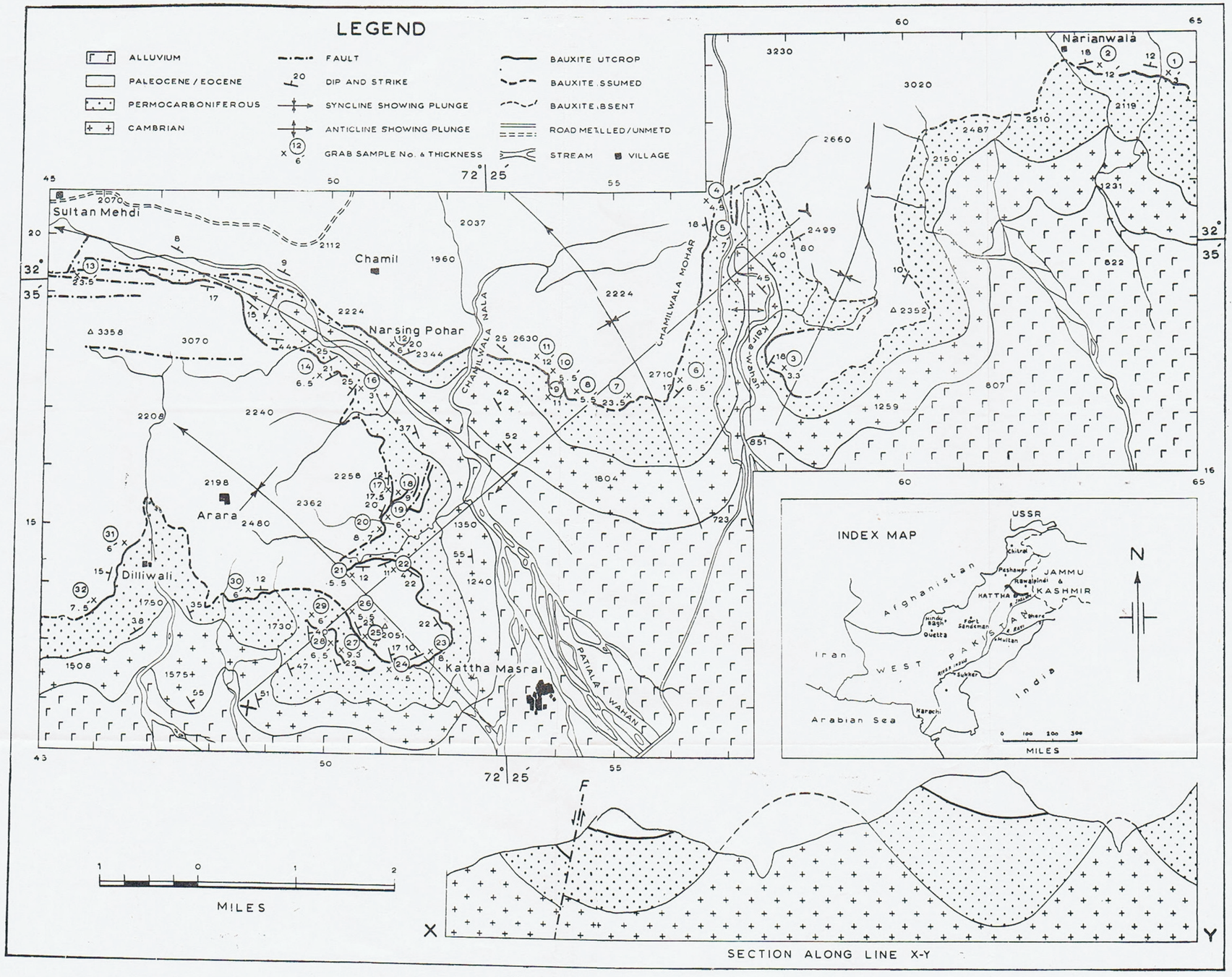

Fig. 1. Geological nmap of Kattha area, Salt Range.

Mapped by : M. Ashraf 1969

Following this criteria the potential bauxite rich localities are found to occur west of Kattha-Pail road and specifically on both sides of the Patiala Wahan. The more important locations are exposed in the Narianwala area, Kalra Wahan, below Chamilwala Mohar along Katha-Pail road, East and West of Chamilwala nala, and south of Sultan Mehdi, north-west of Kattha Masral and west and south-west of Dilliwali. The bauxite horizon, including laterite, occurs on an uneven plane of middle or upper Permian limestone or arenaceous limestone. The overlying calcareous sandstone of yellowish brown to brownish-green colour forms the marker horizon as it is distinctly present everywhere over the bauxite. The bauxite occurs as discontinuous zones in the localities described above. In the intervening areas the bauxite was either not formed or had been covered under the talus of the nodular limestone. Mostly the outcrops are feebly disturbed with gentle synclinal folding and normal faulting. Only the area between Sultan Mehdi and Narsing Pohar is highly disturbed where the outcrops generally dip at higher angles.

Various features of bauxite are described below on the basis of four type localities Fig. 2 of the area :—

(*a*) **Narianwala Section:** The bauxite is exposed near Narianwala spring where its thickness is 6'-3", with the top portion being of white to light greyish in colour and having gritty appearence. The main zone is 5'-9" thick, is light grey to buff coloured with yellowish and red patches around joints. The pisolites are creamish, grey and red coloured. The bulk of the rock is clayey and has a leached-out appearence as is evident from its chemical composition : SiO_2=39.26%, Al_2O_3=46.72%, Fe_2O_3=28% Fig. 2, a.

(*b*) **Section at Location 7 :** This occurs SSW of Chamilwala Mohar Fig. 1. The thickness of the section is 23.5 feet and the exposed length is more than 150 feet. There are three major vertical divisions of the outcrop Fig. 2, b.

(*i*) The upper zone of bauxite is white, yellow, pink to reddish brown in colour and is rather mottled with occasional oolites and pisolites. It has leached out appearence, is light in density, and is fine grained, loosely cemented and clayey. It is about 4 feet thick with average composition of SiO_2=44.52%, Al_2O_3=39.98%, Fe_2O_3=0.87%.

(*ii*) The middle zone consists of yellowish green pisolitic to oolitic bauxite with a little groundmass of the same colour. It is loosley cemented and crumbles easily. Generally, the pisolites are about 5 mm in diameter but some are 10 to 20 mm in diameter. These pisolities are mostly concentric. The thickness of the zone is 12.5 feet with average composition of SiO_2=15.47%, Al_2O_3=55.41%, Fe_2O_3=15.71%.

(*iii*) The basal zone of bauxite resembles the upper zone being mottled and creamish, pink to reddish brown in colour. The zone is highly jointed and the joint planes are incursted with pinkish to reddish brown iron compounds ; the fresh surface, however, is light cream in colour. The thickness is 7 feet and average composition is SiO_2=13,00%, Al_2O_3=68.97%, Fe_2O_3=1.83%.

(*c*) **Mehdi Ziarat Section :** This section is exposed south of Mehdi Ziarat with a thickness of about 23.5 feet. There are five distinct zones Fig. 2, c:-

(*i*) Upper zone, consisting of fine grained clayey looking splintry rock. It is well cemented, has weakly leached appearence and does not have light density as seen at other places. Thickness of the zone is 4 feet and average composition is SiO_2=12.80%, Al_2O_3=72.50%, Fe_2O_3=0.45%.

(*ii*) Upper-middle zone, consisting of some oolites and fine grained compact rock. It is light grey to buff in colour with joints incursted with iron compounds. Thickness of the zone is 7 feet and composition is SiO_2=13.96%, Al_2O_3=70.23, Fe_2O_3=0.88%.

(*iii*) Middle zone, formed of abundant oolites and occasional pisolites and is light grey in colour.

Thickness of the zone is 3·5 feet and average composition is SiO_2=26.17%, Al_2O_3=60.12%, Fe_2O_3=0.72%.

(*iv*) Lower-middle zone, full of pisolites, 2 to 5 mm in diameter, embedded in a groundmass of fine-grained clay-looking material. Both groundmass and pisolites are white to very light grey in colour. Its thickness is 4 feet and average composition is SiO_2=18.70%, Al_2O_3=64.81 %, Fe_2O_3=0.97%.

(*v*) The basal zone, formed of lateritic pisolites and braccia. The brecciated portion consists of lateritized and unweathered pebbles of shales and argillaceous sandstone etc. This zone gradually merges into the lower-middle zone. Colour of the material is dirty red and the thickness is about 5 feet.

(*d*) **Section at Location 17 :** This occurs NW of Kattha Masral where its thickness is 17.5 feet with variable exposed length. Three zones are, distinct in this section. Fig. 2, d.

(*i*) The Upper zone of this section is white, yellowish, pinkish and reddish in colour. It is rather mottled at places, like the upper zone at locality 7 with some sparsely distributed pisolites and oolites. It has also leached out appearence and is light in density as the mass is porous and very fine grained. It is clayey and loosley cemented and soils the finger. It is 2.5 feet thick with average composition of SiO_2=39.30%, Al_2O_3=40.26%, Fe_2O_3=3.50%.

(*ii*) The Middle zone is the most interesting as, besides being loosley cemented and clayey to pisolitic, is highly aluminous. The ground mass of bauxite is creamish to buff coloured and the pisolites are yellowish to reddish, sometime from 3 to 5 mm in diameter. In this zone, about 200 feet NW of locality17, there are 2 to 6 inches thick veinlets composed of fibrous and hard creamish material, probably alunite. This zone is 6 feet thick with composition of SiO_2=9.12% Al_2O_3=71.11%, Fe_2O_3=2.02%.

(*iii*) The basal zone is composed of laterite which has a slightly undulating relationship with the middle zone. This zone is cherry red to red coloured, pisolitic and massive and is hard as compared to the bauxite zones. The pisolites are rounded to oblong and somewhat broken near bottom of the zone. Size of pisolities varies from 4 to 10 mm. Thickness of the zone is about 9 feet.

STRUCTURE

The general strike of the strata is east-west with a northwards dip. The rocks of Cambrian to Permian age have high inclination, over 40°, while the beds of Tertiary age dip gently, from 10° to 20°. Slumping is wide-spread all along the southern escarpment slope and near Ziarat Sultan Mehdi in the north. Slumping is so enormous that sometimes gigantic bed of Eocene is found to have slumped over a long distance and thereby covered the Paleozoic rocks.

The area shows a sort of corrugated structure due to the presence of alternating anticlines and synclines ; where valleys are formed, the anticlinal and synclinal structure can be observed in the uneroded hills. The anticlines and synclines are parts of parallel folds which either die out or show slight inclination in the younger Paleocene-Eocene rocks. While Cambrian to Permo-Carboniferous rocks are steeply folded on the surface, they appear to be dying out in the surface. In the Patiala Wahan, near Narsing Pohar, perfectly parallel anticlinal folds are observed where due to space problem older and younger rocks in the base of fold could no longer be folded concentrically. This lack of space (DeSitter, 1956) in the core of Narsing Pohar anticline created a tendency to broaden the wedge of upward thrust within the centre of the fold resulting into longitudnal crest-fault Fig. 1.

Normal faulting is also wide-spread in the area ; the throw, however, is too small to be mapped. Anyhow, about 10 major faults have been mapped. Most of these faults are either normal

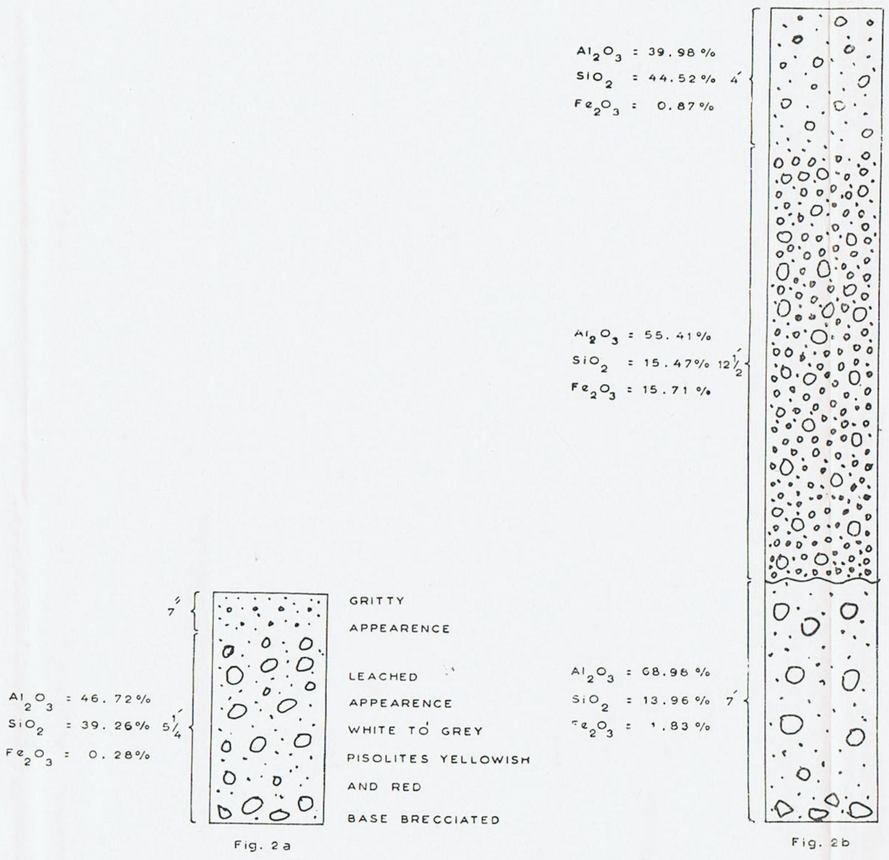

Fig. 2a

Fig. 2b

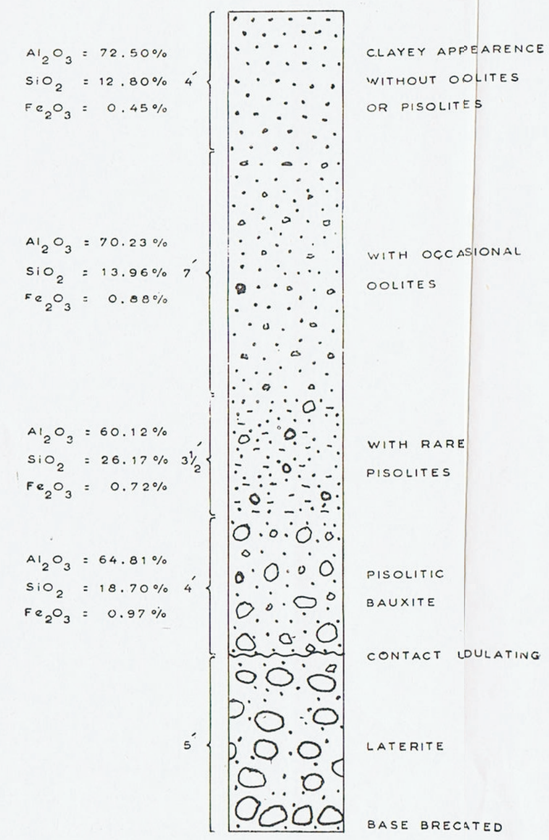

Fig. 2c

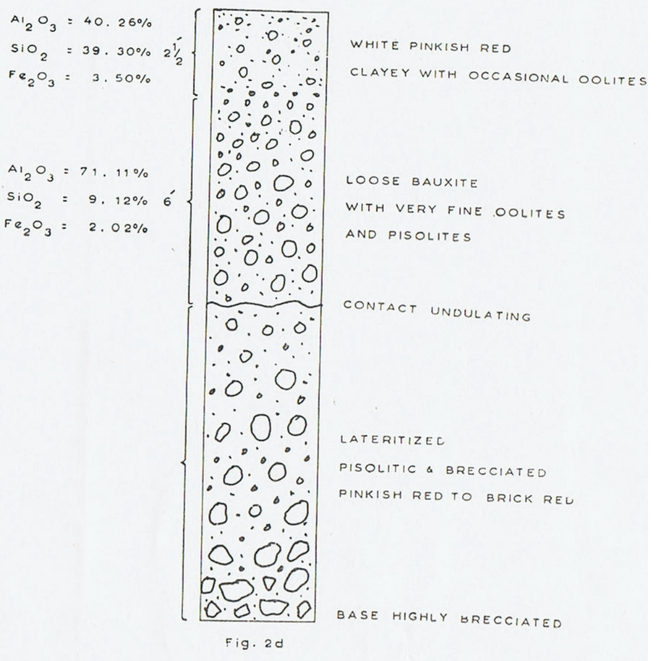

Fig. 2d

Fig. 2. Narianwala Section (2a), Section at location 7 (2b), Mehdi Ziarat Section (2c), Section at location 17 (2d).

gravity faults or step faults. The best exhibition of gravity fault is seen in Kalra Wahan where, on both sides of the valley, down-thrown outcrops of Permian to Eocene can be seen. Step faults appear in Patiala Wahan between 1350 and 2258 feet high peaks. However, one of the faults is a scissors-type normal fault with straitgraphic throw towards north-east. A transitional normal fault is also observed in the southern area between 1730 and 2051 feet high peaks with a steep south-western dip.

ECONOMIC GEOLOGY

The chemical investigations (Table 1) show that bauxite contains Al_2O_3 from 73% to 38.0% but some samples show exceptionally high silica upto 50% in the top bauxitic layer or in the leached out portions of bauxite. Fe_2O_3 is around 1% in a fairly large number of samples, but exceptionally high Fe_2O_3 is also found in some samples. The H_2O content is nearly 14% in almost all the samples with the exception of Nos. 3/25, 5/26, and 7/29 wherein it ranges from 20% to 28%. This indicates that probably both types of bauxite, monohydrated and trihydrated, or mixture of both (diaspore or boehmite and gibbsite) are present. It is also seen that in samples collected from mines or deep quarries, SiO_2 is as low as 9.12% and Al_2O_3 is as high as 72.50% while the samples collected from the outcrops are high in silica (50%) and low in

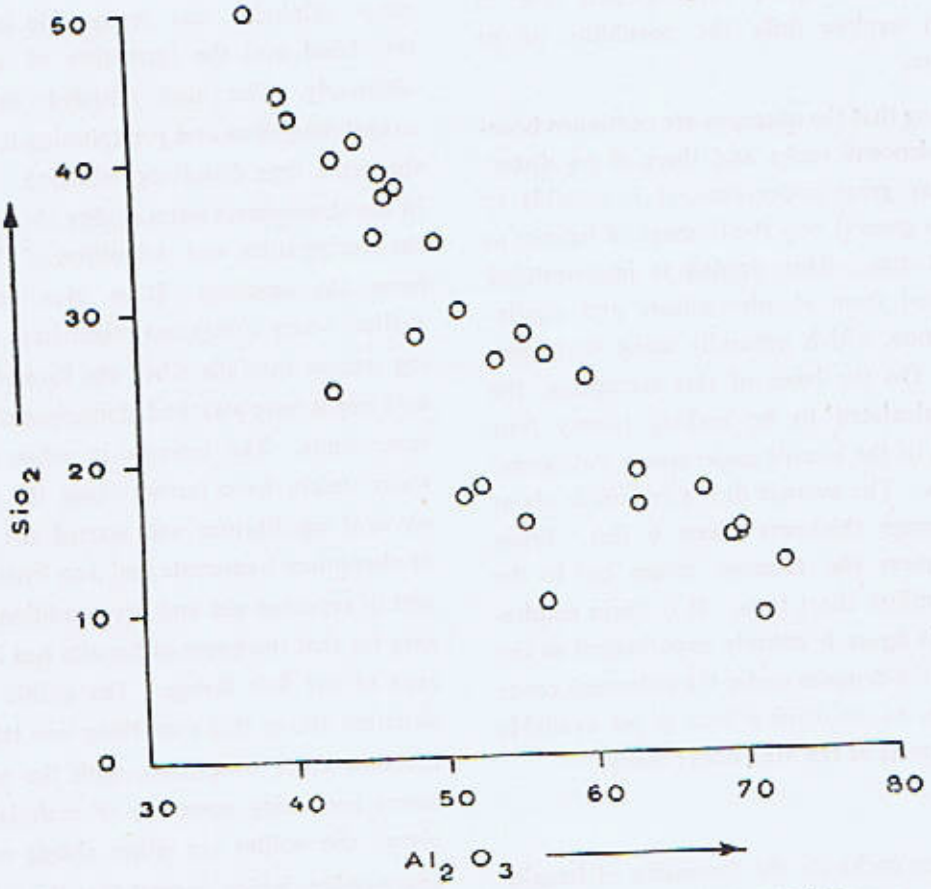

Fig. 3. Relative distribution of alumina and silica in bauxites of Kattha, Salt Range.

alumina (38%). It is possibly due to the wheathering effects on the outcrops due to which bauxite has been leached out in the form of some aluminium salts under arid condition. In Fig. 3, SiO_2 and Al_2O_3 are plotted to see their distribution in the deposits. The relationship shows a reciprocal behaviour such that with increase of alumina, bauxite minerals increase in rock and *visa versa*. Further, it shows either absence or presence of very small amount of impurities as otherwise their abundance would have given rise to rather random distribution in the diagram.

The high content of alumina in some samples indicates that this bauxite is suitable for the manufacture of aluminium chemicals and alumina refractories etc. The trihydrated bauxite is preferred for the preparation of alum. The detailed chemical and mineralogical investigations are in progress to explore fully the possibility of its industrial use.

Assuming that the outcrops are continuos beneath the Paleocene rocks and there is no disturbance of any great importance, it is possible to estimate in a general way the tonnage of bauxite in the mapped area. This deposit is interstratified and is derived from alumino-silicate and argillaceous limestone, which generally make fairly uniform beds. On the basis of this asumption, the area was calculated to be making twenty four square miles of the bauxite undernearth Paleocene/ Eocene rocks. The average dip of bauxite is about 20° and average thickness about 6 feet. From the above figures the tonnage comes out to the tune of 60 million short tons. It is again emphasized that this figure is entirely hypothetical as the continuity of the deposits under the Paleocene cover is not certain, as no drilling data is yet available over various parts of the area under study.

ORIGIN

The source rocks for the formation of bauxite in this area are possibly argillaceous limestone, arenaceous shales, pyritous shales, clays and marls (Table II). All these rocks are present in the older sequence, from Upper Permian-Triassic to Cretaceous (Wadia, 1953). The prevailing conditions at that time, necessary for the bauxite formation, were humid tropical or subtropical climate alongwith the presence of argillaceous material and activity of chemical reagents for conversion of the source rocks to bauxite.

In view of the above, it is concluded that in this part of the Salt Range, aluminosilicates were dissolved by weathering and were impoverished in some easily removable impurities like sodium, potassium, calcium, magnesium and iron. Then a strong bond, established between aluminium and silicon (Kitaisky, 1963), gave rise to kaolinite. Sulphuric acid derived from pyrite and other sulphides was responsible for breaking of this bond and the formation of aluminous ore ultimately. The acid initiated the reaction by coagulating silica and precipitating it rapidly and at the same time dissolving alumina. The increase in the atmospheric water acidity sharply diminished the precipitation and deposition of alumina started from the soutions. It is also conceived that shallow water conditions might have persisted during intense rainfalls when the formation of humic acid might have attacked aluminium to form soluble compounds. The increase in saline and brackish water, might have further upset the chemical and physical equilibrium and started the precipitation of aluminium hydroxide and iron hydroxide. Such sort of repeated wet and dry conditions were necessary for that thickness of bauxite bed in the Kattha area of the Salt Range. The oolitic and pisolitic structure shows that everything was taking place in the near-shore conditions, with the movement of waves producing accretion of material. At some places, the oolites are either absent or present as micro-oolites which suggest that the wave intensity was very low to almost negligible.

TABLE — 1

CHEMICAL ANALYSIS OF SELECTED SPECIMENS

Field No/*	69/1	71/1	67/2	65/3	15/4	17/5	22/6	K/7	19/7	20/7	58/8	57/9	55/10	54/11
SiO_2	24.90	41.00	39.26	50.15	40.04	41.68	34.71	13.00	15.47	41.35	17.90	29.40	25.10	14.50
Al_2O_3	43.00	45.00	46.72	38.04	43.48	45.05	50.30	68.97	55.41	41.83	63.06	51.17	59.65	69.57
Fe_2O_3	19.08	0.50	0.28	0.71	2.12	0.45	1.00	1.83	15.71	1.62	0.94	2.38	0.60	0.95
CaO	0.59	0.19	0.43	0.51	0.28	0.47	0.43	0.70	0.58	0.46	0.37	0.46	0.38	0.32
MgO	0.22	0.11	Traces	Nil	Traces	Traces	0.07	0.20	0.16	0.33	0.08	0.06	0.10	Traces
H_2O	12.08	13.04	13.60	11.50	14.00	12.80	14.00	14.95	12.40	14.70	17.60	16.50	14.00	15.00
Total :	99.87	99.84	100.29	100.91	99.92	100.45	100.51	99.65	99.93	100.29	99.95	99.97	99.83	100.43
Thickness of the zone Analysed	5½′	11′	5¼′	3¾	5½′	6½′	6½′	7′	12½′	4′	5½′	11′	5½′	12′
Colour	Cherry red	Light grey	Grey	Mottled (yellow-ish)	Cream-ish white	Mottled	Cream-ish to white	Mottled creamish pink red	Yellowish cream	Mott-led	Light cream	Cream	Light cream	White to mottled

Analyst : M. Waheed Qureshi, PCSIR Laboratories, Lahore

*Numbers refer to Fig. 1

Contd . . . .

Field No./**	24/12	25/12	26/12	29/13	H/13	H2/13	H3/13	59/14	61/15	63/16	MA/17*	MA/17*	MA/18*	50/20	52/21
SiO_2	35.00	26.48	21.90	12.80	13.96	26.17	18.70	28.12	43.34	37.40	39.30	9.12	10.21	17.68	14.30
Al_2O_3	46.35	54.03	62.80	72.50	70.23	60.12	64.81	48.78	40.58	47.32	40.26	71.11	56.80	67.65	69.46
Fe_2O_3	1.55	3.72	1.77	0.45	0.88	0.72	0.97	8.56	2.02	0.78	3.50	2.02	2.45	0.60	0.71
CaO	0.34	0.30	0.27	0.10	0.12	0.25	0.13	0.67	0.73	0.38	0.52	1.10	7.03	0.41	0.33
MgO	0.03	Nil	Nil	Nil	Nil	Traces	Nil	Nil	0.21	0.07	0.10	0.40	0.35	0.06	0.05
H_2O	16.70	15.40	12.86	14.40	14.62	13.41	15.22	14.10	13.40	14.60	15.33	15.54	16.07	14.10	15.10
CO_2	—	—	—	—	—	—	—	—	—	—	—	—	6.14	—	—
	99.99	99.93	99.60	100.25	99.81	100.67	99.83	100.23	100.28	100.25	99.01	99.29	99.05	100.50	99.95
Thickness of the zone analysed	6½′	6′	6½′	4′	7′	3½′	4′	6½′	5′	3′	2½′	6′	9′	5½′	5½′
Colour	Light cream	Mottled & cream	Light cream	Very light cream	Very light cream	Light grey	Light grey to white	Yellow-ish brown	Mottled	Yellow-ish brown	White pinkish red	Cream	Cream	Light cream	Pinkish greyish white

Analyst : —M. Waheed Qureshi, P.C.S.I.R., Laboratories, Lahore.

*M. Ashraf, P.C.S.I.R., Laboratories, Lahore.

**Numbers refer to Fig. 1

Contd.

Field No./**	53/22	47/23	44/24	3/25	5/26	14/27	11/18	7/29	SF/30*	48M/31*	49M/32
SiO2	26.84	27.20	21.60	18.18	17.60	14.50	23.62	27.40	42.34	39.45	40.46
Al2O3	55.90	55.58	57.08	52.90	51.62	69.57	59.32	48.88	41.21	43.67	42.43
Fe2O3	2.10	1.42	3.32	6.50	1.63	0.95	0.68	0.06	0.21	0.63	0.63
CaO	0.51	0.29	0.38	0.87	0.42	0.32	0.61	0.52	0.23	0.33	0.19
MgO	Traces	0.08	Nil	0.22	0.09	Traces	Nil	Traces	0.05	0.25	0.20
H2O	14.60	15.40	18.00	20.00	28.20	15.00	16.44	23.60	15.54	15.90	15.69
Total :	99.95	99.97	100.38	99.27	99.56	100.34	100.07	100.46	99.58	100.23	99.60
Thickness of the zone analysed	4½′	8′	4½′	4½′	5′	9′	9′	8½′	6′	7′	7½′
Colour	Cream to pinkish cream	Light cream to yellow	Light cream to yellow	Cream	Light cream	White to pinkish white	Creamish white	White	White	Cream	Creamish white

Analyst : —M. Waheed Qureshi, P.C.S.I.R., Laboratories, Lahore.
*M. Ashraf, P.C.S.I.R., Laboratories, Lahore.

**Numbers refer to Fig 1.

TABLE 2

WEATHERED GEOLOGICAL SUCCESSION

Cretaceous Sequence	
2. LUMSHIWAL FORMATION (Lumshiwal Sandstone)	Light-coloured sandstone with carbonaceous shale bands.
1. CHICHALI FORMATION (Belemnite Beds)	Dark green and almost black shales and sandstone with Cephalopods
Jurassic Sequence	
2. SAMANA SUK LIMESTONE (Baroch Limestone)	Grey and purplish, bedded limestone, often semi-porecellaneous
1. DATTA FORMATION (Variegated Beds)	Variegated beds consisting of reddish brown, ferruginous sandstones, carbonaceous shales. Also red shales and laterite.
——UNCOMFORMITY——	
Triassic Sequence	
3. KINGRIALI FORMATION (Kingriali Dolomite)	Massive, light coloured dolomites limestones and sandstones.
2. TREDIAN FORMATION (Kingriali Sandstone)	Variegated sandstones.
1. MIANWALI FORMATION (Ceratite Beds)	(*b*) Mittiwali Shale Member: green shales with minor interbeds of sandstone and limestone.
	(*a*) Kathwai Dolomite Member : brownish weathering thin-bedded dolomite and light-grey limestone.

ACKNOWLEDGEMENTS

The authors are thankful to Farooq Ahmad Khan, Assistant Geologist and Nasrullah Ahmed Apprentice Geologist of Mineral Development Wing, W.P.I.D.C., Karachi for their cooperation during the field work. They also owe a great debt of gratitude to Lt. Col. Shahnawaz Khan of Shanico Mine Owners and Malik Karam Buksh of Chiniot Collieries for the facilities and cooperation extended to us during the field work. Thanks are also due to Prof. Dr. F.A. Shams, Head of Geology Department, Punjab University, Lahore for his critical discussions and correction of the manuscript.

REFERENCES

Dex Sitter, L.U., 1956 STRUCTURAL GEOLOGY. MacGraw Hill Book Co. Inc., New York.

Fox, C.S., 1928 A contribution to the geology of the Punjab Salt Range. *Rec. Geol. Surv. India*, 61, 147.

Gee, E.R., 1944 The age of the Saline Series in the Salt Range of the Punjab. *Proc. Nat. Acad. Sci., India*, 14, (6) Sec. B., pp.

Kataisky, Y.D., 1963 PROSPECTING FOR MINERALS. MIR publishers, Moscow.

Wadia, D.N., 1953 GEOLOGY OF INDIA. 3rd Ed., MacMillan & Co. London.

Wynne, A.B. 1878 On the Geology of the Salt Range in the Punjab. *Mem. Geol. Surv. India*, 14, 1-310.

Received January, 1971

PRELIMINARY ACCOUNT OF THE HARICHAND ULTRAMAFIC COMPLEX, MALAKAND AGENCY, N.W.F.P., PAKISTAN

BY

IJAZ HUSSAIN UPPAL

Geology Department, Punjab University, Lahore

Abstract : *The Harichand Ultramafic Complex, in the Malakand Agency, covering about 45 square miles, has been mapped for the first time on a scale of 6 inches to 1 mile and is presented here on a reduced scale of 1 inch to 1 mile.*

The complex constitutes large bodies of harzburgite with small conformable outcrops of dunite rock. The harzburgite-dunite bodies are partially surrounded by peridotite rock which is serpentinized along its contact with the country rocks, consisting of low grade schists. Two small bodies of metagobbroic rock are present in the metamorphic formations falling within the mapped area.

Chromitite at places is associated with dunite, while orthopyroxenite dykes sporadically traverse the area.

Preliminary account based on field observations and petrographic studies is given, while the results of detailed petrological and chemical work will be presented in a later communication.

INTRODUCTION

Along northern and western border of Pakistan (West) a series of ultramafic bodies are exposed, from Malakand agency in the north to the Chagai District in the south, with the distribution pattern apparently following the regional tectonic trend (Fig. 1). Many of these bodies are chromite-bearing.

The chromite was discovered in Zhob Valley by Vredenburg in 1901, and is being exploited since 1903, but little work on genesis of the host rocks, the ultramafic bodies, has been done. The outcrops of Fort Sandeman, Hindubagh, Khanozai, Chagai and Kharan have been studied by Asrarullah (1960), and Bilgrami (1964, 1968), but little information is available about the rocks from tribal territories of Mohmand, Waziristan and Malakand Agency (The Harichand Complex). The author therefore chose ultramafic rocks of the Malakand agency. It has been named as the Harichand Ultramafic Complex after the locality of Harichand (Long. 71° 48°' E; Lat. 34° 25′ N). It can be reached by a metalled road from Shergarh, and by fair-weather un-metalled road from Dargai. Both these villages are situated along Mardan-Malakand highway.

The Complex is exposed as three large and a few smaller outcrops, making an elongated belt which is about 3 miles wide and extends for about 15 miles from west of Sakhakot (Long. 71° 54′ E ; Lat. 34° 27′ N) on Mardan-Malakand highway to Qila (Long. 71° 41′ 30″ E ; Lat. 34° 27′ 30″ N).

The area is one of the low topography, the average height of the valley floor is about 1500 feet above sea level. Most of the hills are be-

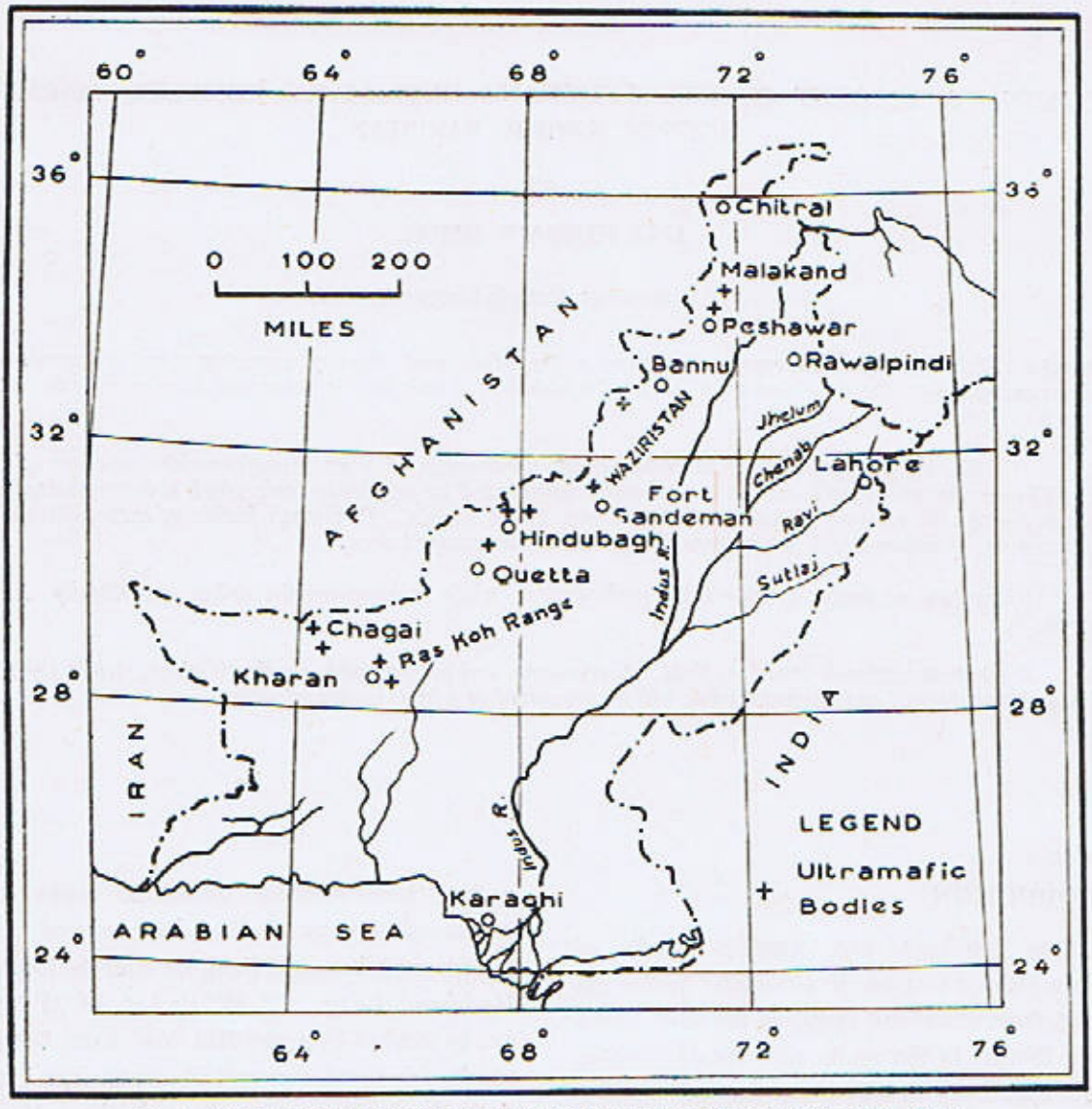

Fig. 1. Known chromite-bearing ultramafic bodies in West Pakistan (Asrarullah, 1960)

tween 2250 and 2750 feet high while the highest peak, Badasar, is about 3356 feet above sea level. The area is drained by few streams which are fed by small seasonal nallas with their numerous tributaries that form a dentritic type of drainage pattern. The rocks are generally free of vegetation and ideally exposed for study. The area is dry and hot in summer, sothat it can be best investigated during winter season.

The occurrence of the complex was mentioned by Asrarullah (1960). Afterward, Ali and Amin (1963) gave a brief account of chemistry of chromite from the area. Recently some rodingite rocks from the area have been described by Qaiser *et al.* (1970).

Very little is known about the geology of the Harichand Ultramafic Complex. General mapping of the complex has been carried out by the

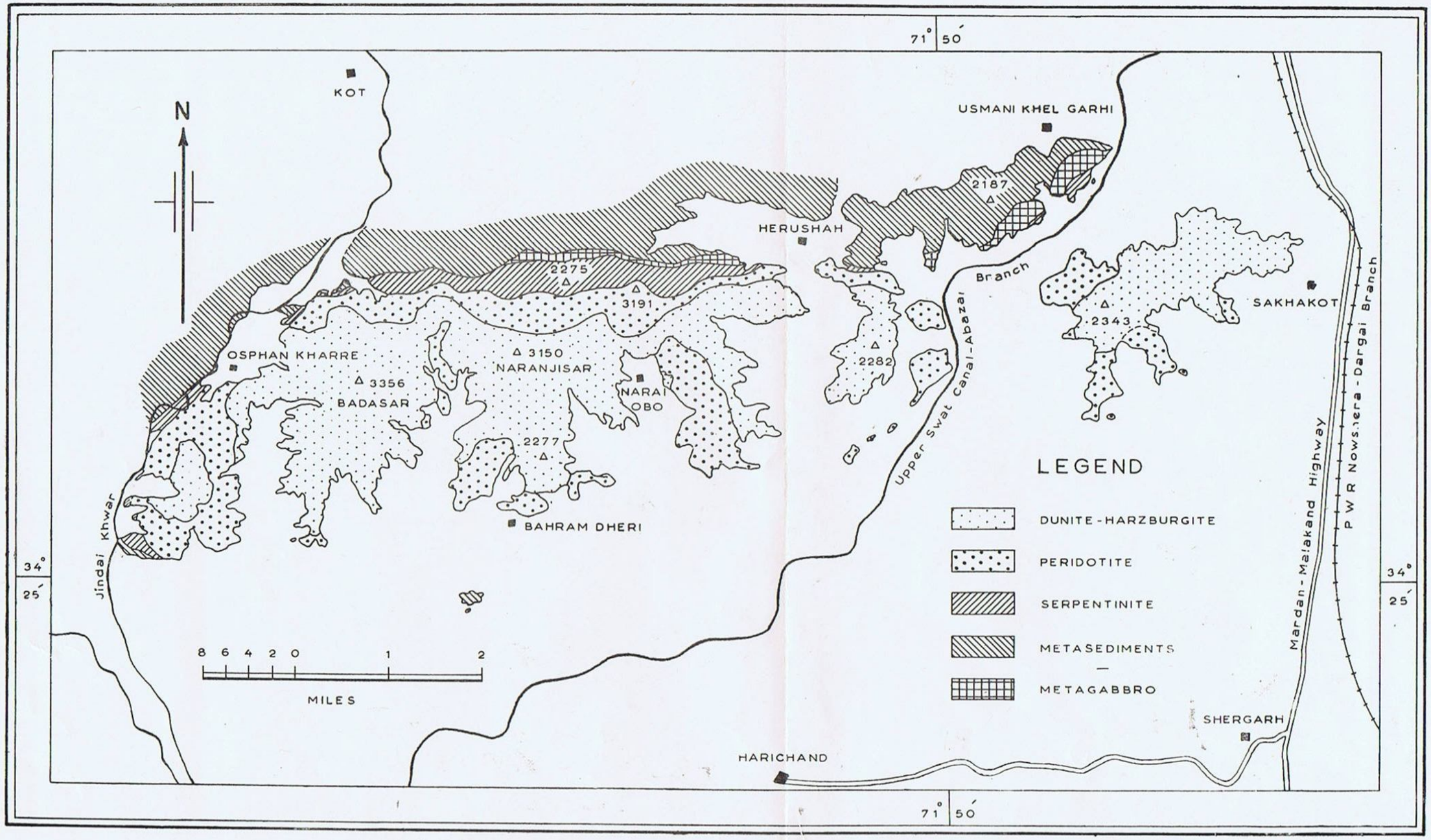

Fig. 2. Geological map of the Harichand ultramafic complex, Malakand Agency, Pakistan, Geology by I.H. Uppal, 1972

author, using photographic enlargements of one inch topographic sheets to a scale of 6 inches to one mile. Detailed laboratory work is in progress and the present note is meant to give a preliminary account of the complex.

GENERAL GEOLOGY

The ultramafic complex has an east-west strike with a northward dip ranging from 60° to 90°, and is partly in contact with a series of low grade metasediments. Along the northern and western borders of the complex, the metasedimentary rocks are well exposed and consist mainly of chlorite schist and phyllite, biotite-muscovite-quartz schist, graphite schist, calcareous schist, talc-schist and soapstone. A small elognated body of metagabbroic rock separates the ultramafic complex and schistose metasediments in west of Herushah (Long. 71° 48′ 30″; Lat. 34° 38′ N). Another body of metagabbroic rock is exposed in the south of Usmanikhel Garhi (Long. 34° 29′ 25″ ; Lat. 70° 51′ 20″ N). In the south and east of the complex, no metasedimentary rock is exposed, except a small knoll of calcareous schist, therefore nothing is known about the contact on these directions.

Thin lenses of rodingite are present within the ultramafic mass along the western and northern contact zone ; these will be dealt with separately in a later communication.

Nearly two third of the ultramafic mass is composed of harzburgite with small conformable but randomly spread outcrops of dunite rock. There are three dunite-harzburgite exposures (Fig. 2) which are partly to completely surrounded by peridotite rock. Outcrops of dunite are present in peridotite as well having relationship similar to that of the former with harzburgite. The contact of harzburgite with peridotite is transitional. The peridotite is in turn surrounded by a narrow zone of serpentinite along the contact of ultramafic complex with the metasediments and other enclosing rocks.

Most of the dunite outcrops are barren, while at places chromite is concentrated to constitute chromitite rock. The latter commonly exhibits layering due to differentiation but sometime it occurs as compact bands and rarely as "grape-shot" ore.

The entire ultramafic mass is sporadically traversed by thin pyroxenite dykes. At places veins of tremolite, talc-tremolite, talc-carbonate and quartz are abundant, but their age relationship is not yet established.

DESCRIPTION OF LITHOLOGIC TYPES

Dunite and Harzburgite

As already mentioned, the harzburgite holds numerous outcrops of dunite rock which are randomly spread in the former. These bodies are always elongated with their longer axes ranging from one foot to dozens of feet and are conformable with general strike of the area. On the scale of mapping adopted at present, it was not possible to map separately dunite from harzburgite due to small sized outcrops of the former ; therefore both types are described collectively.

The harzburgite is brown coloured coarse grained rock, which commonly appears massive, and sometime shows conspicuous layering due to concentration of pyroxene crystals which stand prominently on the weathered surface. The fresh rock is olive-green with easily recogniseable crystals of pyroxene. The individual crystals of olivine, however, are difficult to identify in hand specimen. The dunite appears similar to harzburgite but lacks pyroxene.

Microscopic study reveals that the mineralogy of these rock types is fairly simple. Dunite commonly consists of 98% of olivine which is fresh to partially serpentinized and the harzburgite consists of about 15% orthopyroxene in addition to dominent olivine. Most commonly these rock types show xenomorphic granular texture but sometime it is pseudoporphyritic due to large

subhedral crystals of orthopyroxene and olivine enclosed in a granular matrix of olivine.

Olivine is commonly anhedral (Fig. 3) and frequently displays subparallel translational lamellae. Its composition ranges from forsterite to chrysolite. It commonly contains inclusions of chromite and exhibits all degrees of alteration to serpentine.

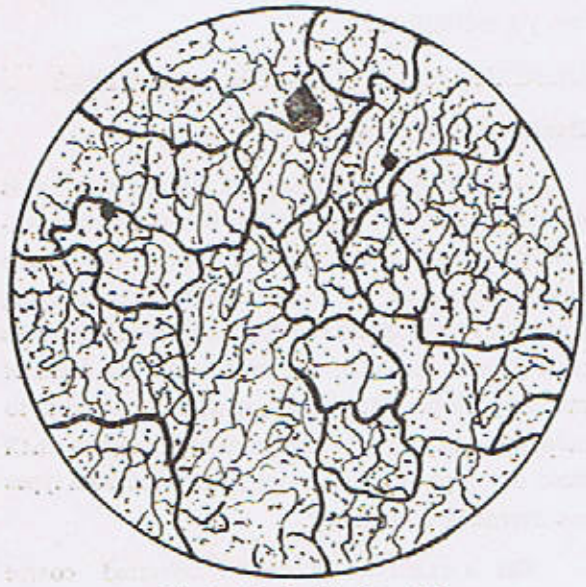

Fig. 3. Typical dunite ×25

Pyroxene composition is commonly in the range of enstatite but bronzite is not uncommon. The poikilitic inclusions of olivine grains inside large pyroxene crystals are noteworthy. Pyroxene is of "Bushveld type", so that it shows conspicuous exsolution texture with lamellae of clinopyroxene oriented parallel to the (100) plane of the orthopyroxene host. Sometime discontinuous rows of small blebs represent the clinopyroxene lamellae (Fig. 4). Pyroxene does not show recogniseable zoning while alteration to fine grained talc is common.

Chromite is a common accessary mineral found in these rocks; it is commonly anhedral, generally fresh, but at places shows alteration to magnetite. Very thin veinlets of carbonate mineral are also seen. Accessary minerals are rare and include limonite and iddingsite.

The compositions of olivine and orthopyroxene in individual rock samples are fairly uniform : olivine from representative samples of dunite and harzburgite is $Fo_{88\cdot5}$ ($\hat{r}=1.676$) and Fo 87.5

Fig. 4. Harzburgite, exhibiting "Bushveld Type" orthoporoxene. ×25

($\hat{r}=1.677$) respectively ; orthopyroxene in the same sample of harzburgite has composition almost $En_{85\cdot0}$ ($\hat{r}=1.678$). Modal composition of the sample is as follows : olivine, 71.5% ; serpentine, 11.4% ; orthopyroxene, 11.2% ; talc 0.6%; chromite 1.0% ; and iddingsite in minor amount.

Peridotite

The peridotite rock appears brownish in field although fresh surface is dark green in colour. It is a coarse grained rock and is generally compact, but at places shows a conspicuous foliation. Randomly distributed crystals of whitish pyroxene are visible on weathered surface while their partial removal produces a sort of pitted effect. The

peridotite also contains small outcrops of dunite which appear similar to those contained inside harzburgite except for their relatively stronger serpentinization.

The peridotite consists chiefly of olivine or serpentine after it, and altered pyroxene with minor amounts of chromite and other accessary minerals. Commonly the rock shows a xenomorphic granular texture, while in partially serpentinized rocks, blades and plates of colourless antigorite project radially along cracks into cores of relict olivine in an "exploded-bomb-fashion." The rock also contains numerous veins of chysotile serpentine and occasionally of structureless serpophite.

The composition of olivine in the peridotite rock ranges from forsterite to chrysolite, while the nature of pyroxene is difficult to identify because of its common alteration. The pyroxene along harzburgite-peridotite contact zone is commonly altered to serpentine but generally to a product which appears colourless to slightly brownish by plane polarized light but between cross nicols shows polarization colours of second order. It could not be identified so far. Rare relicts of augite are recognizeable (Fig. 5).

In general there is considerable secondary iron ore within altered pyroxene crystals displaying lattice texture. Chromite is generally anhedral and fresh but its alteration to magnetite is not uncommon. Other accessary minerals include carbonate, iddingsite and limonite.

Modal composition of a typical sample with olivine $Fo_{86.5}$ ($\hat{\rho} = 1.679$) and augite ($C \wedge Z = 43°$) is: olivine, 62.6%; serpentine after olivine, 22.4%; augite, 0.2%; altered pyroxene, 13.3%; chromite 0.1%; magnetite, 0.1%; limonite and iddingsite, 0.1%.

Serpentinite

The serpentinite of Harichand complex is grey coloured compact rock, with partially bleached red crystals of carbonate. The fresh rock is green coloured. The rock shows no layering except when marked by zones of chromite concentration.

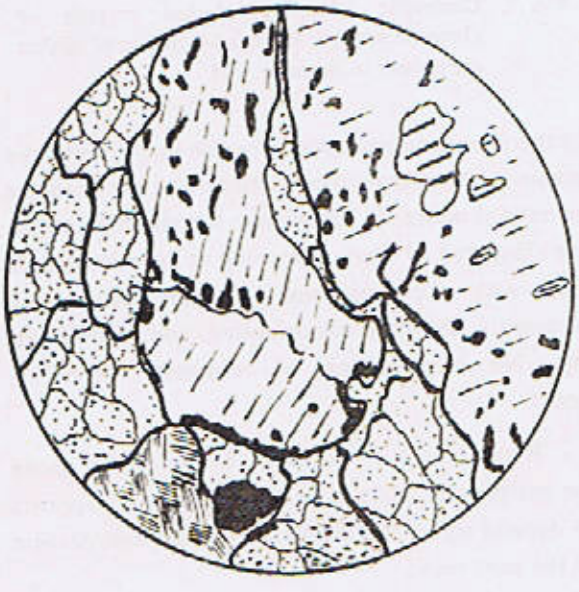

Fig. 5. Peridotite showing alteration of augite mineral. Few relicts of augite and secondary iron ore stand prominently. ×25

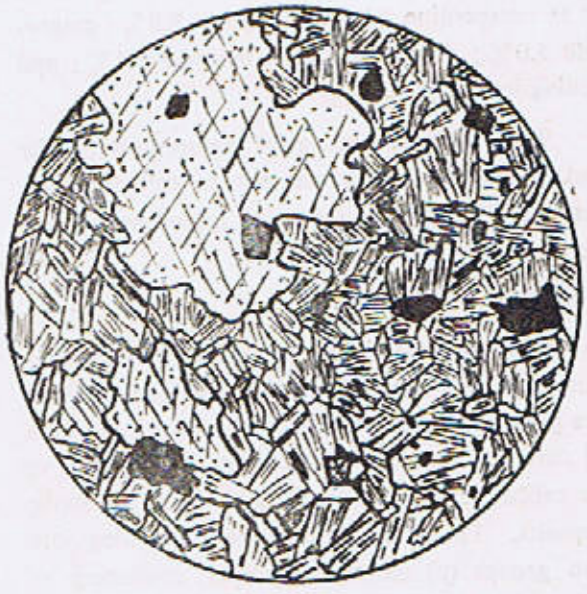

Fig. 6. Carbonate-serpentinite with antigorite displaying rectangular texture. ×25

Microscopically the rock consists mainly of blades and plates of antigorite displaying a rectangular texture (Fig. 6). Occasionally, the chrysotile veinlets reveal a mesh texture enclosing antigorite, rarely with relicts of olivine. At places colourless or light green chlorite, with or without serpentine, is found ; especially along the contacts of ultramafic mass with the enclosing rocks.

Carbonate is present in variable amounts with its outlines controlled by blades and plates of antigorite.

Magnetite occurs as one of the accessary minerals ; it is generally anhedral and is randomly distributed. A lattice texture after pyroxene, consisting of antigorite and magnetite, is commonly seen. The magnetite is clearly formed from two sources : as a by-product of serpentinization and by complete or partial alteration of pre-existing chromite.

Other accessary minerals include fresh chromite, limonite and iddingsit.

Modal composition of a typical rock specimen is as : serpentine, 84.7% carbonate, 9.8% ; magnetite 5.0% ; chromite 0.2% ; limonite 0.1% ; and iddingsite 0.1%.

The rock with rectangular texture of antigorite but lacking lattice texture can be called dunite-serpentinite while the rock with lattice texture can be termed peridotite-serpentinite.

Chromitite

As already mentioned, the dunite rock in harzburgite as well as peridotite and dunite-serpentinite are generally barren, except for local concentration of chromite in sufficient amounts for the rock to be called "chromitite" and may form economic deposits. The chromitite can be subdivided into two groups (*a*) chromitite proper, consisting of almost pure chromite and (*b*) dunite exceptionally rich in chromite. The latter type constitutes rather low grade ore.

The chromitite proper is a medium to coarse grained rock with chromite grains displaying metallic lustre and anhedral to subhedral outlines.

Microscopic study reveals that in chromitite anhedral to subhedral chromite, ranges from 30% to 80%, with rare euhedral crystals (Fig. 7).

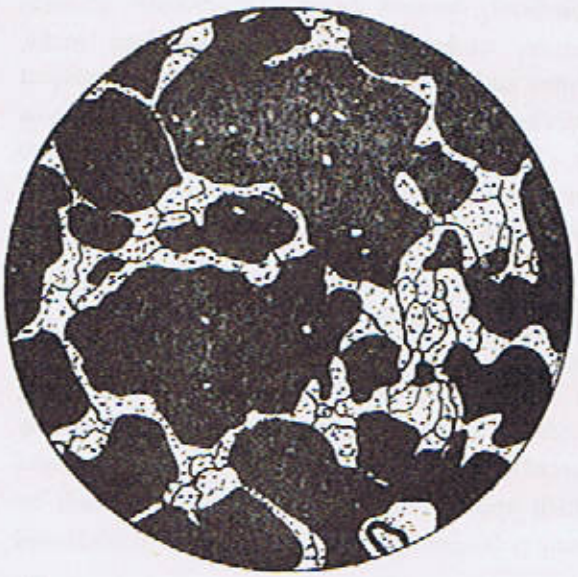

Fig. 7. Chromitite showing anhedral crystals of chromite mineral. Rounded inclusion of olivine are present in chromite. × 25

In the specimens exceptionally rich in chromite, the grains are closely packed, with olivine occurring as interstitial material. Sometime the chromite grains are elongated to mark a layering at the microscopic scale with a conspicuous pull-apart texture and frequently showing microfolding and microfaulting. No cross-cutting of chromite layers is noted.

Replacement of chromite by magnetite along the peripheries and cracks is common and appears to depend upon the degree of the serpentinization of the host rock.

The olivine generally occurs as mosaic of irregular grains, occasionally sheared and foliated. Rounded and elongated inclusions of olivine, or of

serpentine after it, are common in chromite but reverse is also seen.

Replacement of olivine by serpentine is exhibited in all degrees, and the serpentine thus formed commonly displays a mesh texture. The secondary minerals include carbonate, chlorite, iddingsite and limonite.

A typical specimen with olivine Fo_{89-3} (β=1.674) has : chromite, 70.2%; olivine, 16.7%; serpentine, 12.2%; carbonate and iddingsite etc, 0.7%.

Pyroxenite

The dykes of pyroxenite vary in thickness from 9 inches to 2.5 feet and can be traced over hundreds of feet. The pyroxenite is coarse grained, black or dark green in colour and consists mainly of orthopyroxene having a composition varying from enstatite to bronzite. The pyroxene is of "Bushveld type" and commonly exhibits partial alteration to talc.

Fig. 8. Pyroxenite exhibiting xenomorphic texture and replacement of pyroxene by colourless amphibole ×25

At places small amounts of olivine are present either as an interstitial mineral or as poikilitic inclusions in pyroxene. Chromite and carbonate are common accessories, while a colourless amphibole (Fig. 8) and limonite are also frequently present.

A representative sample consisting of bronzite pyroxene, En_{85-2} (β=1.682; -ve) have : pyroxene, 78.6%; talc 13.9%; amphibole 7.3%; and chromite 0.8%.

CHEMISTRY

Chemical analyses of typical samples of different rock types have been carried out and are given in Table I.

CONTACT PHENOMENA

The contact between the ultramafic mass and the metasediments and other enclosing rocks, is every where steep and concordant, but at places exhibits effects of shearing. Despite attempts, no evidence of thermal induration or hornfelsic structure is so far noted in any specimen of the country rock at or near the contact. At places the contact is marked by talc-carbonate, talc-tremolite or chlorite rocks. These and other interesting phenomena will be reported when their detailed field and laboratory investigations are completed.

TABLE 1

	Dunite	*Harzburgite*	*Peridotite*	*Serpentinite*	*Chromitite*	*Pyroxenite*
	13017	13073	12285	12300	13591	13014
SiO_2 ..	38.01	40.98	41.24	39.79	7.93	55.74
Fe_2O_3	6.87	3.33	5.35	4.46	3.67	3.41
FeO ..	5.31	6.96	5.45	4.08	12.68	6.29
Al_2O_3 ..	..	1.18	1.08	3.08	9.91	..
MnO ..	.15	.19	.22	.03	.04	.07
Ti_2O ..	..	..	..	..	.09	.04
P_2O_5 ..	..	..	..	..	.62	..
Cr_2O_3 ..	1.76	.19	1.47	.31	33.25	.35
MgO ..	45.52	41.46	36.68	37.14	22.09	33.04
CaO ..	..	.42	1.98	.18	2.64	1.20
K_2O ..	.04	.09	.01	..	n.d.	.008
Na_2O ..	.13	.03	.18	..	n.d.	.061
H_2O+ ..	1.13	4.75	0.36	11.69	6.08	.15
H_2O^- ..	.33	.09	.59	.03	.23	.30
CO_2 ..	..	..	..	.18	..	..
Total : ..	99.25	99.71	100.60	99.71	100.62	100.659

Analyst : I. H. Uppal.

ACKNOWLEDGEMENT

Thanks are due to Prof. F.A. Shams, Geology Department, Punjab University, Lahore for his constant encouragement, advice and critical reading of the manuscript.

REFERENCES

Asrarullah, M., 1960 Geology of Chromite in West Pakistan. CENTO SYMPOSIUM ON CHROME ORE. Ankara, Turkey, 38-53.

Bilgrami, S.A., 1964 Mineralogy and petrology of the central part of the Hindubagh Igneous Complex, Hindubagh minning district ; Zhob Valley, West Pak. *Rec. Geol. Surv., Pakistan*, **10**, (2c), 1—28.

Bilgrami, S.A., 1968 Geology and chemical mineralogy of the Zhob Valley chromite deposits, W. Pak. *Amer. Min.*, **54**, 134-148.

Challis, G.A., 1965 The origin of New Zealand ultramafic intrusion, *Jour. Petr.*, **6**, 322-364.

Deer, W.A., Howie, R.A., and Zussman J. 1964 AN INTRODUCTION TO THE ROCK FORMING MINERALS. Longmans, Green and Co. Ltd., London.

Hayden, H., 1918 General report of the geological survey of India for the year 1916. *Rec. Geol. Surv., India*, **48**, 12.

Hess, H.H., 1933 Problems of serpentinization and the origin of certain chrysotile Asbestos, talc and soapstone deposits. *Econ. Geol.*, **28**, 634-657.

Hess, H.H., 1952 Orthopyroxenes of the Bushveld type, ion substitutions and changes in unit cell dimensions. *Amer. Jour. Sci.* BOWEN VOL., 73-187.

Johannsen, A., 1963 A DESCRIPTIVE PETROGRAPHY OF THE IGNEOUS ROCKS, **4.** the University of Chicago Press, Chicago.

Qaiser, M.A, Akhtar, S.M., and Khan, A.H., 1970 Rodingite from Naranji Sar, Dargai ultramafic complex, Malakand. *West Pakistan Min. Mag.*, **37**, 735-738.

Shams, F.A., 1964 Structures in chromite bearing serpentinites, Hindubagh, Zhob Valley, W. Pakistan. *Econ. Geol.*, **59**, (7), 1343-1347.

PROBLEMS OF STRATIGRAPHIC NOMENCLATURE IN THE HAZARA DISTRICT, N.W.F.P., PAKISTAN

BY

AFTAB A. BUTT

Geology Department, Punjab University, Lahore

Abstract : *Three formations, Hazara Formation, Abbottabad Formation and Kihal Formation, the last two with five and two members respectively, are recommended for the unfossiliferous sequence of the (?) Paleozoic of Hazara stratigraphy, as opposed to Hazara Group and Abbottabad Group of Latif* (1970).

INTRODUCTION

Waagen & Wynne (1872) for the first time made a systematic attempt to establish the stratigraphy of Hazara. Middlemiss (1896) gave a detailed account of the geology of this region together with a geological map. However, several lithostratigraphic units recognised by these authors did not follow the modern concept of stratigraphic nomenclature, for example the "Infra-Triassic Series" of Moddlemiss ("Below the Trias" of Waagen & Wynne) and the "Numulitic Series" (Nummulitic Formation of Waagen & Wynne). During the years 1960-1970, some publications have appeared concerning the stratigraphic terminology of Hazara (Marks & Muhammad Ali, 1961, 1962 ; Davies & Gardezi, 1965 ; Gardezi & Ghazanfar, 1965 ; Butt, 1968 ; Latif, 1970). The contribution of Latif, despite some shortcomings, is an attempt to define formally the entire succession of Hazara. However, in view of the recommendations of the Stratigraphic Committee of Pakistan many new names proposed by Latif for the Mesozoic and Tertiary are regarded unpurposeful because these units have their extension in the adjoining areas of Salt Range, Kala Chitta, Potwar and Kohat (Samana Range), where they have since long been established with formal, actually acceptable nomenclature. The stratigraphic nomenclature of the unfossiliferous succession of Hazara of doubtful age, (?) Paleozoic, as proposed by Latif, is far from satisfactory. The purpose of the present study is to discuss these units and to attempt to bring them in accordance with the normal practice of stratigraphic nomenclature (see Fig. 1).

STRATIGRAPHIC UNITS

Hazara Formation

The name Hazara Formation has been formalized here for the "Slate Series" of Middlemiss (1896). Marks & Muhammad Ali (1961) named this unit as the Hazara Slate Formation, which name has been followed popularly in later years (Davies & Riaz, 1963 ; Davies, 1963 ; Davies & Gardezi, 1965, Gardezi, 1968), while Latif (1970) proposed the new name of Hazara Group. These rocks belong to the oldest exposed sequence in Hazara of which excellent exposures can be seen along the Lora-Maqsood road and along the Abbottabad-Nathiagali road.

If we study the main lithological features of this lithostratigraphic unit, we find that it is exposed as thick succession of unfossiliferous, well

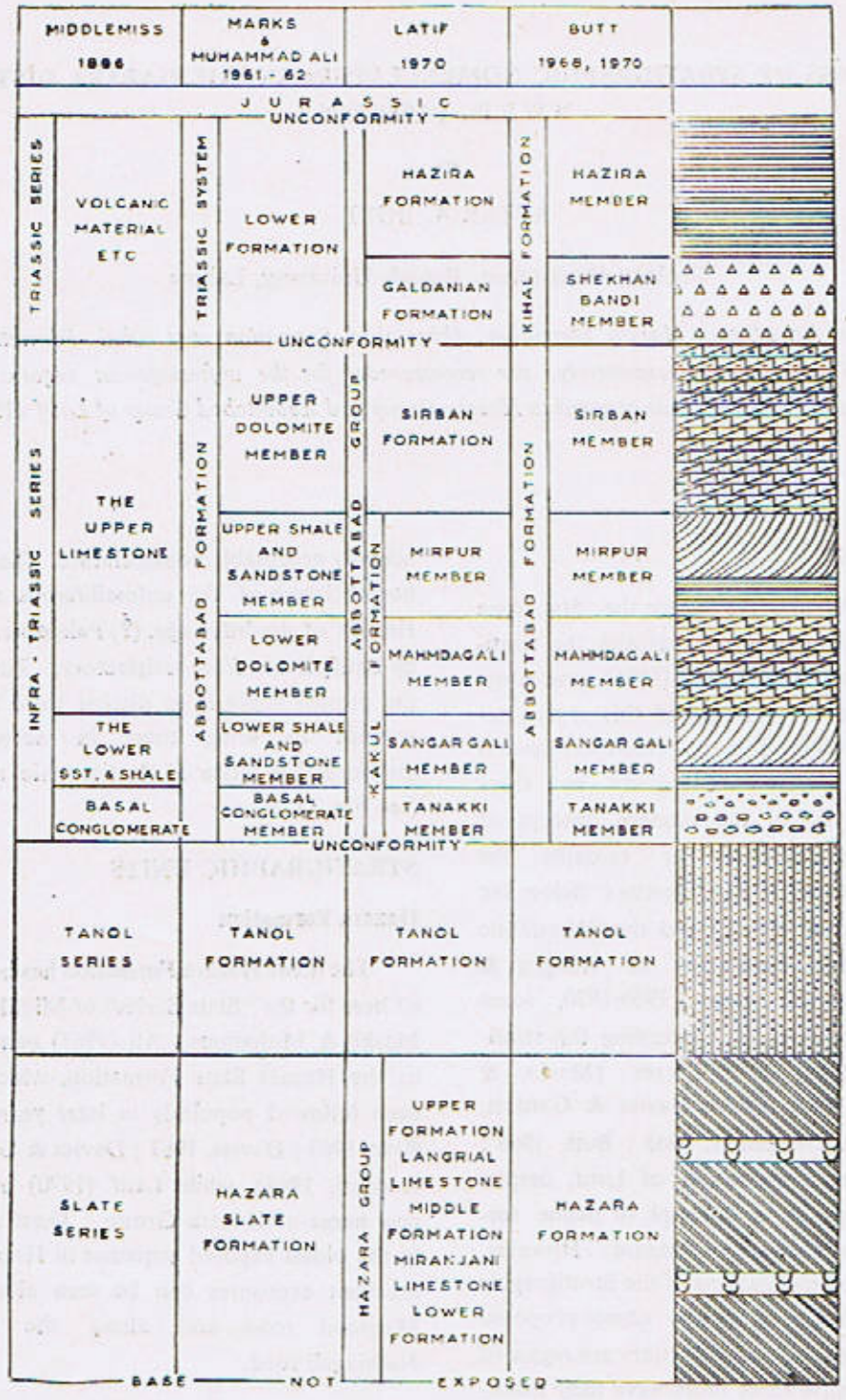

Fig. 1. Lithostratigraphic units of the (?) Paleozoic of Hazara as recognised by different authors.

bedded, largely fissile rocks, commonly showing an alternation of arenaceous and argillaceous deposits. In addition, according to their supposed stratigraphic position and structural characters, two types of algal limestones are also present. According to Gardezi (1968), the lower one is known as the Miranjani Algal Limestone and the upper one, the Langrial Algal Limestone (Lungurial band of Middlemiss, 1896). From the lithological features it is evident that this rock unit is not composed of true slates for which reason the name Hazara Slate Formation cannot be adopted. Even Marks & Muhammad Ali (1961, p. 48) themselves confirm that "Although the various names applied to this formation all stress its slaty appearance, true slates form only small part". Keeping in mind that the rock character is of varied nature, our purpose of nomenclature is best served if we call it as Hazara Formation, named after the Hazara district. Exposures at Baragali can be regarded to form the type locality along the Natiagali-Abbottabad road.

Latif (1970) recognised five formations in his newly proposed Hazara Group, Lower Formation, Miranjani Limestone, Middle Formation, Langrial Limestone, Upper Formation respectively. If we follow his description (p. 10), he states that "The Lower, Middle and Upper Formation all taken together are composed of low grade slates, argillites, silty shales, sub-greywacke sandstones and siltstones, interbedded with gypsum and calcareous shales". This fivefold division on the basis of occurrence of two types of algal limestones is not according to the requirements of stratigraphic nomenclature, because his three formations are not in accordance with the formal definitions, and, moreover, they do not have diagnostic characters to separate them from one another. If we want to put more emphasis on the structural characters of the limestones as a basis of subdivision, we must keep in view this fact that fundamentally these limestones are having the same composition and the variation in the physical character, one showing wavering ridges on the weathering surfaces, and the other typically nodular, can possibly exist when we see the enormous thickness of the flyshoid sediments amongst which occasionally the environments gave rise to the deposition of algal limestones. It can certainly be said here that in the present state of our knowledge there is no sound basis to accord a formational rank to fivefold division, and hence the stratigraphic name Hazara Formation is introduced here.

Waagen & Wynne (1872) applied the name Attock Slates to the Hazara Formation on the basis that the Attock Slates, the type exposures of which are found at Attock along the Grand Trunk Road, do extend in Hazara district. Although there is a striking similarity of the deposits found at Attock and those in Hazara, Tahirkheli (1970) has taken a different view. Under these circumstances it is considered appropriate to use the name Hazara Formation for the deposits exposed in Hazara district.

Abbottabad Formation

Marks & Muhammad Ali (1962) proposed the name Abbottabad Formation for the "Infra-Trias" of Middlemiss (1896) after its occurrence near the town Abbottabad, the type section being exposed 5½ miles south of Abbottabad near Khotedi Qabar along the Hazara Trunk road. They distinguished five members on the basis of their detailed study of these dposits in their previous paper (1961). However, they did not give any geographical name to any of their members. Latif (1970) followed the concept of lithostratigraphic subdivision of the authors in a manner that he separated the topmost member from the Abbottabad Formation to which he gave the new name as Sirban Formation. He recognised the remaining four members which were named by him as Tanakki Member, Sangargali Member, Mahmdagali Member and Mirpur Member. These were combined by him into a single formation, the Kakul Formation,

newly proposed by him. These two formations thus constituted his Abbottabad Group in which two more formations were included, the Galdanian Formation and the Hazira Formation.

The apparent reason of Latif's separation of the topmost member of the Abbottabadd Formation of Marks & Muhammad Ali seems to be due to the fact that the thickness of the uppermost member is considerable, estimated to be 1600 feet, and, therefore, he gave to this member the status of a formation. If we see the lithological features, we find that the Abbottabad Formation begins with clastic deposits represented by a conglomeratic member passing into an arenaceous member. This, in turn, is followed by carbonate deposits, the dolomite member, which is again overlain by an arenaceous member indicating a return to earlier sedimentary conditions. This is finally followed by carbonate deposition represented by a dolomite member. This is an example of rhythmic alternation of arenaceous and calcareous facies. Therefore, it is reasonable to include five units into a single formation. The Sirban Formation of Latif is, therefore, regarded here as Sirban Member of the Abbottabad Formation. Thus the recognition of fivefold division of the Abbottabad Formation follows the original concept of Marks aud Muhammad Ali (1962).

Muhammad Ali (1962) recognised the Abbottabad Formation in the Tanol area as well, where he identified four members, to which he also did not give geographical names either. According to him the lowermost and the uppermost members (now named here as the Tanakki Member and the Sirban Member) compare closely at both localities, while detailed differences exist in between and the general degree of metamorphism is sensibly higer in the Tanol area. If we want to correlate the sequence of the Tanol area with that of the type locality in Abbottabad area, we find that the Mahmdagali Member is not recognisable in the former locality, where on the basis of lithological characters, it would form part of the Mirpur Member.

Kihal Formation

Butt (1968) introduced the name Kihal Formation for the "volcanic material" and "yellow shales" of Middlemiss (1896) found below his "Triassic Series". The name is derived after its occurrence near Kihal village in the vicinity of Abbottabad. The formation is composed of two distinct facies, the one containing argillaceous sediments to which a stratigraphic name, the Hazira Formation was given by Gardezi & Ghazanfar (1965) and it refers to the "yellow shales" of Middlemiss. The other facies which represents "volcanic material" of Middlemiss was designated by them as the Haematite Formation. Both these units belong to the highest sequence of the Abbottabad Group of Latif (1970). Butt (1968) combined the two facies into a single formation, the Kihal Formation which consisted of two members, Hazira Member and Shekhan Bandi Member, the latter name proposed for the Haematite Formation of Gardezi & Ghazanfar (1965).

If we see the stratigraphic position of these two entirely different facies, we find that they occupy similar stratigraphic interval. Each facies is overlying the uppermost member, the Sirban Member of the Abbottabad Formation with apparent conformity and, in turn, is being overlain by the Samana Suk Formation of Jurasssic age. A band of pure white sandstone, 3 feet thick marks the top of each facies. Because of the similar stratigraphic level of these lateral equivalents in the sequence, the author feels appropriate to combine them into a single formation. As the lithological features of these stratigraphic units do not appear to have any comparison with the underlying Abbottabad Formation, they should be separated from the Abbottabad Group of Latif (1970). The view that these deposits merit separate recognition from the Abbottabad Group of Latif, has also been expressed by Fuchs (1970), while discussing the significance of Hazara stratigraphy to the Himalayan geology.

REFERENCES

Butt, A.A., 1968 Remarks on the proposed "Abbottabad Group" of Gardezi & Ghazanfar. *Geol. Bull. Punjab Univ.*, **7**, 79.

Davies, R.G., 1963 Some preliminary observations on the geological structure of the Hazara Slate Formation in the area of the Lora-Maqsud Road. *Ibid*, **3**, 32-35.

Davies, R.G., and Ahmad, R., 1963 Fossils from the Hazara Slate Formation at Baragali, Hazara, West Pakistan. *Ibid.*, **3**, 29-30.

Davies, R.G., and Gardezi, A.H., 1965 The Presence of *Bouleiceras* in Hazara and its geological implications. *Ibid.*, **5**, 23-30.

Fuchs, G., 1970 The significance of Hazara to Himalayan geology. *Jahrb. Geol. Budesanst.*, **15**, 21-23.

Gardezi, A.H., 1968 Note on the geology of area around Nathiagali, district Hazara. *Geol. Bull. Punjab Univ.*, **7**, 71-78.

Gardezi, A.H., and Ghazanfar, M., 1965 A change of facies at the base of the Jurassic in district Hazara, West Pakistan. *Ibid.*, **5**, 53-54.

Latif, M.A., 1970 Explanatory notes on the geology of south eastern Hazara, to accompany the revised geological map. *Jahrb. Geol. Bundesanst.*, **15**, 5-20.

Marks, P., and Muhammad Ali Ch., 1961 The geology of the Abbottabad area with special reference to the Infra-Tria. *Geol. Bull. Punjab Univ.*, **1**, 47-55.

Marks, P., and Muhammad Ali, Ch., 1962 The Abbottabad Formation : new name for Middlemiss' Infra-Trias. *Ibid.*, **2**, 56.

Middlemiss, C.S., 1896 The geology of Hazara and the Black Mountain. *Mem. Geol. Surv., India.* **26**, (1), 1-290.

Muhammad Ali Ch., 1962 The stratigraphy of the southwestern Tanol area, Hazara, West Pakistan. *Geol. Bull. Punjab Univ.*, **2**, 31-38.

Tahirkheli, R.A.K., 1970 The geology of the Attock-Cherat Range, West Pakistan. *Geol. Bull. Peshawar Univ*, **5**, 1-26.

Waagen, W., and Wynne, A.B., 1872 The geology of Mount Sirban in upper Punjab. *Mem. Geol. Surv.. India*, **9**, 331-350.

Received December, 1970.

NOTICES, ABSTRACTS AND REVIEWS

A NOTE ON THE PERSISTENT PARH

The Parh Limestone is one of the most extensive formations of West Pakistan. It runs from Gadani in Las Bela in the south to the tribal teritory of Waziristan in the north (Fig. 1). The most remarkable character of this formation is its persistence in lithology from one end to the other though it passes through variable environments during its deposition.

The formations both below and above it show lateral and vertical variation in lithology. It is not only true of Jurassic strata and the rocks below but also of the *Belemnite* Shales which are generally of Cretaceous age as the Parh itself. The rocks above Parh show much more rapid variation in lithology. In some areas they are represented by shales while in other by limestone or even by sandstone (Figs. 2,3,4). All of them are of Cretaceous age.

The author had a chance to run sections through the Parh Limestone at a number of places from Las Bela to Fort Sandeman and to the west in Raskoh, and east in Gokurt area. It has a big variation in thickness but faithfully maintains its lithology throughout, a character which impresses the regional geologist.

Lithologically the limestone is porcellaneous or sub-lithographic, white, light grey also with pink, green and red colours in places arranged sometimes in alternate bands. The beds range from a few inches to 2 feet in thickness and show conchoidal fracture. In places it contains in various propertions bands of volcanic rocks. Nodules and small thin lenses of chert between the beds are also found in many exposures.

The above lithological description is true for the various parts of Baluchistan geosyncline e.g., Miogeosyncline, Eugeosyncline, Geanticline and submerged ridges.

This factor proved a very reliable guide in mapping and in discerning the structure of the highly disturbed areas. There are areas where the lithologically resembling rocks of different ages are brought in juxtaposition by the structural disturbance. For example, the Ghazij Shales came into contact with the *Belemnite* Shales or Dunghan Limestone has faulted against the Jurrassic limestone of apparently similar lithology. In such cases it is the Parh Limestone along which come to the rescue of the structural geologist as a distinct, easily recognizable and reliable horizon to understand the complexities of the structure.

The figure 1 shows the area of the exposures of Cretaceous rocks where the Parh Limestone is also generally found. Some lines of the sections where the author has seen the Parh Limestone are also shown as a, b, c, d, e, f, and g on it.

(*a*) **Las Bela :** Here the Parh Limestone is exposed below the Pab Sandstone all along the western flank of the Pab Range. Thin lenses of Parh Lime stone are also found in the belt of volcanic rocks from east of Naka Kharai in Las Bela District to Gokurt in Kalat District. The isolated thin layers which are seen caught within the inter-pillows spaces and the volcanic trap has the same lithology as the Parh Limestone of the flank of the Pab Range.

(*b*) **Khuzdar :** In this area the Parh is widely exposed with an unconformity on its top. In Gungo

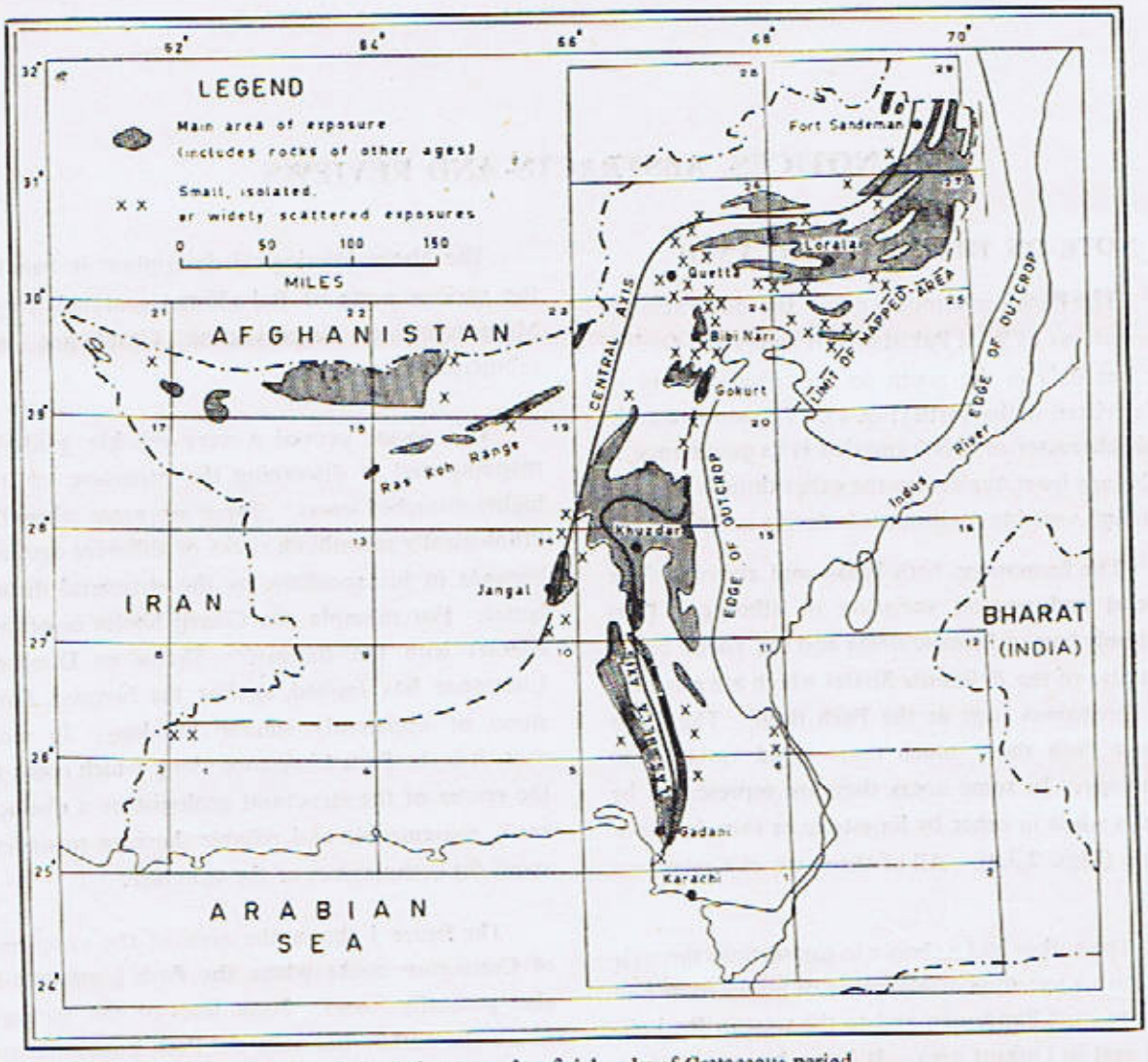

Fig. 1. General location of surficial rocks of Cretaceous period.

area 9 miles W-SW of Khuzdar it is seen interbedded with volcanic traps and overlain by a band of marly shales below the Pab Sandstone. Here also it persists in its lithology and is recognized at the first glance.

(*c*) **Jangal :** Here also the position is the same as in Khuzdar. Though the volcanic beds here increases in frequency but the Parh Limestone maintains its lithological characters.

(*d*) **Raskoh :** In the eastern Raskoh e.g. near Mal Thana on the Nushki-Dalbandin road thin lenticular bands of Parh Limestone are found in Kuchakki volcanics of Cretaceous age. The age of these volcanics is determined to be the same as that of Parh by the Photographic Survey Corporation. Thin lenses have been seen by the author sparsely dispersed in the volcanics west upto Duki Nala south of Dalbandin. Though the lenses are very thin and sparsely dispersed in the thick series of the volcanics but still stick to their individuality of lithology.

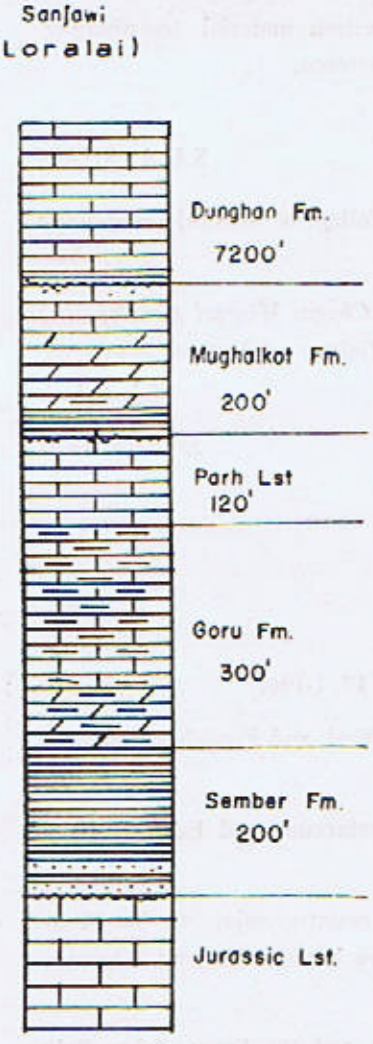

Fig. 2.

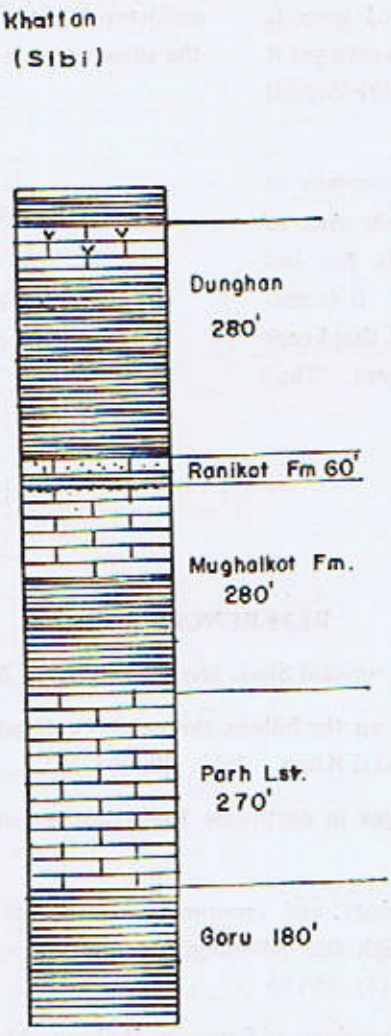

Fig. 3.

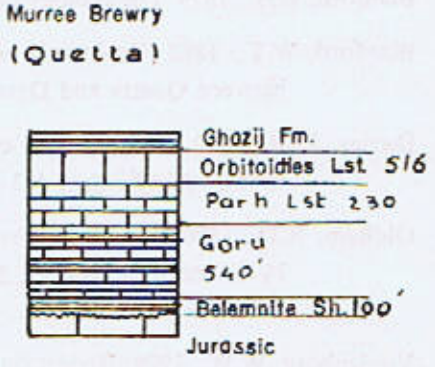

Fig. 4.

(*e*) **Gokurt :** In Gokurt area 15 miles west of Dhadar in Kachhi District the Parh Limestone is exposed below the Moro Formation of the Photographic Survey Corporation. Here also it shows its typical lithological character.

(*f*) **Quetta :** In Quetta area in the Murree Brewery gorge, the thickness of Parh Limestone is very much reduced alongwith other Cretaceous rocks compared to other areas. However, the reduction in thickness could not affect its lithology to any marked degree.

(*g*) **Loralai :** In this area the Parh Limestone shows its best exposures and imparts a beautiful panorama to the surrounding of the Loralai town by its light grey, pink and red shades on the weathered surface. It is in this locality that we can easily study its main characters of lithology though they remain the same as in other localities.

(*h*) **Zhob :** In this district the author has examined the Parh Limestone in many places. The ultrabasic intrusions of Hindubagh and other places in Zhob districts and the volcanic rocks of Chinjan and Kach

areas are supposed to occur within this formation. There also though it has accommodated igneous rocks of much greater thickness than its own yet it refrained them from interfering into its lithological characters to any marked sign.

As it has been stated above, the uniformity of the lithological character in such a wide area of deposition under variable environments has impressed the author to write this article. It is perhaps the only formation of Tethys basin that keeps its lithological characters intact throughout. Thus it provides the Pakistani stratigraphers and the sedimentologists interesting material to discover the causes of this persistence.

S.H.A. SHAH

Pakistan College of Mineral Technology
Quetta.

Presently: Chagai Mineral Development Project, Ministry of Natural Resources, Islamabad.

January, 1970

REFERENCES

Blanford, W.T., 1879 The geology of the western Sind. *Mem. Geol. Surv., India*, **17**, 1-196.

Blanford, W.T., 1883 Geological notes on the hills in the neighbourhood of Sind and Punjab formations between Quetta and Dera Ghazi Khan. *Ibid.*, **20**, 105-240.

Davies, L.M., 1940 Geographical changes in northwest India during Late Cretaceous and Early Tertiary times. *Pacific Sci.*, 483-500.

Oldham, R.D., 1890 Report on the geology and economic resources of the country adjoining the Sind-Pishin railway between Sharigh and Spintangi, and of the country between it and Khattan. *Rec. Geol. Surv., India*, **23**, (3), 93-110.

Vredenburg, W.W., 1909 Report on the geology of Sarawan, Jhalwan, Mekran and the State of Las Bela *Mem. Geol. Surv., India*, **38**, (3), 189-215.

Williams, M.D., 1959 Stratigraphy of the Lower Indus basin, West Pakistan *Proc. 5th World Petroleum Congr. New York*, Sec. 1, paper 19, 377-390.

Hunting Survey Corporation Ltd. 1960 RECONNAISSANCE GEOLOGY OF PART OF WEST PAKISTAN, 231-238. Maracle Press Ltd., Ontario.

A NOTE ON THE CHEMICAL COMPOSITION AND MAGNETIC RESPONSE OF CHROMITES FROM HINDUBAGH, BALUCHISTAN.

The occurrence of chromite in Hindubagh, Baluchistan, was discovered by Vredenburg in 1902 (Hayden, 1918). Since then, about 30,000 tons of high grade ore are recovered annually. In 1969, during a visit to Mine 155, the senior author noticed a heap of discarded ore which appeared significantly different from the main ore (A), due to its black colour and fine-grained texture.

On analysis, specimen of black ore (B) was found to be a fairly good chromite with Cr/Fe ratio of 2.91 as compared with 2.94 for the normal ore. However, a significant difference was found in the ferric iron content which was abnormally high in (B) as compared with (A).

Another interesting observation was made while purifying the specimens for chemical analysis. Ground portions (80-120 mesh) of chromites A and B were treated with bromoform to remove light mineral fractions. The heavy mineral associates were removed with the help of a Frantz Isodynamic magnetic separator. While the chromite mineral, from ore (A), separated almost completely at 0.6A (ampere) current intensity, 15° sideward tilt (S.T.) and 30° forward tilt (F.T.), the black ore (B) showed an entirely different behaviour. The chromite mineral from this ore started separating around 0.1 A and continued to afford sizable fractions uptil 0.44 A ; no chromite fraction was obtained at higher current intensities. To investigate this unusual behaviour of chromite B, fractions were obtained by fixing current intensity at 0.1A, 0.2A and 0.4A which yielded 6%, 30% and 64% portions respectively. The chromites A, B and fractions of B were all analysed, following the modified scheme of Shafeeq (1969), and the data are reported in Table I alongwith certain recasted values.

In order to understand the relationship between chemical composition and magnetic response, Fig. 1 was prepared on the basis of data given in Table 1. The top-most portion of Fig. 1, shows the quantitative relationship between chromite fraction separated and current intensity applied. The position of chromite A has been plotted for comparative purposes. It is interesting that when various curves are extrapolated (dashed portions) they almost join the position of (A) under their normal trend, although the chromite B yields no fraction after 0.44 current intensity.

Following are the additional inferences from Fig. 1 :—

1. Various curves are regular and show a definite relationship between chemistry of chromite fraction and the current intensity applied.

2. Significant variation in chemical composition is shown by the values of Cr_2O_3, Fe_2O_3 and FeO while values of MgO and Al_2O_3 show only minor decrease with increase in current intensity applied.

3. The values of Fe_2O_3 and FeO show distinct reciprocal variation such that while the value of Fe_2O_3 decreases that of FeO increases with increase in current intensity applied.

The graph shows that chromite fractions with higher content of Cr_2O_3 will also require higher intensity to separate. When read in conjunction with curves for FeO and Fe_2O_3, the higher Cr_2O_3 bearing fractions also have higher FeO content and reciprocally lower Fe_2O_3 content ; that the chromite (B) contains abnormally high Fe_2O_3, explains its separation at current intensity significantly lower than that required for separating chromite (A).

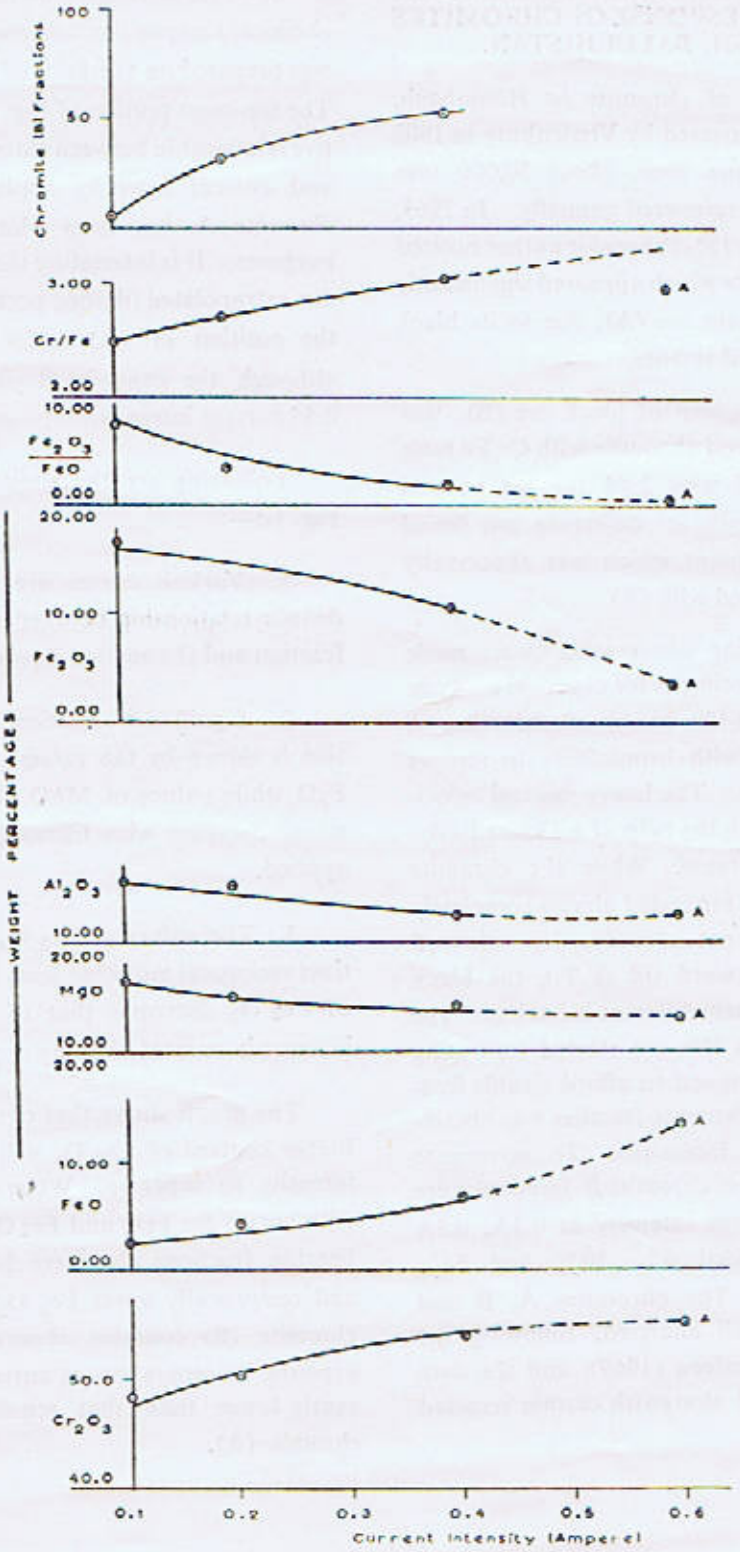

Fig. 1. Showing relationship between chemical composition and magnetic response of high Fe^{3+} Chromite.

TABLE I

Oxides	*Weight percentages*		*Fractions of B at*		
	A	B	0.1A	0.2A	0.4A
Cr_2O_3 ..	55.72	53.48	48.12	50.66	54.44
Al_2O_3 ..	12.59	13.46	15.80	15.25	12.80
Fe_2O_3 ..	3.37	11.45	16.28	13.23	10.35
FeO ..	13.62	5.47	2.30	4.70	6.48
MgO ..	13.56	15.06	16.90	15.30	14.60
MnO ..	0.35	0.33	0.29	0.39	0.29
TiO_2 ..	0.38	0.30	0.31	0.31	0.28
SiO_2 ..	0.28	0.32	0.32	0.35	0.26
Total ..	99.87	99.87	100.32	100.19	99.50
Cr/Fe ..	2.94	2.91	2.50	2.72	3.03
RO/R_2O_3 ..	1.01	1.01	0.79	0.80	0.84
Cautions on basis of 32 (0)					
Cr ..	11.44	10.64	9.37	9.99	10.95
Al ..	3.86	4.01	4.58	4.48	3.84
Fe^{3+} ..	0.66	2.18	3.01	2.48	1.98
Total ..	15.96	16.83	16.96	16.95	16.77
Fe^{2+} ..	2.88	1.16	0.41	0.89	1.32
Mg ..	5.10	5.52	6.09	5.56	5.45
Mn ..	0.08	0.07	0.06	0.08	0.06
Total : ..	8.06	6.75	6.56	6.53	6.83

Analyst : Shafeeq Ahmad

F.A. SHAMS
SHAFEEQ AHMAD
Geology Department
Punjab University, Lahore
December, 1971.

REFERENCES

Hayden, H.H., 1918 General report of the Geological Survey of India for the year 1916. *Rec. Geol. Surv.*, India, **48**, 12.

Shafeeq Ahmad, 1969 An improved scheme for chromite analysis. *Geol. Bull. Punjab Univ.*, **8**, 33-38.

EFFECT OF HEAT ON FeO CONTENT OF CHROMITE MINERAL

During geochemical study of a large number of chromites from Hindubagh, the author found them to have low range of ferric iron content (from 1.10% to 6.54%, in 58 analyses). This is also true of chromites reported from Hindubagh by Bilgrami (1963). However, at Mine 155, small chromite bodies associated with a large chromite deposit, show a totally different structure and general appearance which prompted its detailed study. (Shams and Shafeeq, 1972, in press). Given (Table I) are analyses of normal chromite (A) from the main body and chromite (B) from associated extensions. The latter shows abnormal excess of Fe_2O_3 and simultaneous deficiency in FeO content. Among various factors responsible for this, prevalence of oxidizing conditions was thought as one of them, which may have accounted for higher Fe_2O_3 content of chromite (B) as compared with the normal chromite (A). Considering field association, small fractions of chromite (A) were heated in atmosphere at 500°C, 700°C, 900°C, 1100°C and 1300°C for 24 hours in each case and their FeO percentage determined by Seil's method (1943); the data are given (Table 1-2). The values thus obtained are represented in a graph (Fig. 1), and the main inferences drawn are as follows.

1. The graph shows a gentle fall in FeO content from 500°C to 700°C (FeO 13.10% to 11.38% by weight).

2. After 700°C a sharp fall in FeO percentage takes place upto 900°C when there is only 2.59% FeO by weight.

3. After 900°C the temperature seems to have little effect as FeO weight percentage decreases very slowly and reaches a value of 1.73% by weight at 1300°C.

The position of chromites A and B are also plotted in Fig. 1.

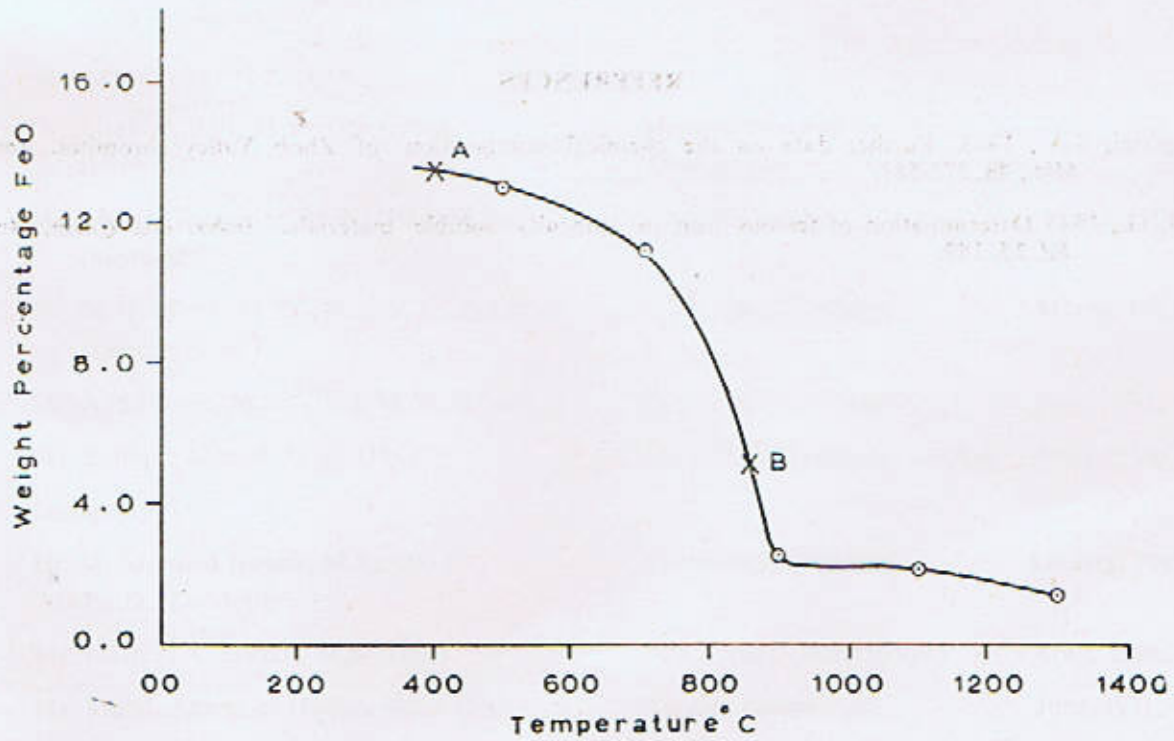

Fig. 1. Curve between temperature and weight percentage of FeO in chromite.

TABLE 1

Chemical Composition of normal Chromite, (A) and high Fe^{3+} Chromite (B).

Oxides	*Weight Percentage*	
	A	B
Cr_2O_3	.. 55.72	53.48
Al_2O_3	.. 12.59	13.46
Fe_2O_3	.. 3.37	11.45
FeO	.. 13.62	5.47
MgO	.. 13.56	15.06
MnO	.. 0.35	0.33
TiO_2	.. 0.38	0.30
SiO_2	.. 0.28	0.32
Total :	.. 99.87	99.87

TABLE 2

FeO content of heated Chromite (A).

Temperature	*Weight Percentage* FeO
500°C	13.10
700°C	11.38
900°C	2.59
1100°C	2.16
1300°C	1.73

SHAFEEQ AHMAD
Geology Department
Punjab University, Lahore
December, 1971

REFERENCES

Bilgrami, S.A., 1963 Further data on the chemical composition of Zhob Valley chromites. *Amer. Min.*, **48**, 573-587.

Seil, G., 1943 Determination of ferrous iron in difficulty soluble materials. *Indus. and Chem. Anal. Ed.* **15**, 189.

STAFF LIST OF THE DEPARTMENT OF GEOLOGY, UNIVERSITY OF THE PUNJAB (AT THE 31st DECEMBER, 1972).

1. Teaching Staff.

Name and Qualifications	*Subject*	*Appointed*
Professor of Geology :		
Prof. F.A. Shams, M.Sc. (Pb.), M.A. (Cantab), Ph.D. (Pb.), Head of the Department.	.. Mineralogy, Petrology, X-Ray Crystallography.	.. November, 1956.
Associate Professors :		
Dr. M.A. Latif, M.Sc. (Pb.) M.Sc. D.I.C., Ph.D. (London), F.P.T.C. (Vienna).	.. Micropaleontology, Stratigraphy.	.. July, 1957.
Dr. Aziz-ur-Rehman, M.Sc. (Pb.), D. Rehr. Nat. (Munich).	.. Applied Geophysics.	.. February, 1960.
Mr. A.H. Gardezi, M.Sc. (Pb.), M.Sc. D.I.C. (London), D.M. (E.N.I. Rome).	.. Petroleum Geology. Structure	.. March, 1962.
Dr. S.F.A. Siddiqui, M.Sc. (Pb.), Ph.D. (London).	.. Mineralogy, Petrology.	.. July, 1960.
Assistant Professors :		
Dr. Aftab A. Butt, M.Sc. (Pb.), Ph.D. (Utrecht).	.. Micropaleontology, Stratigraphy.	.. June, 1959.
Mr. Munir Ghazanfar, M.Sc. (Pb.), M.Sc. (Sheffield).	.. Geomorphology.	.. January, 1965.
Mr. M.H. Malik, M.Sc. (Pb.), M.Sc. D.I.C. (London).	.. Engineering Geology.	.. March, 1965.
Mr. A. Shakoor, M.Sc. (Pb.), M.Sc. (Leeds).	.. Engineering Geology.	.. May, 1965.
Mr. Zulfiqar Ahmad, M.Sc. (Pb.).	.. Mineralogy, Economic Geology	August, 1967.
Lecturers :		
Dr. Mohammad Nawaz, M.Sc. (Pb.), Ph.D. (London).	.. Mineralogy, Petrology.	.. January, 1968.
Mr. Liaquat A. Sheikh, M.Sc. (Pb.)	.. Paleontology, Stratigraphy.	.. April, 1969.
Mr. Mohd. Anwar-ul-Haque, M.Sc. (Pb.).	.. Applied Geophysics.	.. June, 1971.

Name and Qualifications	*Subject*	*Appointed*
Mr. Farooq Ahmad Khan, M.Sc. (Pb.) D.I.C., M. Phil (London).	.. Petroleum Geology. .. Sedimentology	.. November, 1971.
Research Assistants :		
Dr. S. Taseer Hussain*, M.Sc. (Pb.), Ph.D. (Utrecht).	.. Vertebrate .. Paleontology.	.. April, 1966
Dr. Fazal-ur-Rehman, M.Sc. (Pb.), Ph.D. (Pb.).	.. Geochemistry.	.. December, 1966.
Mr. Shafeeq Ahmad, M.Sc. (Pb.).	.. Geochemistry	.. January, 1967.
Mr. Ijaz Hussain, M.Sc. (Pb.).	.. Mineralogy, Petrology.	.. January, 1969.
Demonstrators :		
Sarfraz Ahmad.	.. Paleontology.	.. April, 1971.
Zulfiqar Ahmad Bhatti.	.. Paleontology.	.. April, 1971.
Allah Bakhsh Kausar	.. Mineralogy.	.. April, 1971.
Khalid Saeed	.. Petroleum	.. April, 1971.
Arshad Mahmood Bhutta.	.. Petroleum.	.. April, 1971.
2. Technical and Service Staff :		
Mr. A.Z. Dean, M. Inst. Sc. Tech. (London), M.H.S., B.K.S. (London).	.. Chief Technician.	.. July, 1962.
Mr. Arshad Hussain.	.. Geological Illustrator.	.. March, 1966.
Mr. M. Aslam.	.. Junior Technician.	.. June, 1964.
Mr. H. U. Siddiqui.	.. Junior Technician.	.. June, 1965.
Mr. Mahmood Ahmad.	.. Draftsman.	.. January, 1967.
Mr. G.R. Bhatti.	.. Office Assistant.	.. September, 1963.
Mr. K. Ahmad, B.A. (Pb.).	.. Library Assistant.	.. August, 1965.
Mr. M. Riaz.	.. Stenographer.	.. November, 1967.
Office and Library Staff.	.. 6	
Laboratory Assistants.	.. 9	
Drivers.	.. 1+1 (Summer only).	
Service Staff.	.. 3	

*On duty leave at the Geological Institute, Utrecht, Holland.